



Measurement of the azimuthal anisotropy of charged particles in $\sqrt{s_{NN}} = 5.36$ TeV $^{16}\text{O}+^{16}\text{O}$ and $^{20}\text{Ne}+^{20}\text{Ne}$ collisions with the ATLAS detector

The ATLAS Collaboration

This paper presents the first measurements of the azimuthal anisotropy coefficients v_n , which quantify the n^{th} -order Fourier modulation of charged-particle azimuthal distributions, for $n = 2-4$ in $\sqrt{s_{NN}} = 5.36$ TeV $^{16}\text{O} + ^{16}\text{O}$ and $^{20}\text{Ne} + ^{20}\text{Ne}$ collisions recorded with the ATLAS detector at the Large Hadron Collider in 2025. The v_n coefficients are measured as a function of transverse momentum (p_T), collision centrality, and event multiplicity. They are extracted using two complementary methods: two-particle correlations with a template-fit subtraction of short-range non-flow contributions, and four-particle subevent cumulants, which intrinsically suppress non-flow effects and provide sensitivity to flow fluctuations. The results show a clear hierarchy $v_2 > v_3 > v_4$ and a non-monotonic dependence on p_T , reaching a maximum around 2 GeV, consistent with trends observed in heavy-ion collisions. Detailed comparisons between the two collision systems reveal an enhanced v_2 in central $^{20}\text{Ne} + ^{20}\text{Ne}$ collisions, consistent with theory expectations based on the predicted prolate deformation of neon nuclei, in contrast to the slightly tetrahedral structure predicted for oxygen. The four-particle cumulant results highlight strong event-by-event fluctuations and provide the greatest sensitivity to nuclear shape effects. These measurements can place new constraints on the initial geometry and the hydrodynamic response in light-ion collisions, offering valuable input for models of nuclear structure.

1 Introduction

A hot and dense state of nuclear matter in which the relevant degrees of freedom are strongly coupled quarks and gluons is known as the quark–gluon plasma (QGP). This state can be created transiently in collisions of heavy nuclei at high-energy colliders, such as the Relativistic Heavy Ion Collider (RHIC) and the Large Hadron Collider (LHC) [1–11]. The QGP produced in heavy-ion collisions undergoes collective expansion driven by strong pressure gradients, which convert initial-state spatial anisotropies into momentum anisotropies of the final-state hadron distribution [1–3, 12]. This phenomenon, commonly referred to as collective flow, is well described by nearly inviscid relativistic hydrodynamics and constitutes a key signature of QGP formation (see Ref. [13] and references therein).

The anisotropy of particle distributions in heavy-ion collisions is quantitatively characterized by a Fourier series in the azimuthal angle ϕ [14]:

$$\frac{dN}{d\phi} \propto 1 + 2 \sum_{n=1}^{\infty} v_n \cos(n(\phi - \Psi_n)), \quad (1)$$

where v_n and Ψ_n represent the magnitude and orientation of the n^{th} -order anisotropy, respectively. The v_n are commonly referred to as “flow harmonics,” while the Ψ_n are referred to as “event-plane angles.” The v_n depend on transverse momentum p_T , pseudorapidity¹ (η), and event multiplicity, and fluctuate event-by-event (EbE) [15–18]. These EbE fluctuations arise primarily from variations in the initial geometry and energy density of the nuclear overlap region, which are driven by the fluctuating positions of nucleons and by subnucleonic structure, collectively referred to as geometric fluctuations. Among these coefficients, elliptic flow (v_2) is the largest due to the lenticular geometry of the average overlap region. This is typically followed by triangular flow (v_3), which typically has no contribution from the average geometry and is therefore generated entirely by EbE geometric fluctuations. For higher orders ($n \geq 4$), the flow harmonics are influenced not only by the initial geometry but also by non-linear mode coupling from lower-order harmonics, such as v_4 from v_2^2 and v_5 from v_2v_3 [19]. These contributions make the higher-order harmonics sensitive to both the geometry and the medium’s collective response. Extensive studies of v_n and their EbE fluctuations have provided important constraints on the initial-state geometry and on transport properties of the QGP in nuclear collisions, such as the shear viscosity to entropy density ratio η/s (see Ref. [13] and references therein).

The observation of collective flow was initially regarded as an exclusive signature of QGP formation in collisions of heavy nuclei, such as Au+Au or Pb+Pb systems. However, experiments at the LHC and the RHIC have revealed large v_n signals in much smaller collision systems, including pp and p +Pb at the LHC [20–23] and $p/d/{}^3\text{He}$ +Au at the RHIC [24–27]. Remarkably, the observed v_n hierarchy in these small systems follows patterns consistent with expectations based on geometrical differences between their initial conditions. Detailed theory studies suggest that the measured v_n in small systems can be explained by the collective expansion of the matter produced in the collision, driven by the shape and fluctuations of the initial overlap region [28, 29]. Nevertheless, substantial uncertainties remain regarding the precise nature and properties of the produced matter in small collision systems. These uncertainties arise primarily from the incomplete understanding of the initial conditions in small systems, which are sensitive not only to the

¹ ATLAS uses a right-handed coordinate system with its origin at the nominal interaction point (IP) in the center of the detector and the z -axis along the beam pipe. The x -axis points from the IP to the center of the LHC ring, and the y -axis points upwards. Cylindrical coordinates (r, ϕ) are used in the transverse plane, ϕ being the azimuthal angle around the z -axis. The pseudorapidity is defined in terms of the polar angle θ as $\eta = -\ln \tan(\theta/2)$.

spatial distribution of nucleons within nuclei but also to the internal structure of individual nucleons [24, 30]. Consequently, precise characterization of the initial conditions in small systems is essential to improve the extraction of medium properties such as shear viscosity, pre-hydrodynamic evolution effects, and initial-state momentum anisotropies [31–33].

To address these uncertainties, a promising experimental strategy is to compare v_n harmonics in collisions of nuclei with similar mass numbers but distinct nucleon arrangements [34–36]. Such systems are expected to produce matter with comparable bulk properties and similar final-state collective responses. Therefore, the ratios of v_n between the two systems are expected to be primarily sensitive to differences between their initial conditions [37]. Analogous comparisons have previously been used to study the influence of nuclear structure in large collision systems [38–40]. A key advantage of applying this approach in small collision systems is that the initial-state differences are governed by nucleon distributions that can, in principle, be calculated using state-of-the-art *ab initio* nuclear structure theories [41], providing a theoretical foundation for interpreting experimental observations.

An ideal pair of collision systems for such comparative studies is $^{16}\text{O}+^{16}\text{O}$ and $^{20}\text{Ne}+^{20}\text{Ne}$. Low-energy experiments and theory calculations indicate that ^{16}O has a near-spherical tetrahedral shape, whereas ^{20}Ne is predicted to consist of an ^4He cluster “orbiting” an ^{16}O core [42, 43]. Hydrodynamic simulations incorporating nuclear configurations from *ab initio* calculations predict significant enhancements in v_2 and v_3 for central $^{20}\text{Ne}+^{20}\text{Ne}$ collisions compared with central $^{16}\text{O}+^{16}\text{O}$ collisions² [44]. Furthermore, nuclear structure effects are also predicted to modify the EbE fluctuations of v_2 and v_3 between the two systems [45], providing additional discriminatory power for theory models.

This paper presents measurements of anisotropic flow coefficients v_n for $n = 2$ to 4 in $\sqrt{s_{\text{NN}}} = 5.36$ TeV O+O and Ne+Ne collisions recorded by the ATLAS detector at the LHC in 2025. The analysis employs both two- and four-particle correlation methods [22, 46], which probe different moments of the v_n distributions. These measurements provide valuable constraints on the final-state collective response and on the properties of the produced medium in each system individually, while their comparison offers unique insights into the initial-state geometry and nucleon distributions within these light nuclei.

2 Experimental configuration

The ATLAS detector [47, 48] at the LHC covers nearly the entire solid angle around the collision point. It consists of an inner tracking detector surrounded by a thin superconducting solenoid, electromagnetic and hadronic calorimeters, and a muon spectrometer incorporating three large superconducting air-core toroidal magnets. The primary subsystems relevant to this study include the inner detector (ID), the calorimeter and the trigger and data acquisition infrastructure.

The ID is immersed in a 2 T axial magnetic field and provides charged-particle tracking in the range $|\eta| < 2.5$. The high-granularity silicon pixel detector covers the vertex region and typically provides four measurements per track, the first hit generally being in the insertable B-layer (IBL). It is followed by the SemiConductor Tracker (SCT), which usually provides eight measurements per track. These silicon detectors are complemented by the transition radiation tracker (TRT), which enables radially extended track reconstruction up to $|\eta| = 2.0$.

² For simplicity, ^{16}O and ^{20}Ne are hereafter denoted as O and Ne, respectively.

The calorimetry system includes several components: a liquid argon (LAr) electromagnetic calorimeter covering $|\eta| < 3.2$; a steel–scintillator sampling hadronic calorimeter covering $|\eta| < 1.7$; an additional LAr-based hadronic calorimeter for the region $1.5 < |\eta| < 3.2$; and forward LAr calorimeters (FCal) designed to measure both electromagnetic and hadronic activity in the range $3.2 < |\eta| < 4.9$. Forward neutrons produced from the breakup of nuclei in both hadronic and electromagnetic interactions are measured by compact tungsten sampling Zero Degree Calorimeters (ZDCs) positioned at $z = \pm 140$ meters from the ATLAS interaction point.

Event collection is handled by a two-tiered trigger system [49]. The first level (L1) is implemented through a combination of custom hardware and programmable logic, while the high-level trigger (HLT) uses software algorithms to refine the selection using more detailed detector information.

A software suite [50] is used in data simulation, in the reconstruction and analysis of real and simulated data, in detector operations, and in the trigger and data acquisition systems of the experiment.

3 Datasets, event and track selection

The O+O and Ne+Ne data used in this paper were collected in July 2025. The datasets correspond to integrated luminosities of 2 nb^{-1} for O+O and 0.5 nb^{-1} for Ne+Ne collisions, respectively. Minimum-bias events were selected with an L1 trigger based on the TRT “FastOR” algorithm [51], that required at least one TRT azimuthal sector above threshold, together with an HLT requirement of at least one reconstructed charged-particle track. To increase statistics for the highest-activity events, an additional trigger was used that required the TRT FastOR at L1 and at least 290 reconstructed tracks with $p_T > 200 \text{ MeV}$ at the HLT. A similar trigger with a requirement of 100 reconstructed tracks with $p_T > 200 \text{ MeV}$ at the HLT was employed to supplement the intermediate-activity region. In addition, a trigger requiring an L1 calorimeter transverse energy threshold of 20 GeV , followed by at least one reconstructed track with $p_T > 200 \text{ MeV}$ at the HLT, was also included.

In the offline analysis, the z -position of the primary vertex [52] was required to lie within 10 cm of the nominal interaction point (i.e. within 10 cm of the center of ATLAS). In the recorded O+O and Ne+Ne data, there are sizable contributions from pileup events, in which two or more inelastic collisions occur in the same bunch crossing. The majority of the pileup events are removed by requiring only a single high-quality reconstructed vertex per event. A high-quality vertex is defined as one that is well-constrained in position, having a z -position variance of less than 0.02 mm^2 ; such vertices have many associated tracks pointing to a common origin. Additional background is suppressed by removing events with significantly smaller track multiplicities than expected relative to the total transverse energy recorded in the FCal (ΣE_T^{FCal}) [53]. Similarly, correlations between the energy deposited in the ZDCs and ΣE_T^{FCal} are used to suppress additional pileup by rejecting events for which the energy deposited in the ZDCs is significantly higher than in the majority of collisions. The estimated residual pileup after these selections is found to be at most 0.2%.

As in earlier ATLAS studies of heavy-ion collisions, events are categorized into centrality percentiles based on the ΣE_T^{FCal} [5, 7, 15]. To relate the ΣE_T^{FCal} distribution to the sampled fraction of the total inelastic O+O and Ne+Ne cross-sections, a Glauber-model-based calculation [54, 55] is used to fit the data, to extract the fraction of events selected above a minimum ΣE_T^{FCal} threshold, and to estimate the systematic uncertainties on that fraction [5, 7, 15]. Additionally, the Glauber model is used to extract primary collision characteristics, such as the average number of participating nucleons, $\langle N_{\text{part}} \rangle$, for each centrality interval.

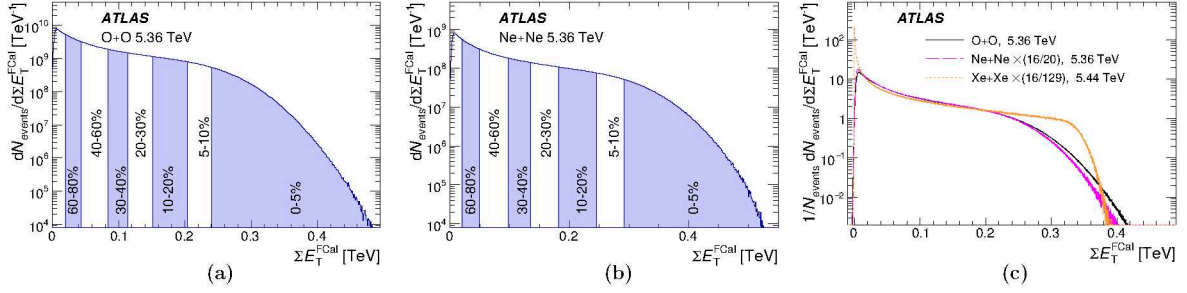


Figure 1: The ΣE_T^{FCal} distribution in minimum-bias events, together with the thresholds for a few centrality intervals, for (a) O+O collisions and (b) Ne+Ne collisions. (c) Comparison to Xe+Xe collisions [7], where the ΣE_T^{FCal} of the Xe+Xe and Ne+Ne systems are scaled by the relative number of nucleons to oxygen. The Ne+Ne and Xe+Xe distributions in panel (c) are normalized to have the same integral as the O+O distribution above 30 GeV.

The distribution of ΣE_T^{FCal} observed in data, along with the threshold values defining various centrality intervals, is illustrated in Figure 1. Figure 1c shows the comparison of the ΣE_T^{FCal} distributions in O+O and Ne+Ne, to that in Xe+Xe collisions (from Ref. [7]). The comparison is done after scaling the Ne+Ne and Xe+Xe ΣE_T^{FCal} distributions by the number of nucleons relative to oxygen. While the Xe+Xe distribution exhibits a sharper fall-off at a scaled ΣE_T^{FCal} of ~ 0.34 TeV and a narrower tail beyond this point, the O+O and Ne+Ne distributions show a significantly more pronounced high- ΣE_T^{FCal} tail. This behavior reflects the larger relative event-by-event fluctuations in particle production in the smaller O+O and Ne+Ne systems compared to Xe+Xe.

Charged-particle tracks and collision vertices are reconstructed from hits in the ID using standard methods [56]. For the nominal analysis, the reconstructed tracks are required to have $p_T > 0.5$ GeV, $|\eta| < 2.5$ and at least one pixel hit, with the additional requirement of a hit in the IBL when one is expected³. If a hit in the IBL is not expected, then a hit is required in the next-to-innermost pixel layer, if such a hit is expected. The tracks are required to have at least six SCT hits. To suppress secondary contributions, the transverse impact parameter of the track with respect to the beam-line, d_0 , and the longitudinal impact parameter of the track relative to the primary vertex, $z_0 \sin(\theta)$, are required to satisfy $|d_0| < 1.5$ mm and $|z_0 \sin(\theta)| < 1.5$ mm. The quantity $N_{\text{ch}}^{\text{rec}}$ is defined as the number of charged-particle tracks in an event that satisfy these selection criteria and have $p_T > 0.5$ GeV. An alternate set of more restrictive selections are used to evaluate systematic uncertainties in the measurement. For these “tight” selections, the number of pixel and SCT hits are raised to two and eight respectively, a requirement of at most one missing hit in the SCT is imposed, and the d_0 and $z_0 \sin(\theta)$ impact parameter selections are decreased to 1 mm. Furthermore, the χ^2 per degree of freedom of the reconstructed track trajectory is required to be less than 6.

Figures 2a and 2b show the correlation between ΣE_T^{FCal} and $N_{\text{ch}}^{\text{rec}}$ in minimum-bias O+O and Ne+Ne events, respectively. These two measures of event activity are found to be well correlated. Figures 2c and 2d show the $N_{\text{ch}}^{\text{rec}}$ distributions in minimum-bias O+O and Ne+Ne events, together with the distributions for several centrality intervals from Fig. 1.

To study the detector performance, a sample of 7 million minimum-bias O+O Monte Carlo (MC) events was generated using the HIJING event generator version 1.38b [57]. Since HIJING does not have any intrinsic mechanism to generate flow, the latter is added after the initial particle generation step using an

³ A hit is expected if the extrapolated track crosses an active region of a silicon-sensor module (pixel or SCT) that has not been disabled, and a hit is said to be “missing” when it is expected but not found. If a track crosses a disabled module, then for the purposes of hit counting, the disabled module is counted as a hit.

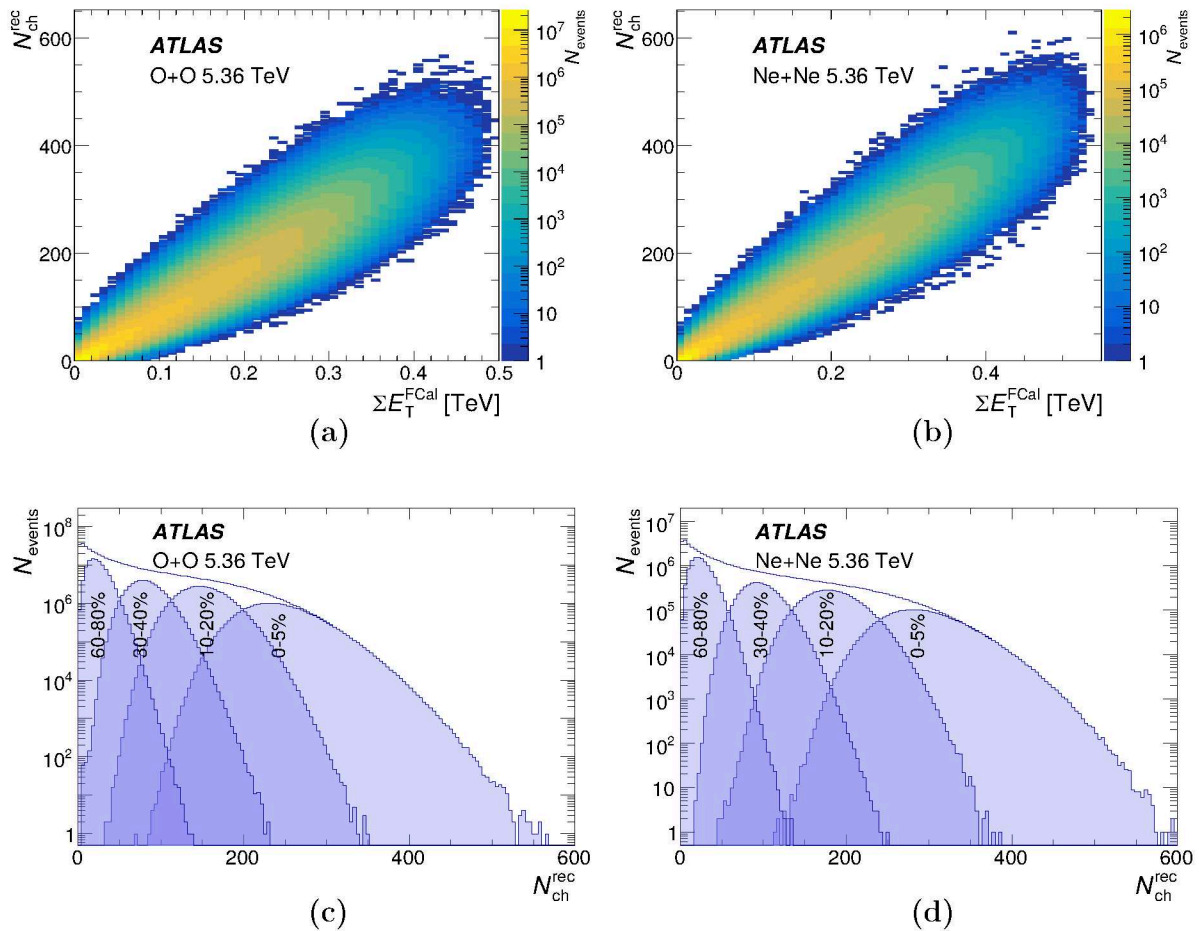


Figure 2: Correlation between $N_{\text{ch}}^{\text{rec}}$ and $\Sigma E_{\text{T}}^{\text{FCal}}$ in minimum-bias events for (a) O+O and (b) Ne+Ne collisions, and distributions of $N_{\text{ch}}^{\text{rec}}$ in minimum-bias events for (c) O+O and (d) Ne+Ne collisions, including the distributions for several centrality intervals.

“afterburner” procedure [58], which slightly shifts the ϕ positions of generated particles to mimic flow. The generated sample was then passed through a full simulation of the ATLAS detector [59] using GEANT4 [60], and the MC events were reconstructed by the same algorithms as the data. The reconstructed particles in the MC events were used to calculate the reconstruction efficiency – the fraction of the generated charged particles that are successfully reconstructed and selected – as a function of p_{T} and η , and denoted by $\epsilon(p_{\text{T}}, \eta)$ below. With the criteria imposed in this analysis, the efficiency at $p_{\text{T}} = 1$ GeV varies between $\sim 65\%$ at $|\eta| = 2.5$ to $\sim 75\%$ at $|\eta| = 2$ and $\sim 85\%$ at $|\eta| = 0$. At mid-rapidity ($|\eta| < 1$) the efficiency is $\sim 80\%$ at $p_{\text{T}} = 0.5$ GeV and increases to $\sim 90\%$ at a p_{T} of 5 GeV. The rate of fake tracks, tracks that do not correspond to any generated particle, denoted by $f(p_{\text{T}}, \eta)$, is also estimated from the MC and stays below $\sim 2\%$ across the p_{T} and η ranges used in this measurement. The reconstructed event multiplicity $N_{\text{ch}}^{\text{rec}}$ is corrected for reconstruction efficiency and fake tracks by weighting each track with:

$$\frac{1 - f(p_{\text{T}}, \eta)}{\epsilon(p_{\text{T}}, \eta)}, \quad (2)$$

where the numerator accounts for fake-track removal and the denominator for the reconstruction efficiency. This efficiency- and fake-corrected multiplicity is referred to as N_{ch} .

4 Methodology

Due to the limited multiplicity per event, the v_n cannot be reliably measured on an EbE basis. Instead, the flow harmonics v_n are estimated from multi-particle correlations, which average over many events and provide access to different moments of the EbE v_n distributions. However, correlations unrelated to collective flow can contaminate the measurement and must be suppressed or removed. For example, jet production and resonance decays produce strongly correlated collinear particles ($|\Delta\eta|, |\Delta\phi| < 1$), and weaker but equally important back-to-back correlations at $\Delta\phi \approx \pi$ that persist even at large $\Delta\eta$. These few-particle, non-global correlations are referred to as “non-flow.” This section describes two approaches for estimating flow harmonics: the two-particle correlations (2PC) method, including its improved template-fit implementation, and the multi-particle cumulant method. In the 2PC approach, a template fit is used to subtract non-flow contributions based on the lowest-multiplicity events, while the multi-particle cumulant method applies a subevent technique to suppress non-flow effects.

4.1 Two-particle correlations and template fit

The 2PC method has been widely used for flow measurements at the RHIC and the LHC [6, 9, 15, 16, 21, 22, 61–69]. Correlations between pairs of charged particles are studied as a function of their relative pseudorapidity, $\Delta\eta = \eta^a - \eta^b$, and relative azimuthal angle, $\Delta\phi = \phi^a - \phi^b$. The indices a and b denote the two particles in the pair, whose kinematic selections may differ. To account for detector acceptance effects, the correlation function is defined as the ratio of the “same-event” pair distribution S , where both particles are taken from the same event, to the “mixed-event” distribution B , where they are taken from different events [15]:

$$C(\Delta\eta, \Delta\phi) = \frac{S(\Delta\eta, \Delta\phi)}{B(\Delta\eta, \Delta\phi)}.$$

The same-event distribution contains both genuine physical correlations and contributions from detector acceptance, inefficiencies and nonuniformities that are not related to the underlying physics. The mixed-event distribution reflects only these non-physical effects, so that their ratio isolates the genuine physical correlations [61]. To ensure this, events used for the B distribution are required to have similar centrality (or multiplicity) and vertex position. When constructing S and B , corrections for track reconstruction inefficiency and fake tracks are applied using a per-pair weight (see Eq. 2):

$$\frac{(1 - f(p_T^a, \eta^a))(1 - f(p_T^b, \eta^b))}{\epsilon(p_T^a, \eta^a) \epsilon(p_T^b, \eta^b)}.$$

Examples of $C(\Delta\eta, \Delta\phi)$ are shown in Figure 3, normalized such that the integral of $B(\Delta\eta, \Delta\phi)$ matches that of $S(\Delta\eta, \Delta\phi)$ for $|\Delta\eta| > 2$. In all cases a prominent peak is observed at $\Delta\eta = \Delta\phi = 0$, arising from short-range correlations such as jet fragmentation, resonance decays, or Hanbury Brown–Twiss (HBT) correlations [70]. At large $\Delta\eta$, long-range correlations are visible both on the near-side ($\Delta\phi \sim 0$) and the away-side ($\Delta\phi \sim \pi$). The near-side correlation, commonly referred to as the “ridge,” originates primarily from collective flow. The away-side correlation receives contributions from both collective flow and back-to-back dijets.

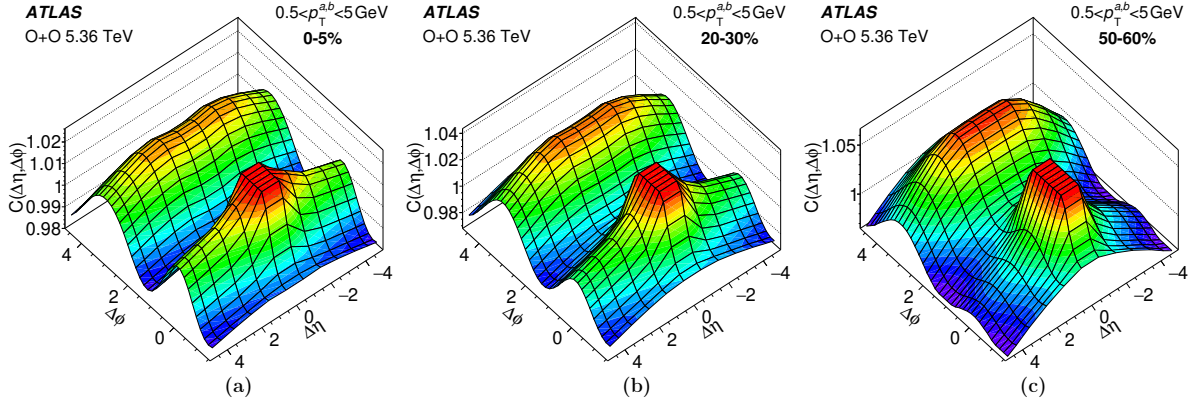


Figure 3: Two-particle $\Delta\eta - \Delta\phi$ correlations in O+O collisions for the (a) 0–5%, (b) 20–30%, and (c) 50–60% centrality intervals. The plots are for $0.5 < p_T^{a,b} < 5$ GeV. The distributions are truncated along the z -axis, to suppress the peak at $\Delta\eta = \Delta\phi = 0$, and are plotted over $|\Delta\eta| < 4.5$ to avoid statistical fluctuations at larger $|\Delta\eta|$.

One-dimensional correlation functions, $C(\Delta\phi)$, are obtained by integrating the S and B distributions over the range $2 < |\Delta\eta| < 5$:

$$C(\Delta\phi) = \frac{\int_2^5 S(|\Delta\eta|, \Delta\phi) d|\Delta\eta|}{\int_2^5 B(|\Delta\eta|, \Delta\phi) d|\Delta\eta|} \equiv \frac{S(\Delta\phi)}{B(\Delta\phi)},$$

where the $|\Delta\eta| > 2$ requirement is imposed to suppress non-flow correlations arising from the peak at $\Delta\eta = \Delta\phi = 0$ seen in Figure 3 [21, 22, 62]. The $C(\Delta\phi)$ are normalized to have an average value of unity. Similar to the single-particle distribution (Eq. 1), the $C(\Delta\phi)$ is parametrized with a Fourier series [15]:

$$C(\Delta\phi) = C_0 \left(1 + 2 \sum_{n=1}^{\infty} v_{n,n}(p_T^a, p_T^b) \cos(n\Delta\phi) \right). \quad (3)$$

To suppress residual non-flow contributions that persist over $|\Delta\eta| > 2$, primarily on the away side ($\Delta\phi \sim \pi$), a commonly used template-fit procedure is employed [22, 24, 64, 71]. In this method, the shape of the non-flow component is estimated from low-multiplicity (peripheral) events and assumed to be unchanged in higher-multiplicity (more central) events. For this analysis, the peripheral reference correlation, $C^{\text{periph}}(\Delta\phi)$, is constructed from events of the same collision species (O+O or Ne+Ne) with centrality greater than 80%. The measured correlation $C(\Delta\phi)$ is then parameterized as the sum of this non-flow reference and an azimuthally modulated pedestal, $C^{\text{ridge}}(\Delta\phi)$, that encodes the collective anisotropy:

$$C(\Delta\phi) = FC^{\text{periph}}(\Delta\phi) + C^{\text{ridge}}(\Delta\phi), \quad (4)$$

with

$$C^{\text{ridge}}(\Delta\phi) \equiv G \left[1 + 2 \sum_{n=2}^5 v_{n,n}(p_T^a, p_T^b) \cos(n\Delta\phi) \right]. \quad (5)$$

The parameters F , G , and the $v_{n,n}$ are determined by the template fit, with F and G constrained such that the integrals of both sides of Eq. 4 are equal. Fourier terms up to fifth order ($v_{2,2}$ – $v_{5,5}$) are included in the fit.

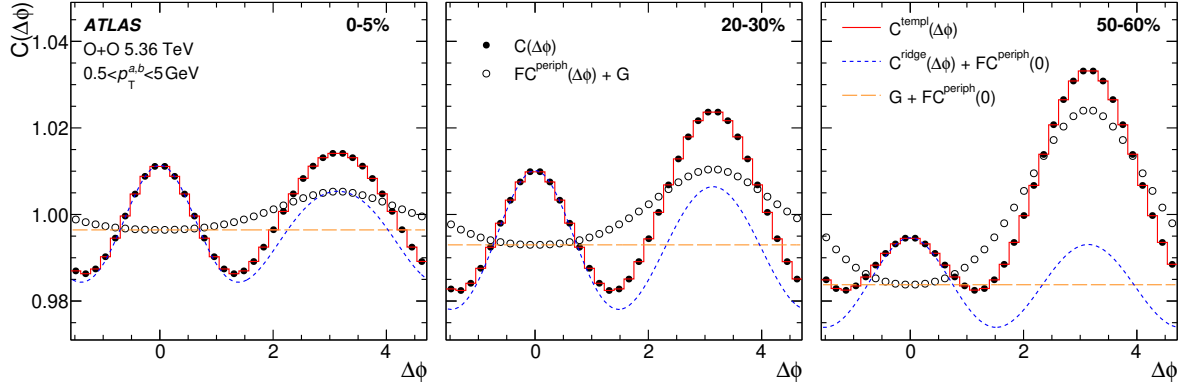


Figure 4: Template fits to correlation functions measured in O+O collisions for the (left) 0–5%, (center) 20–30%, and (right) 50–60% centrality intervals. The plots are for $0.5 < p_T^{a,b} < 5$ GeV. The solid points indicate the measured $C(\Delta\phi)$, and the continuous red line indicates the template fit, $C^{\text{templ}}(\Delta\phi)$. The open points and dashed curves indicate the different components of the template-fit, which are shifted along the y -axis by G or by $FC^{\text{periph}}(0)$, where necessary, for presentation.

Figure 4 shows examples of template fits for O+O collisions, where the template fit is denoted as $C^{\text{templ}}(\Delta\phi)$. In the measured correlations, the away-side peak is the largest in the 50–60% centrality interval and decreases systematically in the 20–30% and 0–5% intervals. A significant fraction of the away-side correlation is described by the scaled peripheral reference ($FC^{\text{periph}}(\Delta\phi)$ term in Eq. 4). The relative contribution of this term decreases monotonically toward mid-central and central events, indicating that non-flow correlations are most important in peripheral collisions. The $C^{\text{ridge}}(\Delta\phi)$ component of the template fit is double-peaked in all intervals, reflecting the dominant contribution from the $v_{2,2}$ term in Eq. 5.

If the pair distribution is entirely determined by a global single-particle distribution, like in Eq. 1, the Fourier coefficients of the $C(\Delta\phi)$ (or $C^{\text{ridge}}(\Delta\phi)$) factorize into the product of single-particle anisotropies [61] as $v_{n,n}(p_T^a, p_T^b) = v_n(p_T^a)v_n(p_T^b)$ and thus:

$$v_n(p_T^b) = \frac{v_{n,n}(p_T^a, p_T^b)}{v_n(p_T^a)} = \frac{v_{n,n}(p_T^a, p_T^b)}{\sqrt{v_{n,n}(p_T^a, p_T^a)}}, \quad (6)$$

For all the 2PC results in this analysis, the $v_n(p_T^b)$ are evaluated using Eq. 6 with $0.5 < p_T^a < 5$ GeV. The upper limit on p_T^a is chosen to suppress non-flow, which increases at high p_T . The template-fit method provides a more reliable treatment of non-flow effects and is therefore regarded as the primary measurement method. Results obtained with the 2PC method are also included in this paper to illustrate the impact of non-flow removal achieved by the template-fit procedure.

4.2 Four-particle cumulants

Multi-particle cumulants extract higher-order azimuthal correlations, providing information about EbE flow fluctuations. The cumulant measurements have the advantage of suppressing correlations from jets and dijets, instead of relying on an explicit procedure to correct v_n as discussed in Section 4.1. The cumulant of order $2k$, where k is an integer, involves correlations between $2k$ particles and suppresses all correlations

involving less than $2k$ particles, including non-flow correlations [72]. The framework for the cumulant measurements is described in Refs. [73–75], but a concise description is provided here for completeness.

As mentioned before, the cumulant method involves the calculation of $2k$ -particle azimuthal correlations $\langle\{2k\}_n\rangle$, and $2k$ -particle cumulants, $c_n\{2k\}$, for the n^{th} -order flow harmonics, where k equals either one or two in this paper. The two- or four-particle azimuthal correlations in one event are evaluated as [73–75]:

$$\langle\{2\}_n\rangle = \left\langle e^{in(\phi_1 - \phi_2)} \right\rangle \quad (7)$$

$$\langle\{4\}_n\rangle = \left\langle e^{in(\phi_1 + \phi_2 - \phi_3 - \phi_4)} \right\rangle \quad (8)$$

where “ $\langle\cdot\rangle$ ” denotes a single-event average over all pairs or quadruplets of distinct particles, respectively. The averages from Eqs. 7 and 8 are expanded into products of per-particle normalized flow vectors [76]:

$$\langle q_n \rangle = \left\langle e^{in(\phi)} \right\rangle, \quad (9)$$

which provides an efficient calculation of multi-particle correlations. The exact details of this procedure follow Ref. [46]. These flow vectors are constructed with per-particle weights that correct for detector non-uniformities, tracking inefficiency, and contributions from fake tracks, similar to Eq. 2 but with additional ϕ -dependent corrections applied.

In the “standard” cumulant method described so far, all $2k$ -particle multiplets involved in the calculations of $\langle\{2k\}_n\rangle$ are selected using the entire detector acceptance. To further suppress the non-flow correlations, which typically involve particles emitted within a localized region in η , the particles can be grouped into several “subevents,” each covering a non-overlapping η interval [75]. The multi-particle correlations are then constructed by correlating particles between different subevents (two and three in this case), further reducing non-flow correlations. For two-subevent correlations, particles 1 and 2 in Eq. 7 are selected from different regions of η . Similarly, in Eq. 8, the pair of particles 1 and 2 are selected from one region of η , and the pair of particles 3 and 4 from another. For the three-subevent correlations, permutations of different choices are made and combined (see Ref. [46] for details). For the results presented here, the subevents used for the two-subevent method cover $-2.5 < \eta < 0$ and $0 < \eta < 2.5$, and those for the three-subevent method cover $-2.5 < \eta < -2.5/3$, $-2.5/3 < \eta < 2.5/3$ and $2.5/3 < \eta < 2.5$.

The two- and four-particle cumulants are then obtained from the azimuthal correlations as:

$$c_n\{2\} = \langle\langle\{2\}_n\rangle\rangle, \quad (10)$$

$$c_n\{4\} = \langle\langle\{4\}_n\rangle\rangle - 2\langle\langle\{2\}_n\rangle\rangle^2, \quad (11)$$

where “ $\langle\langle\cdot\rangle\rangle$ ” represents the average of $\langle\{2k\}_n\rangle$ over an event ensemble. In the absence of non-flow correlations, $c_n\{2k\}$ reflects the moments of the distribution of the flow coefficient v_n :

$$\begin{aligned} c_n\{2\} &= \langle v_n^2 \rangle, \\ c_n\{4\} &= \langle v_n^4 \rangle - 2\langle v_n^2 \rangle^2. \end{aligned} \quad (12)$$

The v_n measured by the 2-particle cumulants is defined as $v_n\{2\} = \sqrt{c_n\{2\}}$. In the absence of non-flow effects, the v_n measured by the 2-particle cumulant is identical to that measured using the 2PC method. However, non-flow contributions lead to differences between the two. Henceforth, the v_n measured with the 2PC and template-fit, methods are denoted as $v_n^{\text{2PC}}\{2\}$ and $v_n^{\text{sub}}\{2\}$, respectively. When making general

statements without reference to a specific method, v_n obtained from any two-particle correlation technique is denoted simply as $v_n\{2\}$.

Under the Gaussian model of eccentricity fluctuations [76], the 2- and 4-particle cumulants can be expressed in terms of an average geometry-driven component \bar{x}_n and a fluctuation component Δ_n as:

$$c_n\{4\} = -\bar{x}_n^4, \quad c_n\{2\} \equiv \langle v_n^2 \rangle = \bar{x}_n^2 + \Delta_n^2. \quad (13)$$

This implies $c_n\{4\} < 0$, and a positive $c_n\{4\}$ signals onset of non-Gaussian flow fluctuations, or significant non-flow contamination. If the sign constraints are obeyed, the corresponding four-particle flow coefficient is then defined as:

$$v_n\{4\} = \sqrt[4]{-c_n\{4\}}, \quad (14)$$

and measures the contribution to the flow from the average-geometry component only.

A comparison of the results of the standard and the two- and three-subevent cumulants in the O+O and Ne+Ne collisions shows that the two- and three-subevent results are consistent. This demonstrates that both subevent methods effectively suppress non-flow in the measured phase space region. For this reason, the $v_n\{4\}$ results presented in this paper uses the two-subevent method.

5 Systematic uncertainties

The systematic uncertainties of the measured v_n using the 2PC, template-fit, and multi-particle cumulant methods are described in this section. The following sources of systematic uncertainty are considered:

1. **MC closure:** The MC closure test compares v_n^{gen} , obtained from MC generated particles, with v_n^{reco} , obtained by applying the full analysis procedure to reconstructed tracks in the MC simulation, as done in data. The difference between the two is within 1% across the p_T and multiplicity ranges considered in this analysis and is conservatively assigned as a systematic uncertainty. This uncertainty accounts for residual reconstruction effects not corrected in the data analysis.
2. **Track selection:** The track selection criteria control the relative contributions of genuine charged particles and fake tracks entering the analysis. The stability of the results with respect to the track selections is evaluated by varying the requirements applied to reconstructed tracks and including the resulting variation in v_n as a systematic uncertainty. The results obtained with the nominal selections are compared with those using the tighter criteria described in Section 2. The differences depend on the harmonic order and are between 0.5–1.5%.
3. **Tracking efficiency:** The uncertainty in the reconstruction efficiency and fake-rate due to ID material modeling in the GEANT4 simulation is accounted for by evaluating the efficiency and fake-rates in alternate MC samples. In each sample, a single modification is applied to the ATLAS ID geometry: the passive material of the ID is increased by 5%, or the passive material of the IBL by 10%, or the passive material in the services region by 25%. These variations capture the full range of data–MC differences observed in dedicated studies of the ID material [77]. The variation in the results when using these alternative models is taken as a systematic uncertainty. This uncertainty is less than 0.25%.

Table 1: The contributions to the systematic uncertainty of v_n in O+O collisions from different sources, as function of centrality. The contributions are expressed in percentages. Items 1–5 are common to all the methods used here (2PC, template-fit and cumulants). Item 6 is specific to the 2PC and template-fit methods. Item 7 is specific to the template-fit method. Item 8 is specific to the cumulant method. The uncertainties are shown for the integrated p_T interval of 0.5–5 GeV.

Source	harmonic order	0–40% [%]	40–70% [%]
1. MC closure	v_2-v_4	1	1
2. Track selection	v_2	0.5	0.5
	v_3	0.75	0.75
	v_4	1.5	1.5
3. Tracking efficiency	v_2-v_4	0.25	0.25
4. Centrality definition	v_2	0.2	0.2–0.6
	v_3	0.2–1.0	1–2
	v_4	0.2	0.2–0.6
5. Residual pileup	v_2-v_4	0.2	0.2
6. Event-mixing	v_2	0.25	0.25
	v_3	0.5	0.5
	v_4	1	1
7. Peripheral reference	v_2	0.5	0.5–3
	v_3	0.75–3.5	3.5–12
	v_4	1.0–4.5	4.5–20
8. Flattening procedure	v_2-v_3	0.25	0.25

4. **Centrality definition:** The centrality definitions used to classify the events into centrality percentiles have a $\sim 1\%$ (2%) uncertainty associated with them in the O+O (Ne+Ne) measurements. This arises from uncertainties in the fraction of the inelastic O+O and Ne+Ne cross-sections accepted by the triggers used in this analysis and is estimated from the Glauber fits to the ΣE_T^{FCal} distributions [5, 6]. The impact of this uncertainty on the v_n is evaluated by varying the ΣE_T^{FCal} thresholds that define the centrality intervals, re-evaluating the v_n , and assigning the observed variation as a systematic uncertainty. This uncertainty is negligible in most central collisions, and increases systematically for more peripheral collisions.
5. **Residual pileup:** Pileup events dilute the measured v_n as there are no correlations between independent collisions. The estimated residual pileup is at most 0.2% in any centrality or multiplicity interval considered in this paper. Because the maximum possible dilution cannot exceed the pileup rate, the entire residual pileup rate of 0.2% is conservatively assigned as a systematic uncertainty on the v_n .
6. **Event-mixing:** As mentioned before, the 2PC method uses event-mixing to account for detector acceptance effects. The nominal mixing matches events that are within a z_{vtx} separation of less than 20 mm. Alternate mixing criteria, where the matching is restricted to within 10 mm and relaxed to 200 mm are used, and the maximum variation in the results is included as a systematic uncertainty. This uncertainty is of order 1% and only affects the 2PC and template-fit measurements.

7. **Peripheral reference:** For the centrality-dependent measurements, the nominal template-fit procedure uses events more peripheral than 80% for building the peripheral reference $C^{\text{periph}}(\Delta\phi)$. For the multiplicity-dependent results, the peripheral references are built from events from the same collision system that have $N_{\text{ch}}^{\text{rec}}$ less than 20. For evaluating uncertainties associated with the assumptions made in the template fit analysis, the centrality and multiplicity dependence measurements are repeated with the peripheral reference built from 5.02 TeV pp events with $N_{\text{ch}}^{\text{rec}}$ less than 20, as was done in Ref. [7]. The difference between the results with this alternate choice of peripheral reference are included as a systematic uncertainty. This uncertainty is relevant only for the template-fit method.
8. **Flattening procedure:** The cumulant measurements use a flattening procedure to remove detector non-uniformities in ϕ [46]. As a conservative estimate of the systematic related to the flattening procedure, the measurements were repeated with the flattening removed, and the resulting variations of $\sim 0.25\%$ are included as a systematic uncertainty on the $v_n\{4\}$.

Table 1 summarizes the final systematic uncertainties for the integrated p_{T} interval of 0.5–5.0 GeV in the O+O measurements. Except for the uncertainties related to the peripheral reference and centrality definition, all other uncertainties are conservatively taken to be constant and sufficiently large to cover the variations across all centrality (or multiplicity) and p_{T} intervals studied here. The dominant uncertainties are the uncertainties related to the MC-closure and the peripheral reference variation. For Ne+Ne, the assigned uncertainties are taken to be the same as for O+O, with values chosen large enough to cover both systems, except for the centrality-definition uncertainty, which is about twice as large. These individual uncertainties are added in quadrature to obtain total uncertainties. For ratios of the Ne+Ne to O+O v_n measurements, all sources of systematic uncertainty are treated as correlated, with the exception of the residual pileup. The latter is not considered correlated, since pileup rates can differ between the two systems due to their distinct running conditions.

6 Results

Figure 5 shows the measured $v_n^{\text{sub}}\{2\}$ and the $v_n^{2\text{PC}}\{2\}$ as a function of p_{T}^b in O+O and Ne+Ne collisions at $\sqrt{s_{\text{NN}}} = 5.36$ TeV. Comparing the template fit v_n and the 2PC v_n , a large potential non-flow contribution is observed in the 2PC results, particularly at higher p_{T}^b and in peripheral collisions. The v_2 results exhibit a linear rise at low p_{T}^b , followed by a decrease in the range of 2–4 GeV for the 0–5% and 20–30% centrality intervals. This behavior is qualitatively similar to what is observed in other collision systems, from Pb+Pb to pp [6, 7, 22, 64]. A hierarchy is also observed, with the magnitude of v_n decreasing as n increases, in agreement with observations from other systems. In peripheral events (50–60% centrality), or at p_{T} above approximately 3 GeV, significant differences are observed between the 2PC and template-fit measurements, highlighting the impact of non-flow background correlations on the 2PC method.

The hydrodynamic response to the initial geometry is best studied as a function of variables that are directly impacted by it, chiefly charged-particle multiplicity and centrality. Figure 6a shows $v_n^{\text{sub}}\{2\}$ and $v_n\{4\}$ for charged particles with $0.5 < p_{\text{T}} < 5.0$ GeV in O+O and Ne+Ne collisions as a function of N_{ch} . In both systems, $v_n^{\text{sub}}\{2\}$ is observed to exceed $v_n\{4\}$ for the same harmonic order n , which reflects the positive contribution of fluctuations to $v_n\{2\}$ as described in Eq. 13. The difference between the $v_2\{2\}$ and $v_2\{4\}$ increases with increasing multiplicity indicating the increased role of the fluctuation component, Δ_2^2 in Eq. 13, relative to the mean geometry component, \bar{x}_2^2 , going from peripheral to central collisions.

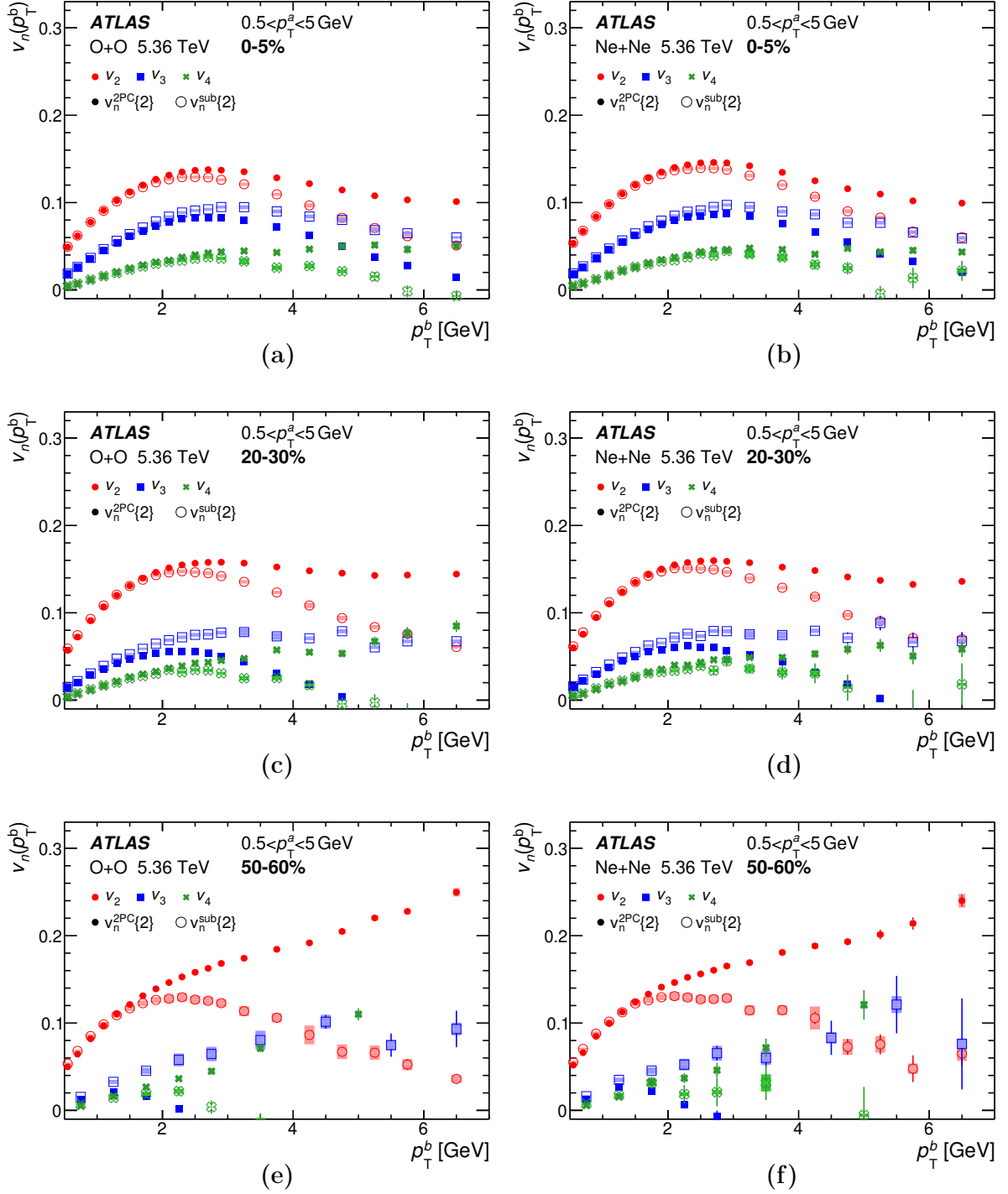


Figure 5: The p_T^b dependence of the $v_n^{2PC}\{2\}$ and $v_n^{\text{sub}}\{2\}$ in the (a, c, e) O+O and (b, d, f) Ne+Ne collisions, for the (a, b) 0–5%, (c, d) 20–30% and (e, f) 50–60% centrality intervals. The solid and open points show the results obtained using the 2PC and the template-fit methods, respectively. The vertical lines and vertical bars indicate statistical and systematic uncertainties, respectively.

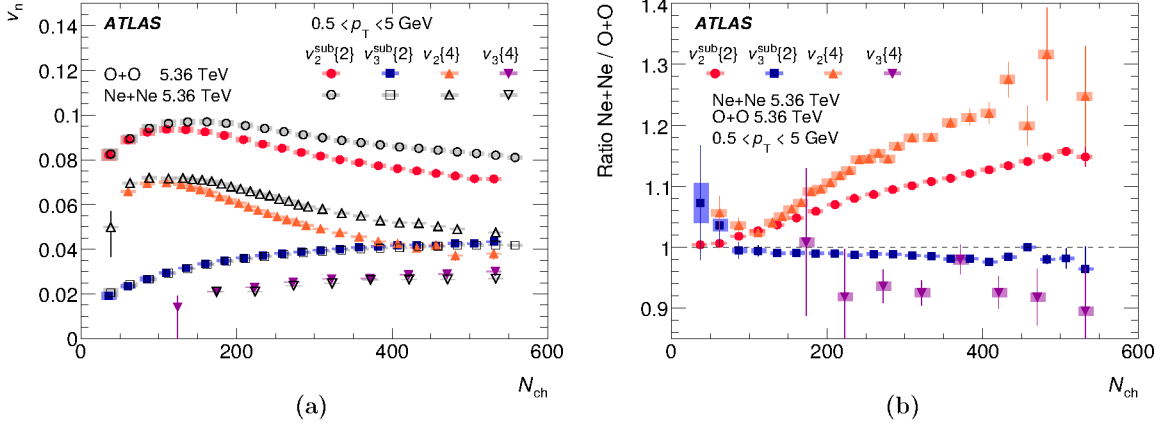


Figure 6: (a) Flow harmonics $v_n^{sub}\{2\}$ and $v_n\{4\}$ for the elliptic and triangular moments in O+O collisions (colored solid markers) and Ne+Ne collisions (open black markers) at $\sqrt{s_{NN}} = 5.36$ TeV, shown as a function of N_{ch} . The Ne+Ne points are slightly displaced along the horizontal axis for visual clarity. (b) Ratios of the flow coefficients in Ne+Ne to those in O+O collisions, corresponding to the results in panel (a). Ratios are shown only for the 0–50% centrality range to suppress large statistical fluctuations in more peripheral intervals. The vertical lines and vertical bars indicate statistical and systematic uncertainties, respectively. For the ratios, systematic uncertainties correlated between the O+O and Ne+Ne measurements largely cancel.

To compare O+O and Ne+Ne v_n directly, their ratio is plotted in Figure 6b. For the elliptic flow, v_2 , there is a growing enhancement in Ne+Ne collisions with increasing N_{ch} . These can be attributed to centrality-dependent changes in the overlap geometry and neon’s deformed nuclear structure, which will be further discussed below, in the context of the centrality-dependent results. Conversely, there is a striking similarity of $v_3^{sub}\{2\}$ in O+O and Ne+Ne collisions as a function of N_{ch} . This provides evidence that the hydrodynamic response and the fluctuation-driven component of the initial-state geometry depend primarily on the particle density. The residual difference and systematically smaller $v_3\{4\}$ may be an indication of differing average triangularity in the initial-state geometry.

To compare the geometric aspects of oxygen and neon nuclei, Figure 7a presents the results as a function of collision centrality, using the same kinematic requirements and analysis techniques as in Figure 6. Although light-ion collisions have large initial-state geometry fluctuations and possibly nuclear deformations, a large contribution to the elliptic geometry is the event-averaged lenticular shape. This event-averaged shape depends on the ratio of the impact parameter to the nuclear radius, which is highly correlated with centrality. For this reason there is closer agreement observed between O+O and Ne+Ne as a function of centrality than N_{ch} . Thus, the ratio of Ne+Ne to O+O flow harmonics is calculated as a function of centrality, in an attempt to remove these average geometric effects. This ratio is shown in Figure 7b. For both $v_2^{sub}\{2\}$ and $v_2\{4\}$, a relatively centrality-independent ratio is observed for centralities more peripheral than 10%, as opposed to the ratios as a function of N_{ch} (Figure 6b). However, over the 0–10% centrality interval, a growing enhancement appears toward the most central collisions. This enhancement is more pronounced in the four-particle cumulant measurement. A similar behavior is observed for the triangular moment: the $v_3^{sub}\{2\}$ ratio exhibits a sudden decrease in the 0–10% centrality interval. For the $v_3\{4\}$ ratio, the statistical uncertainties are too large to observe clear trends.

Figure 8 shows the comparisons of the measured $v_n^{sub}\{2\}$ with the template-fit method to $v_n\{2\}$ calculations from the model described in Ref. [78]. The model combines the Projected Generator Coordinate Method (PGCM), an *ab initio* nuclear structure model for oxygen and neon, with the IPGlasma framework,

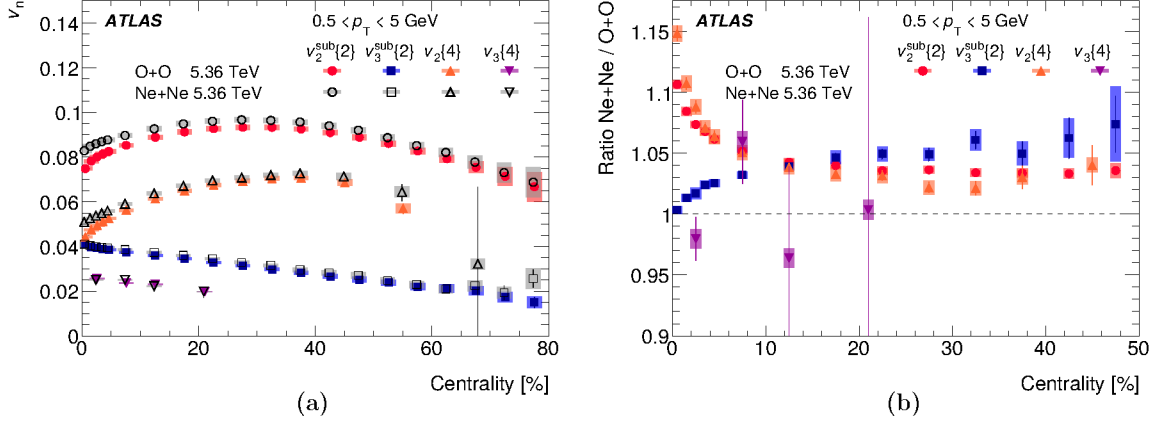


Figure 7: (a) Flow harmonics $v_n^{\text{sub}\{2\}}$ and $v_n\{4\}$ for the elliptic and triangular moments in O+O collisions (colored solid markers) and Ne+Ne collisions (open black markers) at $\sqrt{s_{NN}} = 5.36$ TeV, shown as a function of centrality. (b) Ratios of the flow coefficients in Ne+Ne to those in O+O collisions, corresponding to the results in panel (a). The vertical lines and vertical bars indicate statistical and systematic uncertainties, respectively. For the ratios, systematic uncertainties correlated between the O+O and Ne+Ne measurements largely cancel.

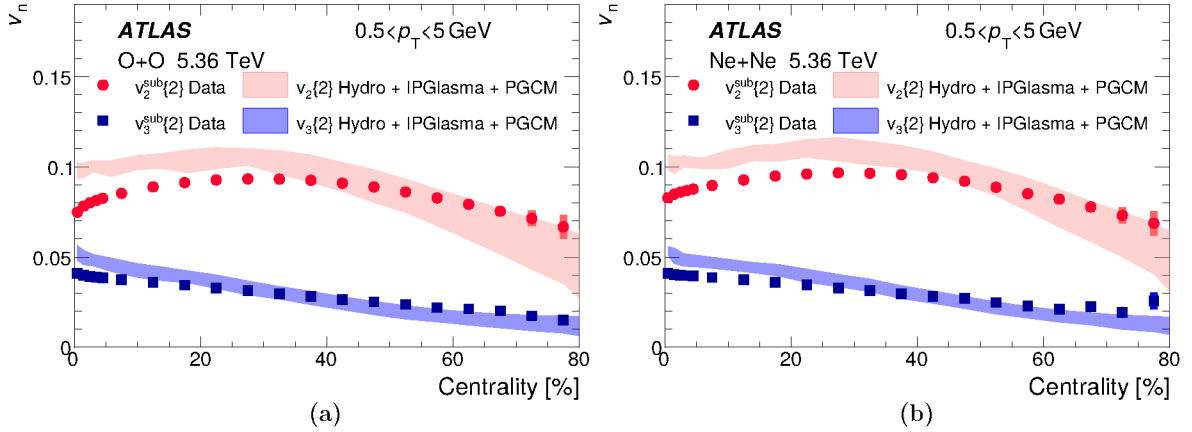


Figure 8: Comparison of $v_2^{\text{sub}\{2\}}$ and $v_3^{\text{sub}\{2\}}$ with theory calculations from the model described in Ref. [78], for (a) O+O and (b) Ne+Ne collisions. The theory calculations are labeled as “Hydro+IPGlasma+PGCM.” For the data, the vertical lines and vertical bars indicate statistical and systematic uncertainties, respectively. The data uncertainties are sometimes too small to be visible. The bands for the theory calculations represent the combined statistical and systematic uncertainties.

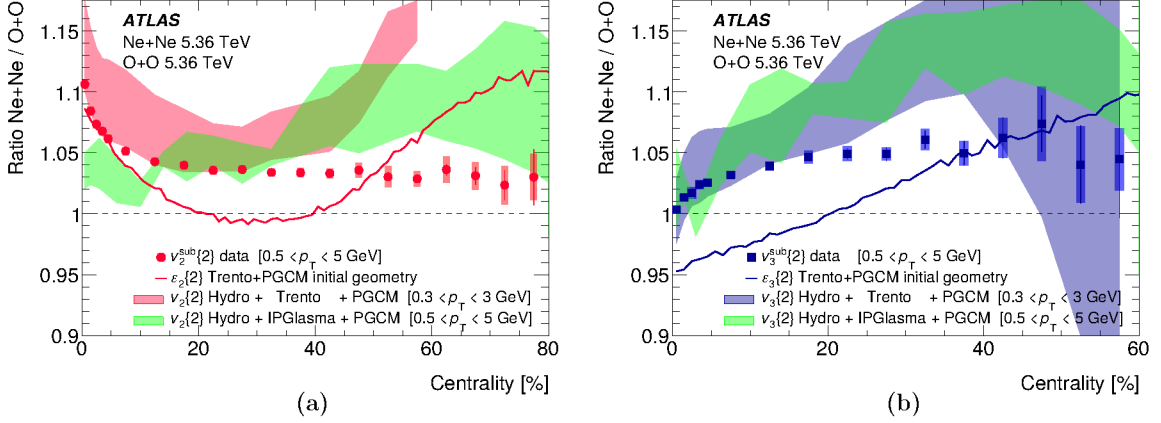


Figure 9: Comparison of the measurements to theory predictions for the ratio of (a) $v_2\{2\}$ and (b) $v_3\{2\}$ between Ne+Ne and O+O. The $v_n\{2\}$ in the data are obtained from the template fit method. The Hydro+Trento+PGCM theory is taken from Ref. [44] and the Hydro+IPGlasma+PGCM is an extension of Ref. [78]. The ratios are also shown for the eccentricities, a quantification of the elliptic (ϵ_2) or triangular (ϵ_3) shape of the initial-state energy density, using the Trento+PGCM model. For the data, the vertical lines and vertical bars indicate statistical and systematic uncertainties, respectively. The bands for the theory calculations represent combined statistical and systematic uncertainties.

including JIMWLK evolution [79], to calculate the initial energy densities of the colliding nuclei. These energy densities are then evolved using viscous relativistic hydrodynamics (MUSIC [80]). Finally, a hadronic afterburner (UrQMD [81, 82]) is applied to obtain the v_n . The centrality is determined with the charged-particle multiplicity at mid-rapidity. The model is denoted as ‘‘Hydro+IPGlasma+PGCM’’ in the figure. The calculations overpredict the v_2 and v_3 in central collisions, but are consistent within uncertainties with the measurements in more peripheral collisions. These comparisons indicate that the light-ion measurements can provide additional constraints for tuning existing theory models.

Figure 9 shows comparisons of the measured ratios for $v_n\{2\}$ between Ne+Ne and O+O collisions, to two theory calculations. The first is the Hydro+IPGlasma+PGCM model introduced above. The second model is described in Ref. [78] and uses PGCM [83] to determine the nuclear configurations of both oxygen and neon, which are then collided, generating initial-state energy densities with the Trento model [84]. These events are then simulated with the Trajectum hydrodynamic framework [85, 86]. This model is labeled as ‘‘Hydro+Trento+PGCM.’’ The model uses mid-rapidity multiplicity to determine centrality. The fluctuations in the model calculations are statistical in nature. The measured $v_n\{2\}$ are obtained from the template-fit method. The event-averaged eccentricity, a quantification of the magnitude of ellipticity ϵ_2 and the triangularity ϵ_3 , ratios for a particular Trento parameter set [87] are also shown in Figure 9. The data and Hydro+Trento+PGCM model agree quantitatively, at the edge of the theory uncertainties, in $v_2\{2\}$ in central collisions. The large enhancement in the $v_2\{2\}$ ratio in the 0–10% central collisions observed in the hydrodynamic theory calculation is attributed to the elongated shape of the neon nucleus, leading to an elliptic initial-state, as can be seen in the $\epsilon_2\{2\}$ ratio. The qualitative behavior of the measured $v_2\{2\}$ ratio supports this picture. The Hydro+IPGlasma+PGCM calculation does not capture this proposed geometrically driven behavior in the 0–10% centrality range. This inability to capture geometric effects in the latter calculation, is also reflected in the data-theory disagreement in Figure 8. In both Ne+Ne and O+O collisions, the measured v_2 decreases in the most central collisions, but this trend is not predicted by the model. Because the nuclear structure model PGCM can capture

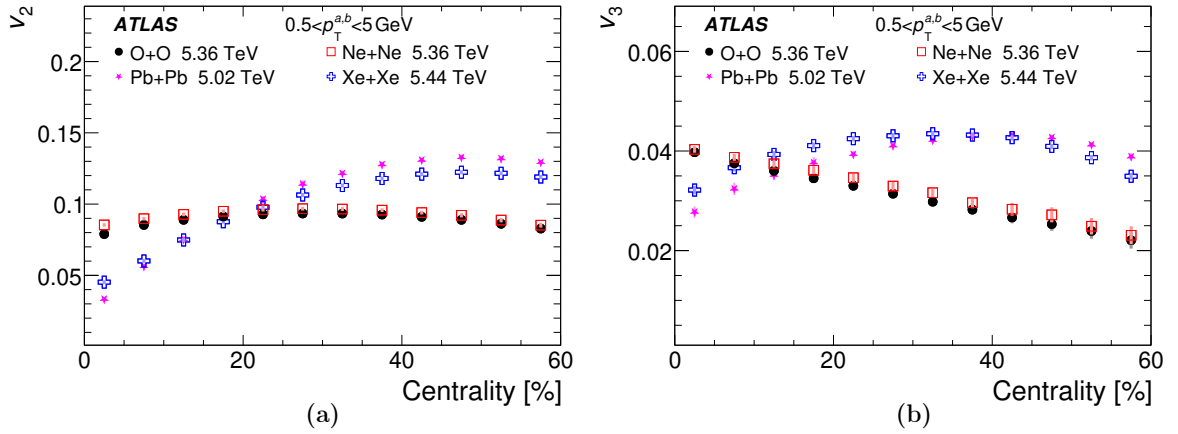


Figure 10: Comparisons of the (a) v_2 and (b) v_3 measured by the template-fit method in O+O and Ne+Ne collisions with prior measurements in Xe+Xe and Pb+Pb collisions from Ref. [7], as a function of centrality. The Xe+Xe and Pb+Pb results are obtained with the 2PC method. The plots are for $0.5 < p_T^{a,b} < 5$ GeV. The vertical lines and vertical bars indicate statistical and systematic uncertainties, respectively.

geometric effects, as seen in the Hydro+Trento+PGCM v_2 ratio agreement with the data, the disagreement with the Hydro+IPGlasma+PGCM calculations could arise in the IPGlasma-with-JIMWLK portion of the initial-state model. It has been noted [78] that this aspect of the model creates large multiplicity fluctuations, reducing the correlation between the centrality and impact parameter. This can lead to the inability of the model to reproduce the centrality dependence trends observed in Figures 8 and 9. For both model comparisons presented in Figure 9, the experimental uncertainties are significantly smaller than the statistical and systematic uncertainties associated with the model calculations. Consequently, further refinement of the theory predictions is required to fully capitalize on the precision of the data.

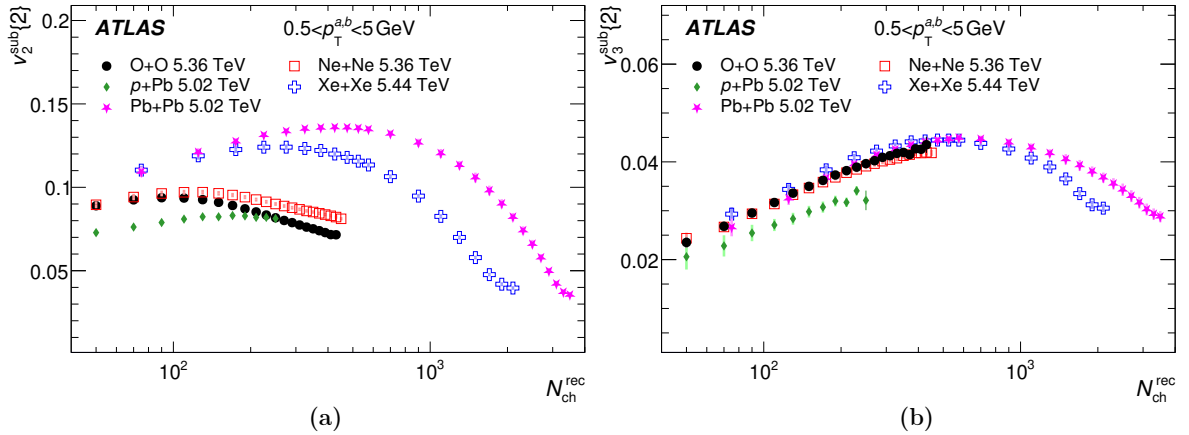


Figure 11: Comparison of the (a) $v_2^{\text{sub}}\{2\}$ and the (b) $v_3^{\text{sub}}\{2\}$ measured in O+O and Ne+Ne collisions with prior measurements in p+Pb, Xe+Xe and Pb+Pb collisions from Ref. [7], as a function of the reconstructed charged-particle multiplicity ($N_{\text{ch}}^{\text{rec}}$). The vertical lines and vertical bars indicate statistical and systematic uncertainties, respectively, and are often too small to be visible.

Figure 10 shows comparisons of $v_n^{\text{sub}}\{2\}$ measurements in O+O and Ne+Ne collisions to previous $v_n^{2\text{PC}}\{2\}$ results in Xe+Xe collisions at 5.44 TeV and Pb+Pb collisions at 5.02 TeV from Ref. [7], as a function of centrality. In heavy-ion collisions, the v_2 is largely determined by the elliptic geometry of the nuclear

overlap, which is strongly correlated with centrality and thus drives the pronounced centrality dependence of v_2 . By contrast, the v_2 in light-ion systems shows a much weaker centrality dependence, highlighting the dominant role of EbE geometry fluctuations in these systems. The v_3 in Xe+Xe and Pb+Pb collisions exhibits a non-monotonic centrality dependence, increasing from central to mid-central collisions and then decreasing. In light-ion collisions, however, the v_3 decreases monotonically from central to peripheral events. Figure 11 shows similar comparisons of $v_n^{\text{sub}}\{2\}$ as a function of reconstructed charged-particle multiplicity, $N_{\text{ch}}^{\text{rec}}$, including results from p +Pb collisions at 5.02 TeV. The most notable feature is the very similar magnitude and $N_{\text{ch}}^{\text{rec}}$ dependence of v_3 in both light- and heavy-ion collisions. This stands in stark contrast to the centrality dependence of v_3 , which differs strongly between light- and heavy-ion systems. Interestingly, the p +Pb v_3 is also comparable in magnitude to the light- and heavy-ion results at the same multiplicities and shows a qualitatively similar multiplicity dependence.

7 Conclusion

This paper presents the first comprehensive measurements of anisotropic flow coefficients v_n ($n = 2-4$) in $\sqrt{s_{\text{NN}}} = 5.36$ TeV O+O and Ne+Ne collisions with the ATLAS detector at the LHC. The results are obtained using two-particle (template-fit) and four-particle (subevent cumulant) methods, and explore the dependence of v_n on transverse momentum, multiplicity, and centrality in each system. To isolate the role of initial-state geometry, ratios of Ne+Ne to O+O v_n are also studied.

The measurements reveal a characteristic rise and fall of v_2 with p_{T} , peaking at 2–4 GeV, large event-by-event fluctuations in the most central collisions, and a clear hierarchy $v_2 > v_3 > v_4$, consistent with hydrodynamic expectations. Multiplicity- and centrality-dependent ratios of $v_2\{2\}$ and $v_2\{4\}$, taken between Ne+Ne and O+O collisions, reveal a marked enhancement in Ne+Ne, consistent with the elongated nuclear shape of neon and reproduced by model calculations. For v_2 , the four-particle cumulant ratios provide the greatest sensitivity to these geometric effects. For $v_3\{2\}$, the Ne+Ne values exceed those in O+O for most centralities, except in the 0–1% most central events where they are comparable. Detailed comparisons of these measurements with model predictions may also provide new sensitivity to α -clustering in the oxygen nucleus [88]. Compared to heavy-ion collisions, the v_2 in light-ions shows a much weaker centrality dependence, underscoring the enhanced role of EbE geometry fluctuations in these systems. As a function of event multiplicity, the v_3 values in O+O and Ne+Ne are quantitatively similar to those measured in Pb+Pb, Xe+Xe, and p +Pb collisions.

These light-ion results offer stringent constraints on hydrodynamic models incorporating *ab initio* nuclear-structure inputs, and provide unique insight into how nucleon-level geometry influences collective flow in small QGP droplets. Future comparisons with detailed model calculations could further constrain key medium and geometric properties, including the temperature dependence of η/s , the role of the pre-hydrodynamic phase, mechanisms of energy deposition in hadronic collisions, and other initial-state effects.

Acknowledgements

We thank CERN for the very successful operation of the LHC and its injectors, as well as the support staff at CERN and at our institutions worldwide without whom ATLAS could not be operated efficiently.

The crucial computing support from all WLCG partners is acknowledged gratefully, in particular from CERN, the ATLAS Tier-1 facilities at TRIUMF/SFU (Canada), NDGF (Denmark, Norway, Sweden), CC-IN2P3 (France), KIT/GridKA (Germany), INFN-CNAF (Italy), NL-T1 (Netherlands), PIC (Spain), RAL (UK) and BNL (USA), the Tier-2 facilities worldwide and large non-WLCG resource providers. Major contributors of computing resources are listed in Ref. [89].

We gratefully acknowledge the support of ANPCyT, Argentina; YerPhI, Armenia; ARC, Australia; BMWF and FWF, Austria; ANAS, Azerbaijan; CNPq and FAPESP, Brazil; NSERC, NRC and CFI, Canada; CERN; ANID, Chile; CAS, MOST and NSFC, China; Minciencias, Colombia; MEYS CR, Czech Republic; DNRF and DNSRC, Denmark; IN2P3-CNRS and CEA-DRF/IRFU, France; SRNSFG, Georgia; BMFTR, HGF and MPG, Germany; GSRI, Greece; RGC and Hong Kong SAR, China; ICHEP and Academy of Sciences and Humanities, Israel; INFN, Italy; MEXT and JSPS, Japan; CNRST, Morocco; NWO, Netherlands; RCN, Norway; MNiSW, Poland; FCT, Portugal; MNE/IFA, Romania; MSTDI, Serbia; MSSR, Slovakia; ARIS and MVZI, Slovenia; DSI/NRF, South Africa; MICIU/AEI, Spain; SRC and Wallenberg Foundation, Sweden; SERI, SNSF and Cantons of Bern and Geneva, Switzerland; NSTC, Taipei; TENMAK, Türkiye; STFC/UKRI, United Kingdom; DOE and NSF, United States of America.

Individual groups and members have received support from BCKDF, CANARIE, CRC and DRAC, Canada; CERN-CZ, FORTE and PRIMUS, Czech Republic; COST, ERC, ERDF, Horizon 2020, ICSC-NextGenerationEU and Marie Skłodowska-Curie Actions, European Union; Investissements d’Avenir Labex, Investissements d’Avenir Idex and ANR, France; DFG and AvH Foundation, Germany; Herakleitos, Thales and Aristeia programmes co-financed by EU-ESF and the Greek NSRF, Greece; BSF-NSF and MINERVA, Israel; NCN and NAWA, Poland; La Caixa Banking Foundation, CERCA Programme Generalitat de Catalunya and PROMETEO and GenT Programmes Generalitat Valenciana, Spain; Göran Gustafssons Stiftelse, Sweden; The Royal Society and Leverhulme Trust, United Kingdom.

In addition, individual members wish to acknowledge support from CERN: European Organization for Nuclear Research (CERN DOCT); Chile: Agencia Nacional de Investigación y Desarrollo (FONDECYT 1230812, FONDECYT 1240864, Fondecyt 3240661); China: Chinese Ministry of Science and Technology (MOST-2023YFA1605700, MOST-2023YFA1609300), National Natural Science Foundation of China (NSFC - 12175119, NSFC 12275265); Czech Republic: Czech Science Foundation (GACR - 24-11373S), Ministry of Education Youth and Sports (ERC-CZ-LL2327, FORTE CZ.02.01.01/00/22_008/0004632), PRIMUS Research Programme (PRIMUS/21/SCI/017); EU: H2020 European Research Council (ERC - 101002463); European Union: European Research Council (BARD No. 101116429, ERC - 948254, ERC 101089007), European Regional Development Fund (SMASH COFUND 101081355, SLO ERDF), European Union, Future Artificial Intelligence Research (FAIR-NextGenerationEU PE00000013), Italian Center for High Performance Computing, Big Data and Quantum Computing (ICSC, NextGenerationEU); France: Agence Nationale de la Recherche (ANR-21-CE31-0022, ANR-22-EDIR-0002); Germany: Deutsche Forschungsgemeinschaft (DFG - 469666862, DFG - CR 312/5-2); China: Research Grants Council (GRF); Italy: Istituto Nazionale di Fisica Nucleare (ICSC, NextGenerationEU), Ministero dell’Università e della Ricerca (NextGenEU I53D23001490006 M4C2.1.1, NextGenEU I53D23000820006 M4C2.1.1, NextGenEU I53D23001490006 M4C2.1.1, SOE2024_0000023); Japan: Japan Society for the Promotion of Science (JSPS KAKENHI JP22H01227, JSPS KAKENHI JP22H04944, JSPS KAKENHI JP22KK0227, JSPS KAKENHI JP24K23939, JSPS KAKENHI JP24KK0251, JSPS KAKENHI JP25H00650, JSPS KAKENHI JP25H01291, JSPS KAKENHI JP25K01023); Norway: Research Council of Norway (RCN-314472); Poland: Ministry of Science and Higher Education (IDUB AGH, POB8, D4 no 9722), Polish National Science Centre (NCN 2021/42/E/ST2/00350, NCN OPUS 2023/51/B/ST2/02507,

NCN UMO-2019/34/E/ST2/00393, UMO-2022/47/O/ST2/00148, UMO-2023/49/B/ST2/04085, UMO-2023/51/B/ST2/00920, UMO-2024/53/N/ST2/00869); Portugal: Foundation for Science and Technology (FCT); Spain: Ministry of Science and Innovation (MCIN & NextGenEU PCI2022-135018-2, MICIN & FEDER PID2021-125273NB, RYC2019-028510-I, RYC2020-030254-I, RYC2021-031273-I, RYC2022-038164-I); Sweden: Carl Trygger Foundation (Carl Trygger Foundation CTS 22:2312), Swedish Research Council (Swedish Research Council 2023-04654, VR 2021-03651, VR 2022-03845, VR 2022-04683, VR 2023-03403, VR 2024-05451), Knut and Alice Wallenberg Foundation (KAW 2018.0458, KAW 2022.0358, KAW 2023.0366); Switzerland: Swiss National Science Foundation (SNSF - PCEFP2_194658); United Kingdom: Royal Society (NIF-R1-231091); United States of America: U.S. Department of Energy (ECA DE-AC02-76SF00515), Neubauer Family Foundation.

References

- [1] STAR Collaboration, *Experimental and theoretical challenges in the search for the quark gluon plasma: The STAR Collaboration's critical assessment of the evidence from RHIC collisions*, *Nucl. Phys. A* **757** (2005) 102, arXiv: [nucl-ex/0501009](#) [[nucl-ex](#)].
- [2] PHOBOS Collaboration, *The PHOBOS perspective on discoveries at RHIC*, *Nucl. Phys. A* **757** (2005) 28, arXiv: [nucl-ex/0410022](#) [[nucl-ex](#)].
- [3] PHENIX Collaboration, *Formation of dense partonic matter in relativistic nucleus-nucleus collisions at RHIC: Experimental evaluation by the PHENIX Collaboration*, *Nucl. Phys. A* **757** (2005) 184, arXiv: [nucl-ex/0410003](#) [[nucl-ex](#)].
- [4] BRAHMS Collaboration, *Quark–gluon plasma and color glass condensate at RHIC? The perspective from the BRAHMS experiment*, *Nucl. Phys. A* **757** (2005) 1, arXiv: [nucl-ex/0410020](#) [[nucl-ex](#)].
- [5] ATLAS Collaboration, *Measurement of the pseudorapidity and transverse momentum dependence of the elliptic flow of charged particles in lead–lead collisions at $\sqrt{s_{NN}} = 2.76$ TeV with the ATLAS detector*, *Phys. Lett. B* **707** (2012) 330, arXiv: [1108.6018](#) [[hep-ex](#)].
- [6] ATLAS Collaboration, *Measurement of the azimuthal anisotropy of charged particles produced in $\sqrt{s_{NN}} = 5.02$ TeV Pb+Pb collisions with the ATLAS detector*, *Eur. Phys. J. C* **78** (2018) 997, arXiv: [1808.03951](#) [[nucl-ex](#)].
- [7] ATLAS Collaboration, *Measurement of the azimuthal anisotropy of charged-particle production in Xe+Xe collisions at $\sqrt{s_{NN}} = 5.44$ TeV with the ATLAS detector*, *Phys. Rev. C* **101** (2020) 024906, arXiv: [1911.04812](#) [[nucl-ex](#)].
- [8] CMS Collaboration, *Measurement of the elliptic anisotropy of charged particles produced in PbPb collisions at $\sqrt{s_{NN}} = 2.76$ TeV*, *Phys. Rev. C* **87** (2013) 014902, arXiv: [1204.1409](#) [[hep-ex](#)].
- [9] CMS Collaboration, *Charged-particle angular correlations in XeXe collisions at $\sqrt{s_{NN}} = 5.44$ TeV*, *Phys. Rev. C* **100** (2019) 044902, arXiv: [1901.07997](#) [[hep-ex](#)].
- [10] ALICE Collaboration, *Elliptic Flow of Charged Particles in Pb-Pb Collisions at $\sqrt{s_{NN}} = 2.76$ TeV*, *Phys. Rev. Lett.* **105** (2010) 252302, arXiv: [1011.3914](#) [[nucl-ex](#)].
- [11] ALICE Collaboration, *Anisotropic flow in Xe-Xe collisions at $\sqrt{s_{NN}} = 5.44$ TeV*, *Phys. Lett. B* **784** (2018) 82, arXiv: [1805.01832](#) [[nucl-ex](#)].

- [12] J.-Y. Ollitrault, *Anisotropy as a signature of transverse collective flow*, *Phys. Rev. D* **46** (1992) 229.
- [13] W. Busza, K. Rajagopal, and W. van der Schee, *Heavy Ion Collisions: The Big Picture, and the Big Questions*, *Ann. Rev. Nucl. Part. Sci.* **68** (2018) 339, arXiv: [1802.04801 \[hep-ph\]](#).
- [14] B. H. Alver, C. Gombeaud, M. Luzum, and J.-Y. Ollitrault, *Triangular flow in hydrodynamics and transport theory*, *Phys. Rev. C* **82** (2010) 034913, arXiv: [1007.5469 \[nucl-th\]](#).
- [15] ATLAS Collaboration, *Measurement of the azimuthal anisotropy for charged particle production in $\sqrt{s_{NN}} = 2.76$ TeV lead–lead collisions with the ATLAS detector*, *Phys. Rev. C* **86** (2012) 014907, arXiv: [1203.3087 \[hep-ex\]](#).
- [16] ATLAS Collaboration, *Measurement of the distributions of event-by-event flow harmonics in lead–lead collisions at $\sqrt{s_{NN}} = 2.76$ TeV with the ATLAS detector at the LHC*, *JHEP* **11** (2013) 183, arXiv: [1305.2942 \[hep-ex\]](#).
- [17] CMS Collaboration, *Non-Gaussian elliptic-flow fluctuations in PbPb collisions at $\sqrt{s_{NN}} = 5.02$ TeV*, *Phys. Lett. B* **789** (2019) 643, arXiv: [1711.05594 \[hep-ex\]](#).
- [18] ALICE Collaboration, *Energy dependence and fluctuations of anisotropic flow in Pb-Pb collisions at $\sqrt{s_{NN}} = 5.02$ and 2.76 TeV*, *JHEP* **07** (2018) 103, arXiv: [1804.02944 \[nucl-ex\]](#).
- [19] ATLAS Collaboration, *Measurement of event-plane correlations in $\sqrt{s_{NN}} = 2.76$ TeV lead–lead collisions with the ATLAS detector*, *Phys. Rev. C* **90** (2014) 024905, arXiv: [1403.0489 \[hep-ex\]](#).
- [20] ALICE Collaboration, *Long-range angular correlations on the near and away side in p-Pb collisions at $\sqrt{s_{NN}} = 5.02$ TeV*, *Phys. Lett. B* **719** (2013) 29, arXiv: [1212.2001 \[nucl-ex\]](#).
- [21] ATLAS Collaboration, *Observation of Associated Near-Side and Away-Side Long-Range Correlations in $\sqrt{s_{NN}} = 5.02$ TeV Proton–Lead Collisions with the ATLAS Detector*, *Phys. Rev. Lett.* **110** (2013) 182302, arXiv: [1212.5198 \[hep-ex\]](#).
- [22] ATLAS Collaboration, *Observation of Long-Range Elliptic Azimuthal Anisotropies in $\sqrt{s} = 13$ and 2.76 TeV pp Collisions with the ATLAS Detector*, *Phys. Rev. Lett.* **116** (2016) 172301, arXiv: [1509.04776 \[hep-ex\]](#).
- [23] CMS Collaboration, *Evidence for collectivity in pp collisions at the LHC*, *Phys. Lett. B* **765** (2017) 193, arXiv: [1606.06198 \[hep-ex\]](#).
- [24] STAR Collaboration, *Measurement of flow coefficients in high-multiplicity p + Au, d + Au, and $^3\text{He} + \text{Au}$ collisions at $\sqrt{s_{NN}} = 200$ GeV*, *Phys. Rev. C* **110** (2024) 064902, arXiv: [2312.07464 \[nucl-ex\]](#).
- [25] STAR Collaboration, *Measurements of the Elliptic and Triangular Azimuthal Anisotropies in Central $^3\text{He} + \text{Au}$, d + Au and p + Au Collisions at $\sqrt{s_{NN}} = 200$ GeV*, *Phys. Rev. Lett.* **130** (2023) 242301, arXiv: [2210.11352 \[nucl-ex\]](#).
- [26] PHENIX Collaboration, *Kinematic dependence of azimuthal anisotropies in p + Au, d + Au, and $^3\text{He} + \text{Au}$ at $\sqrt{s_{NN}} = 200$ GeV*, *Phys. Rev. C* **105** (2022) 024901, arXiv: [2107.06634 \[hep-ex\]](#).
- [27] PHENIX Collaboration, *Creation of quark–gluon plasma droplets with three distinct geometries*, *Nature Phys.* **15** (2019) 214, arXiv: [1805.02973 \[nucl-ex\]](#).

- [28] R. D. Weller and P. Romatschke, *One fluid to rule them all: Viscous hydrodynamic description of event-by-event central $p+p$, $p+Pb$ and $Pb+Pb$ collisions at $\sqrt{s} = 5.02$ TeV*, *Phys. Lett. B* **774** (2017) 351, arXiv: 1701.07145 [nucl-th].
- [29] A. Bzdak, B. Schenke, P. Tribedy, and R. Venugopalan, *Initial-state geometry and the role of hydrodynamics in proton-proton, proton-nucleus, and deuteron-nucleus collisions*, *Phys. Rev. C* **87** (2013) 064906, arXiv: 1304.3403 [nucl-th].
- [30] H. Mäntysaari and B. Schenke, *Evidence of strong proton shape fluctuations from incoherent diffraction*, *Phys. Rev. Lett.* **117** (2016) 052301, arXiv: 1603.04349 [hep-ph].
- [31] G. Giacalone, J. Noronha-Hostler, M. Luzum, and J.-Y. Ollitrault, *Hydrodynamic predictions for 5.44 TeV Xe+Xe collisions*, *Phys. Rev. C* **97** (2018) 034904, arXiv: 1711.08499 [nucl-th].
- [32] V. E. Ambruş, S. Schlichting, and C. Werthmann, *Collective dynamics in heavy and light-ion collisions. II. Determining the origin of collective behavior in high-energy collisions*, *Phys. Rev. D* **111** (2025) 054025, arXiv: 2411.19709 [hep-ph].
- [33] J. Noronha, B. Schenke, C. Shen, and W. Zhao, *Progress and challenges in small systems*, *Int. J. Mod. Phys. E* **33** (2024) 2430005, arXiv: 2401.09208 [nucl-th].
- [34] Z. Citron et al., *Future physics opportunities for high-density QCD at the LHC with heavy-ion and proton beams*, *CERN Yellow Rep. Monogr.* **7** (2019) 1159, ed. by A. Dainese et al., arXiv: 1812.06772 [hep-ph].
- [35] J. Jia et al., *Imaging the initial condition of heavy-ion collisions and nuclear structure across the nuclide chart*, *Nucl. Sci. Tech.* **35** (2024) 220, arXiv: 2209.11042 [nucl-ex].
- [36] STAR Collaboration, *Search for the chiral magnetic effect with isobar collisions at $\sqrt{s_{NN}}=200$ GeV by the STAR Collaboration at the BNL Relativistic Heavy Ion Collider*, *Phys. Rev. C* **105** (2022) 014901, arXiv: 2109.00131 [nucl-ex].
- [37] G. Giacalone, J. Jia, and V. Somà, *Accessing the shape of atomic nuclei with relativistic collisions of isobars*, *Phys. Rev. C* **104** (2021) L041903, arXiv: 2102.08158 [nucl-th].
- [38] ATLAS Collaboration, *Correlations between flow and transverse momentum in Xe+Xe and Pb+Pb collisions at the LHC with the ATLAS detector: A probe of the heavy-ion initial state and nuclear deformation*, *Phys. Rev. C* **107** (2023) 054910, arXiv: 2205.00039 [nucl-ex].
- [39] ALICE Collaboration, *Exploring nuclear structure with multiparticle azimuthal correlations at the LHC*, (2024), arXiv: 2409.04343 [nucl-ex].
- [40] STAR Collaboration, *Imaging shapes of atomic nuclei in high-energy nuclear collisions*, *Nature* **635** (2024) 67, arXiv: 2401.06625 [nucl-ex].
- [41] H. Hergert, *A Guided Tour of ab initio Nuclear Many-Body Theory*, *Front. in Phys.* **8** (2020) 379, arXiv: 2008.05061 [nucl-th].
- [42] K. Wei, Y.-L. Ye, and Z.-H. Yang, *Clustering in nuclei: progress and perspectives*, *Nucl. Sci. Tech.* **35** (2024) 216.

- [43] J. Hiura, Y. Abe, S. Saitō, and O. Endō, *Alpha-Cluster plus ^{16}O -Core Model for ^{20}Ne and Neighboring Nuclei**, *Prog. Theo. Phys.* **42** (1969) 555.
- [44] G. Giacalone et al., *Exploiting ^{20}Ne Isotopes for Precision Characterizations of Collectivity in Small Systems*, *Phys. Rev. Lett.* **135** (2025) 012302, arXiv: 2402.05995 [nucl-th].
- [45] H.-C. Wang, S.-J. Li, L.-M. Liu, J. Xu, and Z.-Z. Ren, *Deformation probes for light nuclei in their collisions at relativistic energies*, *Phys. Rev. C* **110** (2024) 034909, arXiv: 2409.02452 [nucl-th].
- [46] ATLAS Collaboration, *Measurement of long-range multiparticle azimuthal correlations with the subevent cumulant method in pp and $p+Pb$ collisions with the ATLAS detector at the CERN Large Hadron Collider*, *Phys. Rev. C* **97** (2018) 024904, arXiv: 1708.03559 [hep-ex].
- [47] ATLAS Collaboration, *The ATLAS Experiment at the CERN Large Hadron Collider*, *JINST* **3** (2008) S08003.
- [48] ATLAS Collaboration, *The ATLAS experiment at the CERN Large Hadron Collider: a description of the detector configuration for Run 3*, *JINST* **19** (2024) P05063, arXiv: 2305.16623 [physics.ins-det].
- [49] ATLAS Collaboration, *The ATLAS trigger system for LHC Run 3 and trigger performance in 2022*, *JINST* **19** (2024) P06029, arXiv: 2401.06630 [hep-ex].
- [50] ATLAS Collaboration, *Software and computing for Run 3 of the ATLAS experiment at the LHC*, *Eur. Phys. J. C* **85** (2025) 234, arXiv: 2404.06335 [hep-ex].
- [51] ATLAS Collaboration, *The ATLAS transition radiation detector (TRT) Fast-OR trigger*, ATL-INDET-PUB-2009-002, 2009, URL: <https://cds.cern.ch/record/1229213>.
- [52] ATLAS Collaboration, *Vertex Reconstruction Performance of the ATLAS Detector at $\sqrt{s} = 13$ TeV*, ATL-PHYS-PUB-2015-026, 2015, URL: <https://cds.cern.ch/record/2037717>.
- [53] ATLAS Collaboration, *Measurement of flow harmonics with multi-particle cumulants in $Pb+Pb$ collisions at $\sqrt{s_{NN}} = 2.76$ TeV with the ATLAS detector*, *Eur. Phys. J. C* **74** (2014) 3157, arXiv: 1408.4342 [hep-ex].
- [54] M. L. Miller, K. Reygers, S. J. Sanders, and P. Steinberg, *Glauber Modeling in High-Energy Nuclear Collisions*, *Ann. Rev. Nucl. Part. Sci.* **57** (2007) 205, arXiv: nucl-ex/0701025.
- [55] C. Loizides, *Glauber predictions for oxygen and neon collisions at LHC*, (2025), arXiv: 2507.05853 [nucl-th].
- [56] ATLAS Collaboration, *Performance of the ATLAS track reconstruction algorithms in dense environments in LHC Run 2*, *Eur. Phys. J. C* **77** (2017) 673, arXiv: 1704.07983 [hep-ex].
- [57] X.-N. Wang and M. Gyulassy, *HIJING: A Monte Carlo model for multiple jet production in pp , pA , and AA collisions*, *Phys. Rev. D* **44** (1991) 3501.
- [58] J. Jia and S. Mohapatra, *Disentangling flow and nonflow correlations via Bayesian unfolding of the event-by-event distributions of harmonic coefficients in ultrarelativistic heavy-ion collisions*, *Phys. Rev. C* **88** (2013) 014907, arXiv: 1304.1471 [nucl-ex].

- [59] ATLAS Collaboration, *The ATLAS Simulation Infrastructure*, *Eur. Phys. J. C* **70** (2010) 823, arXiv: [1005.4568 \[physics.ins-det\]](#).
- [60] S. Agostinelli et al., *GEANT4 – a simulation toolkit*, *Nucl. Instrum. Meth. A* **506** (2003) 250.
- [61] PHENIX Collaboration, *Dihadron azimuthal correlations in Au+Au collisions at $\sqrt{s_{NN}} = 200$ GeV*, *Phys. Rev. C* **78** (2008) 014901, arXiv: [0801.4545 \[nucl-ex\]](#).
- [62] ATLAS Collaboration, *Measurement of long-range pseudorapidity correlations and azimuthal harmonics in $\sqrt{s_{NN}} = 5.02$ TeV proton–lead collisions with the ATLAS detector*, *Phys. Rev. C* **90** (2014) 044906, arXiv: [1409.1792 \[hep-ex\]](#).
- [63] ATLAS Collaboration, *Measurement of the correlation between flow harmonics of different order in lead–lead collisions at $\sqrt{s_{NN}} = 2.76$ TeV with the ATLAS detector*, *Phys. Rev. C* **92** (2015) 034903, arXiv: [1504.01289 \[hep-ex\]](#).
- [64] ATLAS Collaboration, *Measurements of long-range azimuthal anisotropies and associated Fourier coefficients for pp collisions at $\sqrt{s} = 5.02$ and 13 TeV and $p+Pb$ collisions at $\sqrt{s_{NN}} = 5.02$ TeV with the ATLAS detector*, *Phys. Rev. C* **96** (2017) 024908, arXiv: [1609.06213 \[nucl-ex\]](#).
- [65] CMS Collaboration, *Centrality dependence of dihadron correlations and azimuthal anisotropy harmonics in PbPb collisions at $\sqrt{s_{NN}} = 2.76$ TeV*, *Eur. Phys. J. C* **72** (2012) 2012, arXiv: [1201.3158 \[hep-ex\]](#).
- [66] CMS Collaboration, *Long-range and short-range dihadron angular correlations in central PbPb collisions at $\sqrt{s_{NN}} = 2.76$ TeV*, *JHEP* **07** (2011) 076, arXiv: [1105.2438 \[hep-ex\]](#).
- [67] CMS Collaboration, *Studies of azimuthal dihadron correlations in ultra-central PbPb collisions at $\sqrt{s_{NN}} = 2.76$ TeV*, *JHEP* **02** (2014) 088, arXiv: [1312.1845 \[hep-ex\]](#).
- [68] ALICE Collaboration, *Harmonic decomposition of two-particle angular correlations in Pb-Pb collisions at $\sqrt{s_{NN}} = 2.76$ TeV*, *Phys. Lett. B* **708** (2012) 249, arXiv: [1109.2501 \[nucl-ex\]](#).
- [69] ALICE Collaboration, *Measurements of long-range two-particle correlation over a wide pseudorapidity range in p –Pb collisions at $\sqrt{s_{NN}} = 5.02$ TeV*, *JHEP* **01** (2024) 199, arXiv: [2308.16590 \[nucl-ex\]](#).
- [70] M. A. Lisa, S. Pratt, R. Soltz, and U. Wiedemann, *FEMTOSCOPY IN RELATIVISTIC HEAVY ION COLLISIONS: Two Decades of Progress*, *Ann. Rev. Nucl. Part. Sci.* **55** (2005) 357, arXiv: [nucl-ex/0505014 \[nucl-ex\]](#).
- [71] ATLAS Collaboration, *Measurement of long-range two-particle azimuthal correlations in Z-boson tagged pp collisions at $\sqrt{s} = 8$ and 13 TeV*, *Eur. Phys. J. C* **80** (2020) 64, arXiv: [1906.08290 \[nucl-ex\]](#).
- [72] N. Borghini, P. M. Dinh, and J.-Y. Ollitrault, *Flow analysis from multiparticle azimuthal correlations*, *Phys. Rev. C* **64** (2001) 054901, arXiv: [nucl-th/0105040](#).
- [73] A. Bilandzic, C. H. Christensen, K. Gulbrandsen, A. Hansen, and Y. Zhou, *Generic framework for anisotropic flow analyses with multiparticle azimuthal correlations*, *Phys. Rev. C* **89** (2014) 064904, arXiv: [1312.3572 \[nucl-ex\]](#).
- [74] A. Bilandzic, R. Snellings, and S. Voloshin, *Flow analysis with cumulants: Direct calculations*, *Phys. Rev. C* **83** (2011) 044913, arXiv: [1010.0233 \[nucl-ex\]](#).

- [75] J. Jia, M. Zhou, and A. Trzupek, *Revealing long-range multiparticle collectivity in small collision systems via subevent cumulants*, *Phys. Rev. C* **96** (2017) 034906, arXiv: [1701.03830 \[nucl-th\]](#).
- [76] S. A. Voloshin, A. M. Poskanzer, A. Tang, and G. Wang, *Elliptic flow in the Gaussian model of eccentricity fluctuations*, *Phys. Lett. B* **659** (2008) 537, arXiv: [0708.0800 \[nucl-th\]](#).
- [77] ATLAS Collaboration, *Study of the material of the ATLAS inner detector for Run 2 of the LHC*, *JINST* **12** (2017) P12009, arXiv: [1707.02826 \[hep-ex\]](#).
- [78] H. Mäntysaari, B. Schenke, C. Shen, and W. Zhao, *Collision-Energy Dependence in Heavy-Ion Collisions from Nonlinear QCD Evolution*, *Phys. Rev. Lett.* **135** (2025) 022302, arXiv: [2502.05138 \[nucl-th\]](#).
- [79] B. Schenke, P. Tribedy, and R. Venugopalan, *Fluctuating Glasma initial conditions and flow in heavy ion collisions*, *Phys. Rev. Lett.* **108** (2012) 252301, arXiv: [1202.6646 \[nucl-th\]](#).
- [80] B. Schenke, S. Jeon, and C. Gale, *(3+1)D hydrodynamic simulation of relativistic heavy-ion collisions*, *Phys. Rev. C* **82** (2010) 014903, arXiv: [1004.1408 \[hep-ph\]](#).
- [81] M. Bleicher et al., *Relativistic hadron-hadron collisions in the ultra-relativistic quantum molecular dynamics model*, *J. Phys. G* **25** (1999) 1859, arXiv: [hep-ph/9909407](#).
- [82] S. A. Bass et al., *Microscopic models for ultrarelativistic heavy ion collisions*, *Prog. Part. Nucl. Phys.* **41** (1998) 255, arXiv: [nucl-th/9803035](#).
- [83] D. Lee, *Lattice simulations for few- and many-body systems*, *Prog. Part. Nucl. Phys.* **63** (2009) 117, arXiv: [0804.3501 \[nucl-th\]](#).
- [84] J. S. Moreland, J. E. Bernhard, and S. A. Bass, *Alternative ansatz to wounded nucleon and binary collision scaling in high-energy nuclear collisions*, *Phys. Rev. C* **92** (2015) 011901, arXiv: [1412.4708 \[nucl-th\]](#).
- [85] G. Nijs, W. van der Schee, U. Gürsoy, and R. Snellings, *Bayesian analysis of heavy ion collisions with the heavy ion computational framework Trajectum*, *Phys. Rev. C* **103** (2021) 054909, arXiv: [2010.15134 \[nucl-th\]](#).
- [86] G. Nijs and W. van der Schee, *Predictions and postdictions for relativistic lead and oxygen collisions with the computational simulation code Trajectum*, *Phys. Rev. C* **106** (2022) 044903, arXiv: [2110.13153 \[nucl-th\]](#).
- [87] G. Giacalone, G. Nijs, and W. van der Schee, *Determination of the neutron skin of ^{208}Pb from Ultrarelativistic Nuclear Collisions*, *Phys. Rev. Lett.* **131** (2023) 202302, arXiv: [2305.00015 \[nucl-th\]](#).
- [88] Y. Wang, S. Zhao, B. Cao, H.-j. Xu, and H. Song, *Exploring the compactness of α clusters in ^{16}O nuclei with relativistic $^{16}\text{O}+^{16}\text{O}$ collisions*, *Phys. Rev. C* **109** (2024) L051904, arXiv: [2401.15723 \[nucl-th\]](#).
- [89] ATLAS Collaboration, *ATLAS Computing Acknowledgements*, ATL-SOFT-PUB-2025-001, 2025, URL: <https://cds.cern.ch/record/2922210>.

The ATLAS Collaboration

G. Aad ¹⁰³, E. Aakvaag ¹⁷, B. Abbott ¹²², S. Abdelhameed ^{118a}, K. Abeling ⁵⁵, N.J. Abicht ⁴⁹, S.H. Abidi ³⁰, M. Aboeela ⁴⁵, A. Aboulhorma ^{36e}, H. Abramowicz ¹⁵⁶, Y. Abulaiti ¹¹⁹, B.S. Acharya ^{69a,69b,m}, A. Ackermann ^{63a}, C. Adam Bourdarios ⁴, L. Adamezyk ^{86a}, S.V. Addepalli ¹⁴⁸, M.J. Addison ¹⁰², J. Adelman ¹¹⁷, A. Adiguzel ^{22c}, T. Adye ¹³⁶, A.A. Affolder ¹³⁸, Y. Afik ⁴⁰, M.N. Agaras ¹³, A. Aggarwal ¹⁰¹, C. Agheorghiesei ^{28c}, F. Ahmadov ^{39,ad}, S. Ahuja ⁹⁶, S. Ahuja ¹⁶⁸, X. Ai ^{142b}, G. Aielli ^{76a,76b}, A. Aikot ¹⁶⁸, M. Ait Tamliah ^{36e}, B. Aitbenkikh ^{36a}, T.P.A. Åkesson ⁹⁹, A.V. Akimov ¹⁵⁰, D. Akiyama ¹⁷³, N.N. Akolkar ²⁵, S. Aktas ¹⁷¹, G.L. Alberghi ^{24b}, J. Albert ¹⁷⁰, U. Alberti ²⁰, P. Albicocco ⁵³, G.L. Albouy ⁶⁰, S. Alderweireldt ⁵², Z.L. Alegria ¹²³, M. Aleksa ³⁷, I.N. Aleksandrov ³⁹, C. Alexa ^{28b}, T. Alexopoulos ¹⁰, F. Alfonsi ^{24b}, M. Algren ⁵⁶, M. Alhroob ¹⁷², B. Ali ¹³⁴, H.M.J. Ali ^{92,w}, S. Ali ³², S.W. Alibocus ⁹³, M. Aliev ^{34c}, G. Alimonti ^{71a}, W. Alkakhri ⁵⁵, C. Allaire ⁶⁶, B.M.M. Allbrooke ¹⁵¹, J.S. Allen ¹⁰², J.F. Allen ⁵², P.P. Allport ²¹, A. Aloisio ^{72a,72b}, F. Alonso ⁹¹, C. Alpigiani ¹⁴¹, Z.M.K. Alsolami ⁹², A. Alvarez Fernandez ¹⁰¹, M. Alves Cardoso ⁵⁶, M.G. Alviggi ^{72a,72b}, M. Aly ¹⁰², Y. Amaral Coutinho ^{82b}, A. Ambler ¹⁰⁵, C. Amelung ³⁷, M. Amerl ¹⁰², C.G. Ames ¹¹⁰, T. Amezza ¹²⁹, D. Amidei ¹⁰⁷, B. Amini ⁵⁴, K. Amiric ¹⁶⁰, A. Amirkhanov ³⁹, S.P. Amor Dos Santos ^{132a}, K.R. Amos ¹⁶⁸, D. Amperiadou ¹⁵⁷, S. An ⁸³, C. Anastopoulos ¹⁴⁴, T. Andeen ¹¹, J.K. Anders ⁹³, A.C. Anderson ⁵⁹, A. Andreatta ^{71a,71b}, S. Angelidakis ⁹, A. Angerami ⁴², A.V. Anisenkov ³⁹, A. Annovi ^{74a}, C. Antel ³⁷, E. Antipov ¹⁵⁰, M. Antonelli ⁵³, F. Anulli ^{75a}, M. Aoki ⁸³, T. Aoki ¹⁵⁸, M.A. Aparo ¹⁵¹, L. Aperio Bella ⁴⁸, M. Apicella ³¹, C. Appelt ¹⁵⁶, A. Apyan ²⁷, M. Arampatzi ¹⁰, S.J. Arbiol Val ⁸⁷, C. Arcangeletti ⁵³, A.T.H. Arce ⁵¹, J-F. Arguin ¹⁰⁹, S. Argyropoulos ¹⁵⁷, J.-H. Arling ⁴⁸, O. Arnaez ⁴, H. Arnold ¹⁵⁰, G. Artoni ^{75a,75b}, H. Asada ¹¹², K. Asai ¹²⁰, S. Asatryan ¹⁷⁸, N.A. Asbah ³⁷, R.A. Ashby Pickering ¹⁷², A.M. Aslam ⁹⁶, K. Assamagan ³⁰, R. Astalos ^{29a}, K.S.V. Astrand ⁹⁹, S. Atashi ¹⁶⁴, R.J. Atkin ^{34a}, H. Atmani ^{36f}, P.A. Atlasiddha ¹³⁰, K. Augsten ¹³⁴, A.D. Auriol ⁴¹, V.A. Austrup ¹⁰², A.S. Avad ⁹⁵, G. Avolio ³⁷, K. Axiotis ⁵⁶, A. Azzam ¹³, D. Babal ^{29b}, H. Bachacou ¹³⁷, K. Bachas ^{157,q}, A. Bachiu ³⁵, E. Bachmann ⁵⁰, M.J. Backes ^{63a}, A. Badea ⁴⁰, T.M. Baer ¹⁰⁷, P. Bagnaia ^{75a,75b}, M. Bahmani ¹⁹, D. Bahner ⁵⁴, K. Bai ¹²⁵, J.T. Baines ¹³⁶, L. Baines ⁹⁵, O.K. Baker ¹⁷⁷, E. Bakos ¹⁶, D. Bakshi Gupta ⁸, L.E. Balabram Filho ^{82b}, V. Balakrishnan ¹²², R. Balasubramanian ⁴, E.M. Baldin ³⁸, P. Balek ^{86a}, E. Ballabene ^{24b,24a}, F. Balli ¹³⁷, L.M. Baltes ^{63a}, W.K. Balunas ³³, J. Balz ¹⁰¹, I. Bamwidhi ^{118b}, E. Banas ⁸⁷, M. Bandieramonte ¹³¹, A. Bandyopadhyay ²⁵, S. Bansal ²⁵, L. Barak ¹⁵⁶, M. Barakat ⁴⁸, E.L. Barberio ¹⁰⁶, D. Barberis ^{18b}, M. Barbero ¹⁰³, M.Z. Barel ¹¹⁶, T. Barillari ¹¹¹, M-S. Barisits ³⁷, T. Barklow ¹⁴⁸, P. Baron ¹³⁵, D.A. Baron Moreno ¹⁰², A. Baroncelli ⁶², A.J. Barr ¹²⁸, J.D. Barr ⁹⁷, F. Barreiro ¹⁰⁰, J. Barreiro Guimarães da Costa ¹⁴, M.G. Barros Teixeira ^{132a}, S. Barsov ³⁸, F. Bartels ^{63a}, R. Bartoldus ¹⁴⁸, A.E. Barton ⁹², P. Bartos ^{29a}, M. Baselga ⁴⁹, S. Bashiri ⁸⁷, A. Bassalat ^{66,b}, M.J. Basso ^{161a}, S. Bataju ⁴⁵, R. Bate ¹⁶⁹, R.L. Bates ⁵⁹, S. Batlamous ¹⁰⁰, M. Battaglia ¹³⁸, D. Battulga ¹⁹, M. Baunce ^{75a,75b}, M. Bauer ⁷⁹, P. Bauer ²⁵, L.T. Bayer ⁴⁸, L.T. Bazzano Hurrell ³¹, J.B. Beacham ¹¹¹, T. Beau ¹²⁹, J.Y. Beauchamp ⁹¹, P.H. Beauchemin ¹⁶³, P. Bechtel ²⁵, H.P. Beck ^{20,p}, K. Becker ¹⁷², A.J. Beddall ⁸¹, V.A. Bednyakov ³⁹, C.P. Bee ¹⁵⁰, L.J. Beemster ¹⁶, M. Begalli ^{82d}, M. Begel ³⁰, J.K. Behr ⁴⁸, J.F. Beirer ³⁷, F. Beisiegel ²⁵, M. Belfkir ^{118b}, G. Bella ¹⁵⁶, L. Bellagamba ^{24b}, A. Bellerive ³⁵, C.D. Bellgraph ⁶⁸, P. Bellos ²¹, K. Beloborodov ³⁸, I. Benaoumeur ²¹, D. Benckroun ^{36a}, F. Bendebba ^{36a}, Y. Benhammou ¹⁵⁶, K.C. Benkendorfer ⁶¹, L. Beresford ⁴⁸,

M. Beretta [id⁵³](#), E. Bergeaas Kuutmann [id¹⁶⁶](#), N. Berger [id⁴](#), B. Bergmann [id¹³⁴](#), J. Beringer [id^{18a}](#),
G. Bernardi [id⁵](#), C. Bernius [id¹⁴⁸](#), F.U. Bernlochner [id²⁵](#), A. Berrocal Guardia [id¹³](#), T. Berry [id⁹⁶](#),
P. Berta [id¹³⁵](#), A. Berti [id^{132a}](#), R. Bertrand [id¹⁰³](#), S. Bethke [id¹¹¹](#), A. Betti [id^{75a,75b}](#), A.J. Bevan [id⁹⁵](#),
L. Bezio [id⁵⁶](#), N.K. Bhalla [id⁵⁴](#), S. Bharthuar [id¹¹¹](#), S. Bhatta [id¹⁵⁰](#), P. Bhattarai [id¹⁴⁸](#), Z.M. Bhatti [id¹¹⁹](#),
K.D. Bhide [id⁵⁴](#), V.S. Bhopatkar [id¹²³](#), R.M. Bianchi [id¹³¹](#), G. Bianco [id^{24b,24a}](#), O. Biebel [id¹¹⁰](#),
M. Biglietti [id^{77a}](#), C.S. Billingsley [id⁴⁵](#), Y. Bimgdi [id^{36f}](#), M. Bindi [id⁵⁵](#), A. Bingham [id¹⁷⁶](#), A. Bingul [id^{22b}](#),
C. Bini [id^{75a,75b}](#), G.A. Bird [id³³](#), M. Birman [id¹⁷⁴](#), M. Biros [id¹³⁵](#), S. Biryukov [id¹⁵¹](#), T. Bisanz [id⁴⁹](#),
E. Bisceglie [id^{24b,24a}](#), J.P. Biswal [id¹³⁶](#), D. Biswas [id¹⁴⁶](#), I. Bloch [id⁴⁸](#), A. Blue [id⁵⁹](#), U. Blumenschein [id⁹⁵](#),
V.S. Bobrovnikov [id³⁹](#), L. Boccardo [id^{57b,57a}](#), M. Boehler [id⁵⁴](#), B. Boehm [id¹⁷¹](#), D. Bogavac [id¹³](#),
A.G. Bogdanchikov [id³⁸](#), L.S. Boggia [id¹²⁹](#), V. Boisvert [id⁹⁶](#), P. Bokan [id³⁷](#), T. Bold [id^{86a}](#), M. Bomben [id⁵](#),
M. Bona [id⁹⁵](#), M. Boonekamp [id¹³⁷](#), A.G. Borbély [id⁵⁹](#), I.S. Bordulev [id³⁸](#), G. Borissov [id⁹²](#),
D. Bortoletto [id¹²⁸](#), D. Boscherini [id^{24b}](#), M. Bosman [id¹³](#), K. Bouaouda [id^{36a}](#), N. Bouchhar [id¹⁶⁸](#),
L. Boudet [id⁴](#), J. Boudreau [id¹³¹](#), E.V. Bouhova-Thacker [id⁹²](#), D. Boumediene [id⁴¹](#), R. Bouquet [id^{57b,57a}](#),
A. Boveia [id¹²¹](#), J. Boyd [id³⁷](#), D. Boye [id³⁰](#), I.R. Boyko [id³⁹](#), L. Bozianu [id⁵⁶](#), J. Bracnik [id²¹](#),
N. Brahimy [id⁴](#), G. Brandt [id¹⁷⁶](#), O. Brandt [id³³](#), B. Brau [id¹⁰⁴](#), J.E. Brau [id¹²⁵](#), R. Brenner [id¹⁷⁴](#),
L. Brenner [id¹¹⁶](#), R. Brenner [id¹⁶⁶](#), S. Bressler [id¹⁷⁴](#), G. Brianti [id^{78a,78b}](#), D. Britton [id⁵⁹](#), D. Britzger [id¹¹¹](#),
I. Brock [id²⁵](#), R. Brock [id¹⁰⁸](#), G. Brooijmans [id⁴²](#), A.J. Brooks [id⁶⁸](#), E.M. Brooks [id^{161b}](#), E. Brost [id³⁰](#),
L.M. Brown [id^{170,161a}](#), L.E. Bruce [id⁶¹](#), T.L. Bruckler [id¹²⁸](#), P.A. Bruckman de Renstrom [id⁸⁷](#),
B. Brüers [id⁴⁸](#), A. Bruni [id^{24b}](#), G. Bruni [id^{24b}](#), D. Brunner [id^{47a,47b}](#), M. Bruschi [id^{24b}](#), N. Bruscino [id^{75a,75b}](#),
T. Buanes [id¹⁷](#), Q. Buat [id¹⁴¹](#), D. Buchin [id¹¹¹](#), A.G. Buckley [id⁵⁹](#), O. Bulekov [id⁸¹](#), B.A. Bullard [id¹⁴⁸](#),
S. Burdin [id⁹³](#), C.D. Burgard [id⁴⁹](#), A.M. Burger [id⁹⁰](#), B. Burghgrave [id⁸](#), O. Burlayenko [id⁵⁴](#),
J. Bureson [id¹⁶⁷](#), J.C. Burzynski [id¹⁴⁷](#), E.L. Busch [id⁴²](#), V. Büscher [id¹⁰¹](#), P.J. Bussey [id⁵⁹](#), O. But [id²⁵](#),
J.M. Butler [id²⁶](#), C.M. Buttar [id⁵⁹](#), J.M. Butterworth [id⁹⁷](#), W. Buttinger [id¹³⁶](#), C.J. Buxo Vazquez [id¹⁰⁸](#),
A.R. Buzykaev [id³⁹](#), S. Cabrera Urbán [id¹⁶⁸](#), L. Cadamuro [id⁶⁶](#), H. Cai [id³⁷](#), Y. Cai [id^{24b,113c,24a}](#),
Y. Cai [id^{113a}](#), V.M.M. Cairo [id³⁷](#), O. Cakir [id^{3a}](#), N. Calace [id³⁷](#), P. Calafiura [id^{18a}](#), G. Calderini [id¹²⁹](#),
P. Calfayan [id³⁵](#), L. Calic [id⁹⁹](#), G. Callea [id⁵⁹](#), L.P. Caloba [id^{82b}](#), D. Calvet [id⁴¹](#), S. Calvet [id⁴¹](#),
R. Camacho Toro [id¹²⁹](#), S. Camarda [id³⁷](#), D. Camarero Munoz [id²⁷](#), P. Camarri [id^{76a,76b}](#),
C. Camincher [id¹⁷⁰](#), M. Campanelli [id⁹⁷](#), A. Camplani [id⁴³](#), V. Canale [id^{72a,72b}](#), A.C. Canbay [id^{3a}](#),
E. Canonero [id⁹⁶](#), J. Cantero [id¹⁶⁸](#), Y. Cao [id¹⁶⁷](#), F. Capocasa [id²⁷](#), M. Capua [id^{44b,44a}](#), A. Carbone [id^{71a,71b}](#),
R. Cardarelli [id^{76a}](#), J.C.J. Cardenas [id⁸](#), M.P. Cardiff [id²⁷](#), G. Carducci [id^{44b,44a}](#), T. Carli [id³⁷](#),
G. Carlino [id^{72a}](#), J.I. Carlotto [id¹³](#), B.T. Carlson [id^{131,r}](#), E.M. Carlson [id¹⁷⁰](#), J. Carmignani [id⁹³](#),
L. Carminati [id^{71a,71b}](#), A. Carnelli [id⁴](#), M. Carnesale [id³⁷](#), S. Caron [id¹¹⁵](#), E. Carquin [id^{139g}](#), I.B. Carr [id¹⁰⁶](#),
S. Carrá [id^{73a,73b}](#), G. Carratta [id^{24b,24a}](#), C. Carrion Martinez [id¹⁶⁸](#), A.M. Carroll [id¹²⁵](#), M.P. Casado [id^{13,h}](#),
P. Casolaro [id^{72a,72b}](#), M. Caspar [id⁴⁸](#), F.L. Castillo [id⁴](#), L. Castillo Garcia [id¹³](#), V. Castillo Gimenez [id¹⁶⁸](#),
N.F. Castro [id^{132a,132e}](#), A. Catinaccio [id³⁷](#), J.R. Catmore [id¹²⁷](#), T. Cavaliere [id⁴](#), V. Cavaliere [id³⁰](#),
L.J. Caviedes Betancourt [id^{23b}](#), E. Celebi [id⁸¹](#), S. Cella [id³⁷](#), V. Cepaitis [id⁵⁶](#), K. Cerny [id¹²⁴](#),
A.S. Cerqueira [id^{82a}](#), A. Cerri [id^{74a,74b,am}](#), L. Cerrito [id^{76a,76b}](#), F. Cerutti [id^{18a}](#), B. Cervato [id^{71a,71b}](#),
A. Cervelli [id^{24b}](#), G. Cesarini [id⁵³](#), S.A. Cetin [id⁸¹](#), P.M. Chabrilat [id¹²⁹](#), R. Chakkappai [id⁶⁶](#),
S. Chakraborty [id¹⁷²](#), A. Chambers [id⁶¹](#), J. Chan [id^{18a}](#), W.Y. Chan [id¹⁵⁸](#), J.D. Chapman [id³³](#),
E. Chapon [id¹³⁷](#), B. Chargeishvili [id^{154b}](#), D.G. Charlton [id²¹](#), C. Chauhan [id¹³⁵](#), Y. Che [id^{113a}](#),
S. Chekanov [id⁶](#), G.A. Chelkov [id^{39,a}](#), B. Chen [id¹⁵⁶](#), B. Chen [id¹⁷⁰](#), H. Chen [id³⁰](#), J. Chen [id^{143a}](#),
J. Chen [id¹⁴⁷](#), M. Chen [id¹²⁸](#), S. Chen [id⁸⁸](#), S.J. Chen [id^{113a}](#), X. Chen [id^{143a}](#), X. Chen [id^{15,ah}](#), Z. Chen [id⁶²](#),
C.L. Cheng [id¹⁷⁵](#), H.C. Cheng [id^{64a}](#), S. Cheong [id¹⁴⁸](#), A. Cheplakov [id³⁹](#), E. Cherepanova [id¹¹⁶](#),
R. Cherkaoui El Moursli [id^{36e}](#), E. Cheu [id⁷](#), K. Cheung [id⁶⁵](#), L. Chevalier [id¹³⁷](#), V. Chiarella [id⁵³](#),
G. Chiarelli [id^{74a}](#), G. Chiodini [id^{70a}](#), A.S. Chisholm [id²¹](#), A. Chitan [id^{28b}](#), M. Chitishvili [id¹⁶⁸](#),
M.V. Chizhov [id^{39,s}](#), K. Choi [id¹¹](#), Y. Chou [id¹⁴¹](#), E.Y.S. Chow [id¹¹⁵](#), K.L. Chu [id¹⁷⁴](#), M.C. Chu [id^{64a}](#),
X. Chu [id^{14,113c}](#), Z. Chubinidze [id⁵³](#), J. Chudoba [id¹³³](#), J.J. Chwastowski [id⁸⁷](#), D. Cieri [id¹¹¹](#),

K.M. Ciesla [ID 86a](#), V. Cindro [ID 94](#), A. Ciocio [ID 18a](#), F. Cirotto [ID 72a,72b](#), Z.H. Citron [ID 174](#), M. Citterio [ID 71a](#),
 D.A. Ciubotaru [ID 28b](#), A. Clark [ID 56](#), P.J. Clark [ID 52](#), N. Clarke Hall [ID 97](#), C. Clarry [ID 160](#), S.E. Clawson [ID 48](#),
 C. Clement [ID 47a,47b](#), L. Clissa [ID 24b,24a](#), Y. Coadou [ID 103](#), M. Cobal [ID 69a,69c](#), A. Coccaro [ID 57b](#),
 R.F. Coelho Barrue [ID 132a](#), R. Coelho Lopes De Sa [ID 104](#), S. Coelli [ID 71a](#), L.S. Colangeli [ID 160](#), B. Cole [ID 42](#),
 P. Collado Soto [ID 100](#), J. Collot [ID 60](#), R. Coluccia [ID 70a,70b](#), P. Conde Muiño [ID 132a,132g](#), M.P. Connell [ID 34c](#),
 S.H. Connell [ID 34c](#), E.I. Conroy [ID 128](#), M. Contreras Cossio [ID 11](#), F. Conventi [ID 72a,aj](#),
 A.M. Cooper-Sarkar [ID 128](#), L. Corazzina [ID 75a,75b](#), F.A. Corchia [ID 24b,24a](#), A. Cordeiro Oudot Choi [ID 141](#),
 L.D. Corpe [ID 41](#), M. Corradi [ID 75a,75b](#), F. Corriveau [ID 105,ab](#), A. Cortes-Gonzalez [ID 158](#), M.J. Costa [ID 168](#),
 F. Costanza [ID 4](#), D. Costanzo [ID 144](#), J. Couthures [ID 4](#), G. Cowan [ID 96](#), K. Cranmer [ID 175](#), L. Cremer [ID 49](#),
 D. Cremonini [ID 24b,24a](#), S. Crépe-Renaudin [ID 60](#), F. Crescioli [ID 129](#), T. Cresta [ID 73a,73b](#), M. Cristinziani [ID 146](#),
 M. Cristoforetti [ID 78a,78b](#), E. Critelli [ID 97](#), V. Croft [ID 116](#), G. Crosetti [ID 44b,44a](#), A. Cueto [ID 100](#), H. Cui [ID 97](#),
 Z. Cui [ID 7](#), B.M. Cunnett [ID 151](#), W.R. Cunningham [ID 59](#), F. Curcio [ID 168](#), J.R. Curran [ID 52](#),
 M.J. Da Cunha Sargedas De Sousa [ID 57b,57a](#), J.V. Da Fonseca Pinto [ID 82b](#), C. Da Via [ID 102](#),
 W. Dabrowski [ID 86a](#), T. Dado [ID 37](#), S. Dahbi [ID 153](#), T. Dai [ID 107](#), D. Dal Santo [ID 20](#), C. Dallapiccola [ID 104](#),
 M. Dam [ID 43](#), G. D'amen [ID 30](#), V. D'Amico [ID 110](#), J.R. Dandoy [ID 35](#), M. D'Andrea [ID 57b,57a](#),
 D. Dannheim [ID 37](#), G. D'anniballe [ID 74a,74b](#), M. Danninger [ID 147](#), V. Dao [ID 150](#), G. Darbo [ID 57b](#),
 S.J. Das [ID 30](#), F. Dattola [ID 48](#), S. D'Auria [ID 71a,71b](#), A. D'Avanzo [ID 72a,72b](#), T. Davidek [ID 135](#),
 J. Davidson [ID 172](#), I. Dawson [ID 95](#), K. De [ID 8](#), C. De Almeida Rossi [ID 160](#), R. De Asmundis [ID 72a](#),
 N. De Biase [ID 48](#), S. De Castro [ID 24b,24a](#), N. De Groot [ID 115](#), P. de Jong [ID 116](#), H. De la Torre [ID 117](#),
 A. De Maria [ID 113a](#), A. De Salvo [ID 75a](#), U. De Sanctis [ID 76a,76b](#), F. De Santis [ID 70a,70b](#), A. De Santo [ID 151](#),
 J.B. De Vivie De Regie [ID 60](#), J. Debevc [ID 94](#), D.V. Dedovich [ID 39](#), J. Degens [ID 93](#), A.M. Deiana [ID 45](#),
 J. Del Peso [ID 100](#), L. Delagrane [ID 129](#), F. Deliot [ID 137](#), C.M. Delitzsch [ID 49](#), M. Della Pietra [ID 72a,72b](#),
 D. Della Volpe [ID 56](#), A. Dell'Acqua [ID 37](#), L. Dell'Asta [ID 71a,71b](#), M. Delmastro [ID 4](#), C.C. Delogu [ID 57b,57a](#),
 P.A. Delsart [ID 60](#), S. Demers [ID 177](#), M. Demichev [ID 39](#), S.P. Denisov [ID 38](#), H. Denizli [ID 22a,1](#),
 L. D'Eramo [ID 41](#), D. Derendarz [ID 87](#), F. Derue [ID 129](#), P. Dervan [ID 93,*](#), A.M. Desai [ID 1](#), K. Desch [ID 25](#),
 F.A. Di Bello [ID 57b,57a](#), A. Di Ciaccio [ID 76a,76b](#), L. Di Ciaccio [ID 4](#), A. Di Domenico [ID 75a,75b](#),
 C. Di Donato [ID 72a,72b](#), A. Di Girolamo [ID 37](#), G. Di Gregorio [ID 66](#), A. Di Luca [ID 78a,78b](#),
 B. Di Micco [ID 77a,77b](#), R. Di Nardo [ID 77a,77b](#), K.F. Di Petrillo [ID 40](#), M. Diamantopoulou [ID 35](#), F.A. Dias [ID 116](#),
 M.A. Diaz [ID 139a,139b](#), A.R. Didenko [ID 39](#), M. Didenko [ID 168](#), S.D. Diefenbacher [ID 18a](#), E.B. Diehl [ID 107](#),
 S. Díez Cornell [ID 48](#), C. Díez Pardos [ID 146](#), C. Dimitriadi [ID 149](#), A. Dimitrievska [ID 21](#), A. Dimri [ID 150](#),
 Y. Ding [ID 62](#), J. Dingfelder [ID 25](#), T. Dingley [ID 128](#), I-M. Dinu [ID 28b](#), S.J. Dittmeier [ID 63b](#), F. Dittus [ID 37](#),
 M. Divisek [ID 135](#), B. Dixit [ID 93](#), F. Djama [ID 103](#), T. Djobava [ID 154b](#), C. Doglioni [ID 102,99](#), A. Dohnalova [ID 29a](#),
 Z. Dolezal [ID 135](#), K. Domijan [ID 86a](#), K.M. Dona [ID 40](#), M. Donadelli [ID 82d](#), B. Dong [ID 108](#), J. Donini [ID 41](#),
 A. D'Onofrio [ID 72a,72b](#), M. D'Onofrio [ID 93](#), J. Dopke [ID 136](#), A. Doria [ID 72a](#), N. Dos Santos Fernandes [ID 132a](#),
 I.A. Dos Santos Luz [ID 82e](#), P. Dougan [ID 102](#), M.T. Dova [ID 91](#), A.T. Doyle [ID 59](#), M.P. Drescher [ID 55](#),
 E. Dreyer [ID 174](#), I. Drivas-koulouris [ID 10](#), M. Drnevich [ID 119](#), D. Du [ID 62](#), T.A. du Pree [ID 116](#), Z. Duan [ID 113a](#),
 M. Dubau [ID 4](#), F. Dubinin [ID 39](#), M. Dubovsky [ID 29a](#), E. Duchovni [ID 174](#), G. Duckeck [ID 110](#), P.K. Duckett [ID 97](#),
 O.A. Ducu [ID 28b](#), D. Duda [ID 52](#), A. Dudarev [ID 37](#), M.M. Dudek [ID 87](#), E.R. Duden [ID 27](#), M. D'uffizi [ID 102](#),
 L. Duflost [ID 66](#), M. Dührssen [ID 37](#), I. Duminica [ID 28g](#), A.E. Dumitriu [ID 28b](#), M. Dunford [ID 63a](#),
 K. Dunne [ID 47a,47b](#), A. Duperrin [ID 103](#), H. Duran Yildiz [ID 3a](#), A. Durglishvili [ID 154b](#), G.I. Dyckes [ID 18a](#),
 M. Dyndal [ID 86a](#), B.S. Dziejczak [ID 37](#), Z.O. Earnshaw [ID 151](#), G.H. Eberwein [ID 128](#), B. Eckerova [ID 29a](#),
 S. Eggebrecht [ID 55](#), E. Egidio Purcino De Souza [ID 82e](#), G. Eigen [ID 17](#), K. Einsweiler [ID 18a](#), T. Ekelof [ID 166](#),
 P.A. Ekman [ID 99](#), S. El Farkh [ID 36b](#), Y. El Ghazali [ID 62](#), H. El Jarrari [ID 105](#), A. El Moussaouy [ID 36a](#),
 D. Elitez [ID 37](#), M. Ellert [ID 166](#), F. Ellinghaus [ID 176](#), T.A. Elliot [ID 96](#), N. Ellis [ID 37](#), J. Elmsheuser [ID 30](#),
 M. Elsayy [ID 118a](#), M. Elsing [ID 37](#), D. Emeliyanov [ID 136](#), Y. Enari [ID 83](#), S. Epari [ID 109](#),
 D. Ernani Martins Neto [ID 87](#), F. Ernst [ID 37](#), M. Escalier [ID 66](#), C. Escobar [ID 168](#), E. Etzion [ID 156](#),
 G. Evans [ID 132a,132b](#), H. Evans [ID 68](#), L.S. Evans [ID 48](#), A. Ezhilov [ID 38](#), S. Ezzarqtouni [ID 36a](#),

F. Fabbri [ID24b,24a](#), L. Fabbri [ID24b,24a](#), G. Facini [ID97](#), V. Fadeyev [ID138](#), R.M. Fakhruddinov [ID38](#),
 D. Fakoudis [ID101](#), S. Falciano [ID75a](#), L.F. Falda Ulhoa Coelho [ID27](#), F. Fallavollita [ID111](#), G. Falsetti [ID44b,44a](#),
 J. Faltova [ID135](#), C. Fan [ID167](#), K.Y. Fan [ID64b](#), Y. Fan [ID14](#), Y. Fang [ID14,113c](#), M. Fanti [ID71a,71b](#),
 M. Faraj [ID69a,69b](#), Z. Farazpay [ID98](#), A. Farbin [ID8](#), A. Farilla [ID77a](#), K. Farman [ID153](#), T. Farooque [ID108](#),
 J.N. Farr [ID177](#), M.S. Farrington⁶¹, S.M. Farrington [ID136,52](#), F. Fassi [ID36e](#), D. Fassouliotis [ID9](#),
 L. Fayard [ID66](#), P. Federic [ID135](#), P. Federicova [ID133](#), O.L. Fedin [ID38,a](#), M. Feickert [ID175](#), L. Feligioni [ID103](#),
 D.E. Fellers [ID18a](#), C. Feng [ID142a](#), Y. Feng¹⁴, Z. Feng [ID116](#), M.J. Fenton [ID164](#), L. Ferencz [ID48](#),
 B. Fernandez Barbadillo [ID92](#), P. Fernandez Martinez [ID67](#), M.J.V. Fernoux [ID103](#), J. Ferrando [ID92](#),
 A. Ferrari [ID166](#), P. Ferrari [ID116,115](#), R. Ferrari [ID73a](#), D. Ferrere [ID56](#), C. Ferretti [ID107](#), M.P. Fewell [ID1](#),
 D. Fiacco [ID75a,75b](#), F. Fiedler [ID101](#), P. Fiedler [ID134](#), S. Filimonov [ID39](#), M.S. Filip [ID28b,t](#), A. Filipčič [ID94](#),
 E.K. Filmer [ID161a](#), F. Filthaut [ID115](#), M.C.N. Fiolhais [ID132a,132c,c](#), L. Fiorini [ID168](#), W.C. Fisher [ID108](#),
 T. Fitschen [ID102](#), P.M. Fitzhugh¹³⁷, I. Fleck [ID146](#), P. Fleischmann [ID107](#), T. Flick [ID176](#), M. Flores [ID34d,ag](#),
 L.R. Flores Castillo [ID64a](#), F.M. Follega [ID78a,78b](#), N. Fomin [ID33](#), J.H. Foo [ID160](#), A. Formica [ID137](#),
 A.C. Forti [ID102](#), E. Fortin [ID37](#), A.W. Fortman [ID18a](#), L. Foster [ID18a](#), L. Fountas [ID9,i](#), D. Fournier [ID66](#),
 H. Fox [ID92](#), P. Francavilla [ID74a,74b](#), S. Francescato [ID61](#), S. Franchellucci [ID56](#), M. Franchini [ID24b,24a](#),
 S. Franchino [ID63a](#), D. Francis³⁷, L. Franco [ID48](#), L. Franconi [ID48](#), M. Franklin [ID61](#), G. Frattari [ID27](#),
 Y.Y. Frid [ID156](#), J. Friend [ID59](#), N. Fritzsche [ID37](#), A. Froch [ID56](#), D. Froidevaux [ID37](#), J.A. Frost [ID128](#),
 Y. Fu [ID108](#), S. Fuenzalida Garrido [ID139g](#), M. Fujimoto [ID150](#), K.Y. Fung [ID64a](#),
 E. Furtado De Simas Filho [ID82e](#), M. Furukawa [ID158](#), J. Fuster [ID168](#), A. Gaa [ID55](#), A. Gabrielli [ID24b,24a](#),
 A. Gabrielli [ID160](#), P. Gadow [ID37](#), G. Gagliardi [ID57b,57a](#), L.G. Gagnon [ID18a](#), S. Gaid [ID84b](#),
 S. Galantzan [ID156](#), J. Gallagher [ID1](#), E.J. Gallas [ID128](#), A.L. Gallen [ID166](#), B.J. Gallop [ID136](#), K.K. Gan [ID121](#),
 S. Ganguly [ID158](#), Y. Gao [ID52](#), A. Garabaglu [ID141](#), F.M. Garay Walls [ID139a,139b](#), C. García [ID168](#),
 A. Garcia Alonso [ID116](#), A.G. Garcia Caffaro [ID177](#), J.E. García Navarro [ID168](#), M.A. Garcia Ruiz [ID23b](#),
 M. Garcia-Sciveres [ID18a](#), G.L. Gardner [ID130](#), R.W. Gardner [ID40](#), N. Garelli [ID163](#), R.B. Garg [ID148](#),
 J.M. Gargan [ID33](#), C.A. Garner¹⁶⁰, C.M. Garvey [ID34a](#), V.K. Gassmann¹⁶³, G. Gaudio [ID73a](#), V. Gautam¹³,
 P. Gauzzi [ID75a,75b](#), J. Gavranovic [ID94](#), I.L. Gavrilenko [ID132a](#), A. Gavrilyuk [ID38](#), C. Gay [ID169](#),
 G. Gaycken [ID125](#), E.N. Gazis [ID10](#), A. Gekow¹²¹, C. Gemme [ID57b](#), M.H. Genest [ID60](#), A.D. Gentry [ID114](#),
 S. George [ID96](#), T. Geralis [ID46](#), A.A. Gerwin [ID122](#), P. Gessinger-Befurt [ID37](#), M. Ghani [ID172](#),
 K. Ghorbanian [ID95](#), A. Ghosal [ID146](#), A. Ghosh [ID164](#), A. Ghosh [ID7](#), B. Giacobbe [ID24b](#), S. Giagu [ID75a,75b](#),
 T. Giani [ID116](#), A. Giannini [ID62](#), S.M. Gibson [ID96](#), M. Gignac [ID138](#), D.T. Gil [ID86b](#), A.K. Gilbert [ID86a](#),
 B.J. Gilbert [ID42](#), D. Gillberg [ID35](#), G. Gilles [ID116](#), D.M. Gingrich [ID2,ai](#), M.P. Giordani [ID69a,69c](#),
 P.F. Giraud [ID137](#), G. Giugliarelli [ID69a,69c](#), D. Giugni [ID71a](#), F. Giuli [ID76a,76b](#), I. Gkialas [ID9,i](#),
 L.K. Gladilin [ID38](#), C. Glasman [ID100](#), M. Glazewska [ID20](#), R.M. Gleason [ID164](#), G. Glemža [ID48](#),
 M. Glisic¹²⁵, I. Gnesi [ID44b](#), Y. Go [ID30](#), M. Goblirsch-Kolb [ID37](#), B. Gocke [ID49](#), D. Godin¹⁰⁹,
 B. Gokturk [ID22a](#), S. Goldfarb [ID106](#), T. Golling [ID56](#), M.G.D. Gololo [ID34c](#), D. Golubkov [ID38](#),
 J.P. Gombas [ID108](#), A. Gomes [ID132a,132b](#), G. Gomes Da Silva [ID146](#), A.J. Gomez Delegido [ID37](#),
 R. Gonçalves [ID132a](#), L. Gonella [ID21](#), A. Gongadze [ID154c](#), F. Gonnella [ID21](#), J.L. Gonski [ID148](#),
 R.Y. González Andana [ID52](#), S. González de la Hoz [ID168](#), M.V. Gonzalez Rodrigues [ID48](#),
 R. Gonzalez Suarez [ID166](#), S. Gonzalez-Sevilla [ID56](#), L. Goossens [ID37](#), B. Gorini [ID37](#), E. Gorini [ID70a,70b](#),
 A. Gorišek [ID94](#), T.C. Gosart [ID130](#), A.T. Goshaw [ID51](#), M.I. Gostkin [ID39](#), S. Goswami [ID123](#),
 C.A. Gottardo [ID37](#), S.A. Gotz [ID110](#), M. Goughri [ID36b](#), A.G. Goussiou [ID141](#), N. Govender [ID34c](#),
 R.P. Grabarczyk [ID128](#), I. Grabowska-Bold [ID86a](#), K. Graham [ID35](#), E. Gramstad [ID127](#),
 S. Grancagnolo [ID70a,70b](#), C.M. Grant¹, P.M. Gravila [ID28f](#), F.G. Gravili [ID70a,70b](#), H.M. Gray [ID18a](#),
 M. Greco [ID111](#), M.J. Green [ID1](#), C. Grefe [ID25](#), A.S. Grefsrud [ID17](#), I.M. Gregor [ID48](#), K.T. Greif [ID164](#),
 P. Grenier [ID148](#), S.G. Grewe¹¹¹, A.A. Grillo [ID138](#), K. Grimm [ID32](#), S. Grinstein [ID13,x](#), J.-F. Grivaz [ID66](#),
 E. Gross [ID174](#), J. Grosse-Knetter [ID55](#), L. Guan [ID107](#), G. Guerrieri [ID37](#), R. Guevara [ID127](#), R. Gugel [ID101](#),
 J.A.M. Guhit [ID107](#), A. Guida [ID19](#), E. Guilloton [ID172](#), S. Guindon [ID37](#), F. Guo [ID14,113c](#), J. Guo [ID143a](#),

L. Guo ⁴⁸, L. Guo ^{113b,v}, Y. Guo ¹⁰⁷, A. Gupta ⁴⁹, R. Gupta ¹³¹, S. Gupta ²⁷, S. Gurbuz ²⁵,
 S.S. Gurdasani ⁴⁸, G. Gustavino ^{75a,75b}, P. Gutierrez ¹²², L.F. Gutierrez Zagazeta ¹³⁰,
 M. Gutsche ⁵⁰, C. Gutschow ⁹⁷, C. Gwenlan ¹²⁸, C.B. Gwilliam ⁹³, E.S. Haaland ¹²⁷,
 A. Haas ¹¹⁹, M. Habedank ⁵⁹, C. Haber ^{18a}, H.K. Hadavand ⁸, A. Haddad ⁴¹, A. Hadeef ⁵⁰,
 A.I. Hagan ⁹², J.J. Hahn ¹⁴⁶, E.H. Haines ⁹⁷, M. Haleem ¹⁷¹, J. Haley ¹²³, G.D. Hallewell ¹⁰³,
 J.A. Hallford ⁴⁸, K. Hamano ¹⁷⁰, H. Hamdaoui ¹⁶⁶, M. Hamer ²⁵, S.E.D. Hammoud ⁶⁶,
 E.J. Hampshire ⁹⁶, J. Han ^{142a}, L. Han ^{113a}, L. Han ⁶², S. Han ¹⁴, K. Hanagaki ⁸³,
 M. Hance ¹³⁸, D.A. Hangal ⁴², H. Hanif ¹⁴⁷, M.D. Hank ¹³⁰, J.B. Hansen ⁴³, P.H. Hansen ⁴³,
 T. Harenberg ¹⁷⁶, S. Harkusha ¹⁷⁸, M.L. Harris ¹⁰⁴, Y.T. Harris ²⁵, J. Harrison ¹³,
 P.F. Harrison ¹⁷², M.L.E. Hart ⁹⁷, N.M. Hartman ¹¹¹, N.M. Hartmann ¹¹⁰, R.Z. Hasan ^{96,136},
 Y. Hasegawa ¹⁴⁵, F. Haslbeck ¹²⁸, S. Hassan ¹⁷, R. Hauser ¹⁰⁸, M. Haviernik ¹³⁵,
 C.M. Hawkes ²¹, R.J. Hawkings ³⁷, Y. Hayashi ¹⁵⁸, D. Hayden ¹⁰⁸, C. Hayes ¹⁰⁷,
 R.L. Hayes ¹¹⁶, C.P. Hays ¹²⁸, J.M. Hays ⁹⁵, H.S. Hayward ⁹³, M. He ^{14,113c}, Y. He ⁴⁸,
 Y. He ⁹⁷, N.B. Heatley ⁹⁵, V. Hedberg ⁹⁹, J. Heilman ³⁵, S. Heim ⁴⁸, T. Heim ^{18a},
 J.J. Heinrich ¹²⁵, L. Heinrich ¹¹¹, J. Hejbal ¹³³, M. Helbig ⁵⁰, A. Held ¹⁷⁵, S. Hellesund ¹⁷,
 C.M. Helling ¹⁶⁹, S. Hellman ^{47a,47b}, A.M. Henriques Correia ³⁷, H. Herde ⁹⁹,
 Y. Hernández Jiménez ¹⁵⁰, L.M. Herrmann ²⁵, T. Herrmann ⁵⁰, G. Herten ⁵⁴, R. Hertenberger ¹¹⁰,
 L. Hervas ³⁷, M.E. Hesping ¹⁰¹, N.P. Hessey ^{161a}, J. Hessler ¹¹¹, M. Hidaoui ^{36b}, N. Hidic ¹³⁵,
 E. Hill ¹⁶⁰, T.S. Hillersoy ¹⁷, S.J. Hillier ²¹, J.R. Hinds ¹⁰⁸, F. Hinterkeuser ²⁵, M. Hirose ¹²⁶,
 S. Hirose ¹⁶², D. Hirschbuehl ¹⁷⁶, T.G. Hitchings ¹⁰², B. Hiti ⁹⁴, J. Hobbs ¹⁵⁰, R. Hobincu ^{28e},
 N. Hod ¹⁷⁴, A.M. Hodges ¹⁶⁷, M.C. Hodgkinson ¹⁴⁴, B.H. Hodgkinson ¹²⁸, A. Hoecker ³⁷,
 D.D. Hofer ¹⁰⁷, J. Hofer ¹⁶⁸, J. Hofner ¹⁰¹, M. Holzbock ³⁷, L.B.A.H. Hommels ³³,
 V. Homsak ¹²⁸, J.J. Hong ⁶⁸, T.M. Hong ¹³¹, B.H. Hooberman ¹⁶⁷, W.H. Hopkins ⁶,
 M.C. Hoppesch ¹⁶⁷, Y. Horii ¹¹², M.E. Horstmann ¹¹¹, S. Hou ¹⁵³, M.R. Housenga ¹⁶⁷,
 J. Howarth ⁵⁹, J. Hoya ⁶, M. Hrabovsky ¹²⁴, T. Hryn'ova ⁴, P.J. Hsu ⁶⁵, S.-C. Hsu ¹⁴¹,
 T. Hsu ⁶⁶, M. Hu ^{18a}, Q. Hu ⁶², S. Huang ³³, X. Huang ^{14,113c}, Y. Huang ¹³⁵, Y. Huang ^{113b},
 Y. Huang ¹⁴, Z. Huang ⁶⁶, Z. Hubacek ¹³⁴, F. Huegging ²⁵, T.B. Huffman ¹²⁸,
 M. Hufnagel Maranha De Faria ^{82a}, C.A. Hugli ⁴⁸, M. Huhtinen ³⁷, S.K. Huiberts ¹²⁷,
 R. Hulskens ¹⁰⁵, C.E. Hultquist ^{18a}, D.L. Humphreys ¹⁰⁴, N. Huseynov ¹², J. Huston ¹⁰⁸,
 J. Huth ⁶¹, L. Huth ⁴⁸, R. Hyneman ⁷, G. Iacobucci ⁵⁶, G. Iakovidis ³⁰,
 L. Iconomidou-Fayard ⁶⁶, J.P. Iddon ³⁷, P. Iengo ^{72a,72b}, Y. Iiyama ¹⁵⁸, T. Iizawa ¹⁵⁸,
 Y. Ikegami ⁸³, D. Iliadis ¹⁵⁷, N. Ilic ¹⁶⁰, H. Imam ^{36a}, G. Inacio Goncalves ^{82d},
 S.A. Infante Cabanas ^{139c}, T. Ingebretsen Carlson ^{47a,47b}, J.M. Inglis ⁹⁵, G. Introzzi ^{73a,73b},
 M. Iodice ^{77a}, V. Ippolito ^{75a,75b}, R.K. Irwin ⁹³, M. Ishino ¹⁵⁸, W. Islam ¹⁷⁵, C. Issever ¹⁹,
 S. Istin ^{22a,ao}, K. Itabashi ¹²⁶, H. Ito ¹⁷³, R. Iuppa ^{78a,78b}, A. Ivina ¹⁷⁴, V. Izzo ^{72a}, P. Jacka ¹³⁴,
 P. Jackson ¹, P. Jain ⁴⁸, K. Jakobs ⁵⁴, T. Jakoubek ¹⁷⁴, J. Jamieson ⁵⁹, W. Jang ¹⁵⁸,
 S. Jankovych ¹³⁵, M. Javurkova ¹⁰⁴, P. Jawahar ¹⁰², L. Jeanty ¹²⁵, J. Jejelava ^{154a,ae}, P. Jenni ^{54,f},
 C.E. Jessiman ³⁵, C. Jia ^{142a}, H. Jia ¹⁶⁹, J. Jia ¹⁵⁰, X. Jia ^{111,113c}, Z. Jia ^{113a}, C. Jiang ⁵²,
 Q. Jiang ^{64b}, S. Jiggins ⁴⁸, M. Jimenez Ortega ¹⁶⁸, J. Jimenez Pena ¹³, S. Jin ^{113a}, A. Jinaru ^{28b},
 O. Jinnouchi ¹⁴⁰, P. Johansson ¹⁴⁴, K.A. Johns ⁷, J.W. Johnson ¹³⁸, F.A. Jolly ⁴⁸,
 D.M. Jones ¹⁵¹, E. Jones ⁴⁸, K.S. Jones ⁸, P. Jones ³³, R.W.L. Jones ⁹², T.J. Jones ⁹³,
 H.L. Joos ⁵⁵, R. Joshi ¹²¹, J. Jovicevic ¹⁶, X. Ju ^{18a}, J.J. Junggeburth ³⁷, T. Junkermann ^{63a},
 A. Juste Rozas ^{13,x}, M.K. Juzek ⁸⁷, S. Kabana ^{139f}, A. Kaczmarska ⁸⁷, S.A. Kadir ¹⁴⁸,
 M. Kado ¹¹¹, H. Kagan ¹²¹, M. Kagan ¹⁴⁸, A. Kahn ¹³⁰, C. Kahra ¹⁰¹, T. Kaji ¹⁵⁸,
 E. Kajomovitz ¹⁵⁵, N. Kakati ¹⁷⁴, N. Kakoty ¹³, I. Kalaitzidou ⁵⁴, S. Kandel ⁸, N.J. Kang ¹³⁸,
 D. Kar ³⁴ⁱ, E. Karentzos ²⁵, K. Karki ⁸, O. Karkout ¹¹⁶, S.N. Karpov ³⁹, Z.M. Karpova ³⁹,
 V. Kartvelishvili ^{92,154b}, A.N. Karyukhin ³⁸, E. Kasimi ¹⁵⁷, J. Katzy ⁴⁸, S. Kaur ³⁵,

K. Kawade ¹⁴⁵, M.P. Kawale ¹²², C. Kawamoto ⁸⁸, T. Kawamoto ⁶², E.F. Kay ³⁷,
 S. Kazakos ¹⁰⁸, V.F. Kazanin ³⁸, J.M. Keaveney ^{34a}, R. Keeler ¹⁷⁰, G.V. Kehris ⁶¹,
 J.S. Keller ³⁵, J.M. Kelly ¹⁷⁰, J.J. Kempster ¹⁵¹, O. Kepka ¹³³, J. Kerr ^{161b}, B.P. Kerridge ¹³⁶,
 B.P. Kerševan ⁹⁴, L. Keszezhova ^{29a}, R.A. Khan ¹³¹, A. Khanov ¹²³, A.G. Kharlamov ³⁸,
 T. Kharlamova ³⁸, E.E. Khoda ¹⁴¹, M. Kholodenko ^{132a}, T.J. Khoo ¹⁹, G. Khorauli ¹⁷¹,
 Y. Khoulaki ^{36a}, Y.A.R. Khwaira ¹²⁹, B. Kibirige ³⁴ⁱ, D. Kim ⁶, D.W. Kim ^{18b}, Y.K. Kim ⁴⁰,
 N. Kimura ⁹⁷, M.K. Kingston ⁵⁵, A. Kirchhoff ⁵⁵, C. Kirfel ²⁵, F. Kirfel ²⁵, J. Kirk ¹³⁶,
 A.E. Kiryunin ¹¹¹, S. Kita ¹⁶², O. Kivernyk ²⁵, M. Klassen ¹⁶³, C. Klein ³⁵, L. Klein ¹⁷¹,
 M.H. Klein ⁴⁵, S.B. Klein ⁵⁶, U. Klein ⁹³, A. Klimentov ³⁰, T. Klioutchnikova ³⁷, P. Kluit ¹¹⁶,
 S. Kluth ¹¹¹, E. Kneringer ⁷⁹, T.M. Knight ¹⁶⁰, A. Knue ⁴⁹, M. Kobel ⁵⁰, D. Kobylanski ¹⁷⁴,
 S.F. Koch ¹²⁸, M. Kocian ¹⁴⁸, P. Kodyš ¹³⁵, D.M. Koeck ¹²⁵, T. Koffas ³⁵, O. Kolay ⁵⁰,
 I. Koletsou ⁴, T. Komarek ⁸⁷, K. Köneke ⁵⁵, A.X.Y. Kong ¹, T. Kono ¹²⁰, N. Konstantinidis ⁹⁷,
 P. Kontaxakis ⁵⁶, B. Konya ⁹⁹, R. Kopeliansky ⁴², S. Koperny ^{86a}, R. Koppenhofer ⁵⁴,
 K. Korcyl ⁸⁷, K. Kordas ^{157,d}, A. Korn ⁹⁷, S. Korn ⁵⁵, I. Korolkov ¹³, N. Korotkova ³⁸,
 B. Kortman ¹¹⁶, O. Kortner ¹¹¹, S. Kortner ¹¹¹, W.H. Kostecka ¹¹⁷, M. Kostov ^{29a},
 V.V. Kostyukhin ¹⁴⁶, A. Kotsokechagia ³⁷, A. Kotwal ⁵¹, A. Koulouris ³⁷,
 A. Kourkoumeli-Charalampidi ^{73a,73b}, C. Kourkoumelis ⁹, E. Kourlitis ¹¹¹, O. Kovanda ¹²⁵,
 R. Kowalewski ¹⁷⁰, W. Kozanecki ¹²⁵, A.S. Kozhin ³⁸, V.A. Kramarenko ³⁸, G. Kramberger ⁹⁴,
 P. Kramer ²⁵, M.W. Krasny ¹²⁹, A. Krasznahorkay ¹⁰⁴, A.C. Kraus ¹¹⁷, J.W. Kraus ¹⁷⁶,
 J.A. Kremer ⁴⁸, N.B. Krengel ¹⁴⁶, T. Kresse ⁵⁰, L. Kretschmann ¹⁷⁶, J. Kretzschmar ⁹³,
 P. Krieger ¹⁶⁰, K. Krizka ²¹, K. Kroeninger ⁴⁹, H. Kroha ¹¹¹, J. Kroll ¹³³, J. Kroll ¹³⁰,
 K.S. Krowpman ¹⁰⁸, U. Kruchonak ³⁹, H. Krüger ²⁵, N. Krumnack ⁸⁰, M.C. Kruse ⁵¹,
 O. Kuchinskaia ³⁹, S. Kудay ^{3a}, S. Kuehn ³⁷, R. Kuesters ⁵⁴, T. Kuhl ⁴⁸, V. Kukhtin ³⁹,
 Y. Kulchitsky ³⁹, S. Kuleshov ^{139d,139b}, J. Kull ¹, E.V. Kumar ¹¹⁰, M. Kumar ³⁴ⁱ, N. Kumari ⁴⁸,
 P. Kumari ^{161b}, A. Kupco ¹³³, A. Kupich ³⁸, O. Kuprash ⁵⁴, H. Kurashige ⁸⁵,
 L.L. Kurchaninov ^{161a}, O. Kurdysh ⁴, A. Kurova ³⁸, M. Kuze ¹⁴⁰, A.K. Kvam ¹⁰⁴, J. Kvita ¹²⁴,
 N.G. Kyriacou ¹⁴¹, M. Laassiri ³⁰, C. Lacasta ¹⁶⁸, F. Lacava ^{75a,75b}, H. Lacker ¹⁹, D. Lacour ¹²⁹,
 N.N. Lad ⁹⁷, E. Ladygin ³⁹, A. Lafarge ⁴¹, B. Laforge ¹²⁹, T. Lagouri ¹⁷⁷, F.Z. Lahbabi ^{36a},
 S. Lai ^{55,37}, W.S. Lai ⁹⁷, I.K. Lakomic ⁵⁵, J.E. Lambert ¹⁷⁰, S. Lammers ⁶⁸, W. Lampl ⁷,
 C. Lampoudis ^{157,d}, G. Lamprinoudis ¹⁰¹, A.N. Lancaster ¹¹⁷, E. Lançon ³⁰, U. Landgraf ⁵⁴,
 M.P.J. Landon ⁹⁵, V.S. Lang ⁵⁴, A.J. Lankford ¹⁶⁴, F. Lanni ³⁷, K. Lantzsch ²⁵, A. Lanza ^{73a},
 M. Lanzac Berrocal ¹⁶⁸, J.F. Laporte ¹³⁷, T. Lari ^{71a}, D. Larsen ¹⁷, L. Larson ¹¹,
 F. Lasagni Manghi ^{24b}, M. Lassnig ³⁷, S.D. Lawlor ¹⁴⁴, R. Lazaridou ¹⁶⁴, M. Lazzaroni ^{71a,71b},
 E.T.T. Le ¹⁶⁴, H.D.M. Le ¹⁰⁸, E.M. Le Boulicaut ¹⁷⁷, L.T. Le Pottier ^{18a}, B. Leban ^{24b,24a},
 F. Ledroit-Guillon ⁶⁰, T.F. Lee ^{161b}, L.L. Leeuw ^{34c}, M. Lefebvre ¹⁷⁰, C. Leggett ^{18a},
 G. Lehmann Miotto ³⁷, M. Leigh ⁵⁶, W.A. Leight ¹⁰⁴, W. Leinonen ¹¹⁵, A. Leisos ^{157,u},
 M.A.L. Leite ^{82c}, C.E. Leitgeb ¹⁹, R. Leitner ¹³⁵, K.J.C. Leney ⁴⁵, T. Lenz ²⁵, S. Leone ^{74a},
 C. Leonidopoulos ⁵², A. Leopold ¹⁴⁹, J.H. Lepage Bourbonnais ³⁵, R. Les ¹⁰⁸, C.G. Lester ³³,
 M. Levchenko ³⁸, J. Levêque ⁴, L.J. Levinson ¹⁷⁴, G. Levrini ^{24b,24a}, M.P. Lewicki ⁸⁷,
 C. Lewis ¹⁴¹, D.J. Lewis ⁴, L. Lewitt ¹⁴⁴, A. Li ³⁰, B. Li ^{142a}, C. Li ¹⁰⁷, C-Q. Li ¹¹¹, H. Li ^{142a},
 H. Li ¹⁰², H. Li ¹⁵, H. Li ⁶², H. Li ^{142a}, J. Li ^{143a}, K. Li ¹⁴, L. Li ^{143a}, R. Li ¹⁷⁷, S. Li ^{14,113c},
 S. Li ^{143b,143a}, T. Li ⁵, X. Li ¹⁰⁵, Y. Li ¹⁴, Z. Li ¹⁵⁸, Z. Li ^{14,113c}, Z. Li ⁶², S. Liang ^{14,113c},
 Z. Liang ¹⁴, M. Liberatore ¹³⁷, B. Liberti ^{76a}, G.B. Libotte ^{82d}, K. Lie ^{64c}, J. Lieber Marin ^{82e},
 H. Lien ⁶⁸, H. Lin ¹⁰⁷, S.F. Lin ¹⁵⁰, L. Linden ¹¹⁰, R.E. Lindley ⁷, J.H. Lindon ³⁷, J. Ling ⁶¹,
 E. Lipeles ¹³⁰, A. Lipniacka ¹⁷, A. Lister ¹⁶⁹, J.D. Little ⁶⁸, B. Liu ¹⁴, B.X. Liu ^{113b},
 D. Liu ¹⁵⁵, D. Liu ¹³⁸, E.H.L. Liu ²¹, J.K.K. Liu ¹¹⁹, K. Liu ^{143b}, K. Liu ^{143b,143a}, M. Liu ⁶²,
 M.Y. Liu ⁶², P. Liu ¹⁴, Q. Liu ¹⁴⁸, S. Liu ¹⁵⁰, X. Liu ^{142a}, Y. Liu ^{113b,113c}, Y. Liu ¹⁶⁷,





















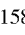

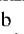








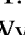


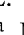
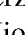

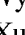


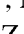


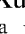
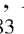




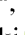
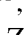




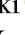




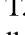
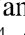


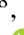


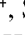



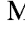




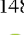
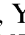


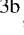


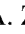















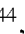




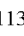
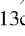
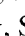
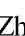
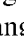

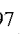
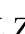
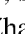



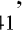
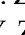




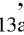
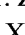
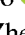
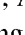


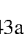
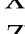
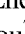
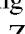
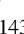


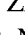
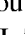
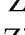


Y.L. Liu ^{142a}, Y.W. Liu ⁶², Z. Liu ^{66,k}, Z. Liu ⁶², S.L. Lloyd ⁹⁵, E.M. Lobodzinska ⁴⁸,
 P. Loch ⁷, E. Lodhi ¹⁶⁰, K. Lohwasser ¹⁴⁴, E. Loiacono ⁴⁸, J.D. Lomas ²¹, J.D. Long ⁴²,
 I. Longarini ¹⁶⁴, R. Longo ¹⁶⁷, A. Lopez Solis ¹³, N.A. Lopez-canelas ⁷, N. Lorenzo Martinez ⁴,
 A.M. Lory ¹¹⁰, M. Losada ^{118a}, G. Löschcke Centeno ⁴, X. Lou ^{47a,47b}, X. Lou ^{14,113c},
 A. Lounis ⁶⁶, P.A. Love ⁹², M. Lu ⁶⁶, S. Lu ¹³⁰, Y.J. Lu ¹⁵³, H.J. Lubatti ¹⁴¹, C. Luci ^{75a,75b},
 F.L. Lucio Alves ^{113a}, F. Luehring ⁶⁸, B.S. Lunday ¹³⁰, O. Lundberg ¹⁴⁹, J. Lunde ³⁷,
 N.A. Luongo ⁶, M.S. Lutz ³⁷, A.B. Lux ²⁶, D. Lynn ³⁰, R. Lysak ¹³³, V. Lysenko ¹³⁴,
 E. Lytken ⁹⁹, V. Lyubushkin ³⁹, T. Lyubushkina ³⁹, M.M. Lyukova ¹⁵⁰, M.Firdaus M. Soberi ⁵²,
 H. Ma ³⁰, K. Ma ⁶², L.L. Ma ^{142a}, W. Ma ⁶², Y. Ma ¹²³, J.C. MacDonald ¹⁰¹,
 P.C. Machado De Abreu Farias ^{82e}, D. Macina ³⁷, R. Madar ⁴¹, T. Madula ⁹⁷, J. Maeda ⁸⁵,
 T. Maeno ³⁰, P.T. Mafa ^{34c,j}, H. Maguire ¹⁴⁴, M. Maheshwari ³³, V. Maiboroda ⁶⁶,
 A. Maio ^{132a,132b,132d}, K. Maj ^{86a}, O. Majersky ⁴⁸, S. Majewski ¹²⁵, R. Makhmanazarov ³⁸,
 N. Makovec ⁶⁶, V. Maksimovic ¹⁶, B. Malaescu ¹²⁹, J. Malamant ¹²⁷, Pa. Malecki ⁸⁷,
 V.P. Maleev ³⁸, F. Malek ^{60,o}, M. Mali ⁹⁴, D. Malito ⁹⁶, A. Maloizel ⁵, S. Maltezos ¹⁰,
 A. Malvezzi Lopes ^{82d}, S. Malyukov ³⁹, J. Mamuzic ⁹⁴, G. Mancini ⁵³, M.N. Mancini ²⁷,
 G. Manco ^{73a,73b}, J.P. Mandalia ⁹⁵, S.S. Mandarry ¹⁵¹, I. Mandić ⁹⁴,
 L. Manhaes de Andrade Filho ^{82a}, I.M. Maniatis ¹⁷⁴, J. Manjarres Ramos ⁹⁰, D.C. Mankad ¹⁷⁴,
 A. Mann ¹¹⁰, T. Manoussos ³⁷, M.N. Mantinan ⁴⁰, S. Manzoni ³⁷, L. Mao ^{143a},
 X. Mapekula ^{34c}, A. Marantis ¹⁵⁷, R.R. Marcelo Gregorio ⁹⁵, G. Marchiori ⁵, C. Marcon ^{71a},
 E. Maricic ¹⁶, M. Marinescu ⁴⁸, S. Marium ⁴⁸, M. Marjanovic ¹²², A. Markhoos ⁵⁴,
 M. Markovitch ⁶⁶, M.K. Maroun ¹⁰⁴, M.C. Marr ¹⁴⁷, G.T. Marsden ¹⁰², E.J. Marshall ⁹²,
 Z. Marshall ^{18a}, S. Marti-Garcia ¹⁶⁸, J. Martin ⁹⁷, T.A. Martin ¹³⁶, V.J. Martin ⁵²,
 B. Martin dit Latour ¹⁷, L. Martinelli ^{75a,75b}, M. Martinez ^{13,x}, P. Martinez Agullo ¹⁶⁸,
 V.I. Martinez Outschoorn ¹⁰⁴, P. Martinez Suarez ³⁷, S. Martin-Haugh ¹³⁶, G. Martinovicova ¹³⁵,
 V.S. Martoiu ^{28b}, A.C. Martyniuk ⁹⁷, A. Marzin ³⁷, D. Mascione ^{78a,78b}, L. Masetti ¹⁰¹,
 J. Masik ¹⁰², A.L. Maslennikov ³⁹, S.L. Mason ⁴², P. Massarotti ^{72a,72b}, P. Mastrandrea ^{74a,74b},
 A. Mastroberardino ^{44b,44a}, T. Masubuchi ¹²⁶, T.T. Mathew ¹²⁵, J. Matousek ¹³⁵, D.M. Mattern ⁴⁹,
 K. Mauer ⁴⁸, J. Maurer ^{28b}, T. Maurin ⁵⁹, A.J. Maury ⁶⁶, B. Maček ⁹⁴, C. Mavungu Tsava ¹⁰³,
 D.A. Maximov ³⁸, A.E. May ¹⁰², E. Mayer ⁴¹, R. Mazini ³⁴ⁱ, I. Maznas ¹¹⁷, S.M. Mazza ¹³⁸,
 E. Mazzeo ³⁷, J.P. Mc Gowan ¹⁷⁰, S.P. Mc Kee ¹⁰⁷, C.A. Mc Lean ⁶, C.C. McCracken ¹⁶⁹,
 E.F. McDonald ¹⁰⁶, A.E. McDougall ¹¹⁶, L.F. Mcelhinney ⁹², J.A. Mcfayden ¹⁵¹,
 R.P. McGovern ¹³⁰, R.P. Mckenzie ³⁴ⁱ, T.C. McLachlan ⁴⁸, D.J. McLaughlin ⁹⁷, S.J. McMahon ¹³⁶,
 C.M. Mcpartland ⁹³, R.A. McPherson ^{170,ab}, S. Mehlhase ¹¹⁰, A. Mehta ⁹³, D. Melini ¹⁶⁸,
 B.R. Mellado Garcia ³⁴ⁱ, A.H. Melo ⁵⁵, F. Meloni ⁴⁸, A.M. Mendes Jacques Da Costa ¹⁰²,
 L. Meng ⁹², S. Menke ¹¹¹, M. Mentink ³⁷, E. Meoni ^{44b,44a}, G. Mercado ¹¹⁷, S. Merianos ¹⁵⁷,
 C. Merlassino ^{69a,69c}, C. Meroni ^{71a,71b}, J. Metcalfe ⁶, A.S. Mete ⁶, E. Meuser ¹⁰¹, C. Meyer ⁶⁸,
 J-P. Meyer ¹³⁷, Y. Miao ^{113a}, R.P. Middleton ¹³⁶, M. Mihovilovic ⁶⁶, L. Mijović ⁵²,
 G. Mikenberg ¹⁷⁴, M. Mikestikova ¹³³, M. Mikuž ⁹⁴, H. Mildner ¹⁰¹, A. Milic ³⁷,
 D.W. Miller ⁴⁰, E.H. Miller ¹⁴⁸, A. Milov ¹⁷⁴, D.A. Milstead ^{47a,47b}, T. Min ^{113a}, A.A. Minaenko ³⁸,
 I.A. Minashvili ^{154b}, A.I. Mincer ¹¹⁹, B. Mindur ^{86a}, M. Mineev ³⁹, Y. Mino ⁸⁸, L.M. Mir ¹³,
 M. Miralles Lopez ⁵⁹, M. Mironova ^{18a}, M. Missio ⁴¹, A. Mitra ¹⁷², V.A. Mitsou ¹⁶⁸,
 Y. Mitsumori ¹¹², O. Miu ¹⁶⁰, P.S. Miyagawa ⁹⁵, T. Mkrtychyan ³⁷, M. Mlinarevic ⁹⁷,
 T. Mlinarevic ⁹⁷, M. Mlynarikova ¹³⁵, L. Mlynarska ^{86a}, C. Mo ^{143a}, S. Mobius ²⁰,
 M.H. Mohamed Farook ¹¹⁴, S. Mohapatra ⁴², S. Mohiuddin ¹²³, G. Mokgatitswane ³⁴ⁱ,
 L. Moleri ¹⁷⁴, U. Molinatti ¹²⁸, L.G. Mollier ²⁰, B. Mondal ¹³³, S. Mondal ¹³⁴, K. Mönig ⁴⁸,
 E. Monnier ¹⁰³, L. Monsonis Romero ¹⁶⁸, J. Montejo Berlingen ¹³, A. Montella ^{47a,47b},
 M. Montella ¹²¹, F. Montekali ^{77a,77b}, F. Monticelli ⁹¹, S. Monzani ^{69a,69c}, A. Morancho Tarda ⁴³,

N. Morange ⁶⁶, A.L. Moreira De Carvalho ⁴⁸, M. Moreno Llácer ¹⁶⁸, C. Moreno Martinez ⁵⁶,
 J.M. Moreno Perez ^{23b}, P. Morettini ^{57b}, S. Morgenstern ³⁷, M. Morii ⁶¹, M. Morinaga ¹⁵⁸,
 M. Moritsu ⁸⁹, F. Morodei ^{75a,75b}, P. Moschovakos ³⁷, B. Moser ⁵⁴, M. Mosidze ^{154b},
 T. Moskalets ⁴⁵, P. Moskvitina ¹¹⁵, J. Moss ³², P. Moszkowicz ^{86a}, A. Moussa ^{36d}, Y. Moyal ¹⁷⁴,
 H. Moyano Gomez ¹³, E.J.W. Moyse ¹⁰⁴, L.J. Mozarsky ⁴², T.G. Mroz ⁸⁷, S. Muanza ¹⁰³,
 M. Mucha ²⁵, J. Mueller ¹³¹, R. Müller ³⁷, G.A. Mullier ¹⁶⁶, A.J. Mullin ³³, J.J. Mullin ⁵¹,
 A.C. Mullins ⁴⁵, A.E. Mulski ⁶¹, D.P. Mungo ¹⁶⁰, D. Munoz Perez ¹⁶⁸, F.J. Munoz Sanchez ¹⁰²,
 W.J. Murray ^{172,136}, M. Muškinja ⁹⁴, C. Mwewa ⁴⁸, A.G. Myagkov ^{38,a}, A.J. Myers ⁸,
 G. Myers ¹⁰⁷, M. Myska ¹³⁴, B.P. Nachman ¹⁴⁸, K. Nagai ¹²⁸, K. Nagano ⁸³, R. Nagasaka ¹⁵⁸,
 J.L. Nagle ^{30,al}, E. Nagy ¹⁰³, A.M. Nairz ³⁷, Y. Nakahama ⁸³, K. Nakamura ⁸³, K. Nakkalil ⁵,
 A. Nandi ^{63b}, H. Nanjo ¹²⁶, E.A. Narayanan ⁴⁵, Y. Narukawa ¹⁵⁸, I. Naryshkin ³⁸,
 L. Nasella ^{71a,71b}, S. Nasri ^{118b}, C. Nass ²⁵, G. Navarro ^{23a}, A. Nayaz ¹⁹, P.Y. Nechaeva ³⁸,
 S. Nechaeva ^{24b,24a}, F. Nechansky ¹³³, L. Nedic ¹²⁸, T.J. Neep ²¹, A. Negri ^{73a,73b},
 M. Negrini ^{24b}, C. Nellist ¹¹⁶, C. Nelson ¹⁰⁵, K. Nelson ¹⁰⁷, S. Nemecek ¹³³, M. Nessi ^{37,g},
 M.S. Neubauer ¹⁶⁷, J. Newell ⁹³, P.R. Newman ²¹, Y.W.Y. Ng ¹⁶⁷, B. Ngair ^{118a},
 H.D.N. Nguyen ¹⁰⁹, J.D. Nichols ¹²², R.B. Nickerson ¹²⁸, R. Nicolaidou ¹³⁷, J. Nielsen ¹³⁸,
 M. Niemeyer ⁵⁵, J. Niermann ³⁷, N. Nikiforou ³⁷, V. Nikolaenko ^{38,a}, I. Nikolic-Audit ¹²⁹,
 P. Nilsson ³⁰, I. Ninca ⁴⁸, G. Ninio ¹⁵⁶, A. Nisati ^{75a}, R. Nisius ¹¹¹, N. Nitika ¹⁷⁴,
 E.K. Nkadimeng ^{34b}, T. Nobe ¹⁵⁸, D. Noll ¹⁴⁸, T. Nommensen ¹⁵², M.B. Norfolk ¹⁴⁴,
 B.J. Norman ³⁵, L.C. Nosler ^{18a}, M. Noury ^{36a}, J. Novak ⁹⁴, T. Novak ⁹⁴, R. Novotny ¹³⁴,
 L. Nozka ¹²⁴, K. Ntekas ¹⁶⁴, D. Ntonis ¹⁴⁸, N.M.J. Nunes De Moura Junior ^{82b}, J. Ocariz ¹²⁹,
 I. Ochoa ^{132a}, A. Odella Rodriguez ¹³, S. Oerdek ^{48,y}, J.T. Offermann ⁴⁰, A. Ogrodnik ⁸⁷,
 A. Oh ¹⁰², C.C. Ohm ¹⁴⁹, H. Oide ⁸³, M.L. Ojeda ³⁷, Y. Okumura ¹⁵⁸, L.F. Oleiro Seabra ^{132a},
 I. Oleksiyuk ⁵⁶, G. Oliveira Correa ¹³, D. Oliveira Damazio ³⁰, J.L. Oliver ¹⁶⁴, R. Omar ⁶⁸,
 Ö.O. Öncel ⁵⁴, A.P. O'Neill ²⁰, A. Onofre ^{132a,132e,e}, P.U.E. Onyisi ¹¹, M.J. Oreglia ⁴⁰,
 D. Orestano ^{77a,77b}, R. Orlandini ^{77a,77b}, R.S. Orr ¹⁶⁰, L.M. Osojnak ⁴², Y. Osumi ¹¹²,
 G. Otero y Garzon ³¹, H. Otono ⁸⁹, M. Ouchrif ^{36d}, F. Ould-Saada ¹²⁷, T. Ovsiannikova ¹⁴¹,
 M. Owen ⁵⁹, R.E. Owen ¹³⁶, V.E. Ozcan ^{22a}, F. Ozturk ⁸⁷, N. Ozturk ⁸, S. Ozturk ⁸¹,
 H.A. Pacey ¹²⁸, K. Pachal ^{161a}, A. Pacheco Pages ¹³, C. Padilla Aranda ¹³, G. Padovano ^{75a,75b},
 S. Pagan Griso ^{18a}, J. Pampel ²⁵, J. Pan ¹⁷⁷, D.K. Panchal ¹¹, C.E. Pandini ⁶⁰,
 J.G. Panduro Vazquez ¹³⁶, H.D. Pandya ¹, H. Pang ¹³⁷, P. Pani ⁴⁸, G. Panizzo ^{69a,69c},
 L. Panwar ¹²⁹, L. Paolozzi ⁵⁶, S. Parajuli ¹⁶⁷, A. Paramonov ⁶, C. Paraskevopoulos ⁵³,
 D. Paredes Hernandez ^{64b}, S.R. Paredes Saenz ⁵², A. Pareti ^{73a,73b}, K.R. Park ⁴², T.H. Park ¹¹¹,
 F. Parodi ^{57b,57a}, J.A. Parsons ⁴², U. Parzefall ⁵⁴, B. Pascual Dias ⁴¹, L. Pascual Dominguez ¹⁰⁰,
 E. Pasqualucci ^{75a}, S. Passaggio ^{57b}, F. Pastore ⁹⁶, P. Patel ⁸⁷, U.M. Patel ⁵¹, J.R. Pater ¹⁰²,
 T. Pauly ³⁷, F. Pauwels ¹³⁵, C.I. Pazos ¹⁶³, M. Pedersen ¹²⁷, R. Pedro ^{132a}, S.V. Peleganchuk ³⁸,
 O. Penc ¹³³, S. Peng ¹⁵, G.D. Penn ¹⁷⁷, K.E. Pensi ¹¹⁰, M. Penzin ³⁸, B.S. Peralva ^{82d},
 A.P. Pereira Peixoto ¹⁴¹, L. Pereira Sanchez ¹⁴⁸, D.V. Perepelitsa ^{30,al}, G. Perera ¹⁰⁴,
 E. Perez Codina ³⁷, M. Perganti ¹⁰, H. Pernegger ³⁷, S. Perrella ^{75a,75b}, K. Peters ⁴⁸,
 R.F.Y. Peters ¹⁰², B.A. Petersen ³⁷, T.C. Petersen ⁴³, E. Petit ¹⁰³, V. Petousis ¹³⁴,
 A.R. Petri ^{71a,71b}, C. Petridou ^{157,d}, T. Petru ¹³⁵, M. Pettee ^{18a}, A. Petukhov ⁸¹, K. Petukhova ³⁷,
 R. Pezoa ^{139g}, L. Pezzotti ^{24b,24a}, G. Pezzullo ¹⁷⁷, L. Pfaffenbichler ³⁷, A.J. Pflieger ⁷⁹,
 T.M. Pham ¹⁷⁵, T. Pham ¹⁰⁶, P.W. Phillips ¹³⁶, G. Piacquadio ¹⁵⁰, E. Pianori ^{18a}, F. Piazza ¹²⁵,
 R. Piegai ³¹, D. Pietreanu ^{28b}, A.D. Pilkington ¹⁰², M. Pinamonti ^{69a,69c}, J.L. Pinfeld ²,
 G. Pinheiro Matos ⁴², B.C. Pinheiro Pereira ^{132a}, J. Pinol Bel ¹³, A.E. Pinto Pinoargote ¹²⁹,
 L. Pintucci ^{69a,69c}, K.M. Piper ¹⁵¹, A. Pirttikoski ⁵⁶, D.A. Pizzi ³⁵, L. Pizzimento ^{64b},
 A. Plebani ³³, M.-A. Pleier ³⁰, V. Pleskot ¹³⁵, E. Plotnikova ³⁹, G. Poddar ⁹⁵, R. Poettgen ⁹⁹,

L. Poggioli [id](#)¹²⁹, S. Polacek [id](#)¹³⁵, G. Polesello [id](#)^{73a}, A. Poley [id](#)¹⁴⁷, A. Polini [id](#)^{24b}, C.S. Pollard [id](#)¹⁷²,
 Z.B. Pollock [id](#)¹²¹, E. Pompa Pacchi [id](#)¹²², N.I. Pond [id](#)⁹⁷, D. Ponomarenko [id](#)⁶⁸, L. Pontecorvo [id](#)³⁷,
 S. Popa [id](#)^{28a}, G.A. Popeneciu [id](#)^{28d}, A. Poreba [id](#)³⁷, D.M. Portillo Quintero [id](#)^{161a}, S. Pospisil [id](#)¹³⁴,
 M.A. Postill [id](#)¹⁴⁴, P. Postolache [id](#)^{28c}, K. Potamianos [id](#)¹⁷², P.A. Potepa [id](#)^{86a}, I.N. Potrap [id](#)³⁹,
 C.J. Potter [id](#)³³, H. Potti [id](#)¹⁵², J. Poveda [id](#)¹⁶⁸, M.E. Pozo Astigarraga [id](#)³⁷, R. Pozzi [id](#)³⁷,
 A. Prades Ibanez [id](#)^{76a,76b}, S.R. Pradhan [id](#)¹⁴⁴, J. Pretel [id](#)¹⁷⁰, D. Price [id](#)¹⁰², M. Primavera [id](#)^{70a},
 L. Primomo [id](#)^{69a,69c}, M.A. Principe Martin [id](#)¹⁰⁰, R. Privara [id](#)¹²⁴, T. Procter [id](#)^{86b}, M.L. Proffitt [id](#)¹⁴¹,
 N. Proklova [id](#)¹³⁰, K. Prokofiev [id](#)^{64c}, G. Proto [id](#)¹¹¹, J. Proudfoot [id](#)⁶, M. Przybycien [id](#)^{86a},
 W.W. Przygoda [id](#)^{86b}, A. Psallidas [id](#)⁴⁶, J.E. Puddefoot [id](#)¹⁴⁴, D. Pudzha [id](#)⁵³, H.I. Purnell [id](#)¹,
 D. Pyatiizbyantseva [id](#)¹¹⁵, J. Qian [id](#)¹⁰⁷, R. Qian [id](#)¹⁰⁸, D. Qichen [id](#)¹²⁸, Y. Qin [id](#)¹³, T. Qiu [id](#)⁵²,
 A. Quadt [id](#)⁵⁵, M. Queitsch-Maitland [id](#)¹⁰², G. Quetant [id](#)⁵⁶, R.P. Quinn [id](#)¹⁶⁹, G. Rabanal Bolanos [id](#)⁶¹,
 D. Rafanoharana [id](#)¹¹¹, F. Raffaelli [id](#)^{76a,76b}, F. Ragusa [id](#)^{71a,71b}, J.L. Rainbolt [id](#)⁴⁰, S. Rajagopalan [id](#)³⁰,
 E. Ramakoti [id](#)³⁹, L. Rambelli [id](#)^{57b,57a}, I.A. Ramirez-Berend [id](#)³⁵, K. Ran [id](#)^{107,113c}, D.S. Rankin [id](#)¹³⁰,
 N.P. Rapheeha [id](#)³⁴ⁱ, H. Rasheed [id](#)^{28b}, A. Rastogi [id](#)^{18a}, S. Rave [id](#)¹⁰¹, S. Ravera [id](#)^{57b,57a}, B. Ravina [id](#)³⁷,
 I. Ravinovich [id](#)¹⁷⁴, M. Raymond [id](#)³⁷, A.L. Read [id](#)¹²⁷, N.P. Radioff [id](#)¹⁴⁴, D.M. Rebutti [id](#)^{73a,73b},
 A.S. Reed [id](#)⁵⁹, K. Reeves [id](#)²⁷, D. Reikher [id](#)³⁷, A. Rej [id](#)⁴⁹, C. Rembser [id](#)³⁷, H. Ren [id](#)⁶², M. Renda [id](#)^{28b},
 F. Renner [id](#)⁴⁸, A.G. Rennie [id](#)⁵⁹, M. Repik [id](#)⁵⁶, A.L. Rescia [id](#)^{57b,57a}, S. Resconi [id](#)^{71a},
 M. Ressegotti [id](#)^{57b,57a}, S. Rettie [id](#)¹¹⁶, W.F. Rettie [id](#)³⁵, M.M. Revering [id](#)³³, E. Reynolds [id](#)^{18a},
 O.L. Rezanova [id](#)³⁹, P. Reznicek [id](#)¹³⁵, H. Riani [id](#)^{36d}, N. Ribaric [id](#)⁵¹, B. Ricci [id](#)^{69a,69c}, E. Ricci [id](#)^{78a,78b},
 R. Richter [id](#)¹¹¹, S. Richter [id](#)^{47a,47b}, E. Richter-Was [id](#)^{86b}, M. Ridel [id](#)¹²⁹, S. Ridouani [id](#)^{36d}, P. Rieck [id](#)¹¹⁹,
 P. Riedler [id](#)³⁷, E.M. Riefel [id](#)^{47a,47b}, J.O. Rieger [id](#)¹¹⁶, M. Rijssenbeek [id](#)¹⁵⁰, M. Rimoldi [id](#)^{34c},
 L. Rinaldi [id](#)^{24b,24a}, P. Rincke [id](#)^{166,55}, G. Ripellino [id](#)¹⁶⁶, I. Riu [id](#)¹³, J.C. Rivera Vergara [id](#)¹⁷⁰,
 F. Rizatdinova [id](#)¹²³, E. Rizvi [id](#)⁹⁵, B.R. Roberts [id](#)⁴⁰, S.S. Roberts [id](#)¹³⁸, D. Robinson [id](#)³³, A. Robson [id](#)⁵⁹,
 A. Rocchi [id](#)^{76a,76b}, C. Roda [id](#)^{74a,74b}, F.A. Rodriguez [id](#)¹¹⁷, S. Rodriguez Bosca [id](#)³⁷,
 Y. Rodriguez Garcia [id](#)^{23a}, A.M. Rodríguez Vera [id](#)¹¹⁷, S. Roe [id](#)³⁷, J.T. Roemer [id](#)³⁷, O. Røhne [id](#)¹²⁷,
 R.A. Rojas [id](#)³⁷, C.P.A. Roland [id](#)¹²⁹, A. Romaniouk [id](#)⁷⁹, E. Romano [id](#)^{73a,73b}, M. Romano [id](#)^{24b},
 A.C. Romero Hernandez [id](#)¹⁶⁷, N. Rompotis [id](#)⁹³, L. Roos [id](#)¹²⁹, S. Rosati [id](#)^{75a}, B.J. Rosser [id](#)⁴⁰,
 E. Rossi [id](#)¹²⁸, E. Rossi [id](#)^{72a,72b}, L.P. Rossi [id](#)⁶¹, L. Rossini [id](#)⁵⁴, R. Rosten [id](#)¹²¹, M. Rotaru [id](#)^{28b},
 D. Rousseau [id](#)⁶⁶, D. Rousso [id](#)⁴⁸, S. Roy-Garand [id](#)¹⁶⁰, A. Rozanov [id](#)¹⁰³, Z.M.A. Rozario [id](#)⁵⁹,
 Y. Rozen [id](#)¹⁵⁵, A. Rubio Jimenez [id](#)¹⁶⁸, V.H. Ruelas Rivera [id](#)¹⁹, T.A. Ruggeri [id](#)¹, A. Ruggiero [id](#)¹²⁸,
 A. Ruiz-Martinez [id](#)¹⁶⁸, A. Rummler [id](#)³⁷, Z. Rurikova [id](#)⁵⁴, N.A. Rusakovich [id](#)³⁹, S. Ruscelli [id](#)⁴⁹,
 H.L. Russell [id](#)¹⁷⁰, G. Russo [id](#)^{75a,75b}, J.P. Rutherford [id](#)⁷, S. Rutherford Colmenares [id](#)³³, M. Rybar [id](#)¹³⁵,
 P. Rybczynski [id](#)^{86a}, A. Ryzhov [id](#)⁴⁵, H.F-W. Sadrozinski [id](#)¹³⁸, F. Safai Tehrani [id](#)^{75a}, S. Saha [id](#)¹,
 M. Sahinsoy [id](#)⁸¹, B. Sahoo [id](#)¹⁷⁴, A. Saibel [id](#)¹⁶⁸, B.T. Saifuddin [id](#)¹²², M. Saimpert [id](#)¹³⁷, G.T. Saito [id](#)^{82c},
 M. Saito [id](#)¹⁵⁸, T. Saito [id](#)¹⁵⁸, A. Sala [id](#)^{71a,71b}, A. Salmikov [id](#)¹⁴⁸, J. Salt [id](#)¹⁶⁸, A. Salvador Salas [id](#)¹⁵⁶,
 F. Salvatore [id](#)¹⁵¹, A. Salzburger [id](#)³⁷, D. Sammel [id](#)⁵⁴, E. Sampson [id](#)⁹², D. Sampsonidis [id](#)^{157,d},
 D. Sampsonidou [id](#)¹²⁵, M.A.A. Samy [id](#)⁵⁹, J. Sánchez [id](#)¹⁶⁸, V. Sanchez Sebastian [id](#)¹⁶⁸, H. Sandaker [id](#)¹²⁷,
 C.O. Sander [id](#)⁴⁸, J.A. Sandesara [id](#)¹⁷⁵, M. Sandhoff [id](#)¹⁷⁶, C. Sandoval [id](#)^{23b}, L. Sanfilippo [id](#)^{63a},
 D.P.C. Sankey [id](#)¹³⁶, T. Sano [id](#)⁸⁸, A. Sansoni [id](#)⁵³, M. Santana Queiroz [id](#)^{18b}, L. Santi [id](#)³⁷, C. Santoni [id](#)⁴¹,
 H. Santos [id](#)^{132a,132b}, A. Santra [id](#)¹⁷⁴, E. Sanzani [id](#)^{24b,24a}, K.A. Saoucha [id](#)^{84b}, J.G. Saraiva [id](#)^{132a,132d},
 J. Sardain [id](#)⁷, O. Sasaki [id](#)⁸³, K. Sato [id](#)¹⁶², C. Sauer [id](#)³⁷, E. Sauvan [id](#)⁴, P. Savard [id](#)^{160,ai}, R. Sawada [id](#)¹⁵⁸,
 C. Sawyer [id](#)¹³⁶, L. Sawyer [id](#)⁹⁸, A.M. Sayed [id](#)²⁷, C. Sbarra [id](#)^{24b}, A. Sbrizzi [id](#)^{24b,24a}, T. Scanlon [id](#)⁹⁷,
 J. Schaarschmidt [id](#)¹⁴¹, U. Schäfer [id](#)¹⁰¹, A.C. Schaffer [id](#)^{66,45}, D. Schaile [id](#)¹¹⁰, R.D. Schamberger [id](#)¹⁵⁰,
 C. Scharf [id](#)¹⁹, M.M. Schefer [id](#)²⁰, V.A. Schegelsky [id](#)³⁸, D. Scheirich [id](#)¹³⁵, M. Schernau [id](#)^{139f},
 C. Scheulen [id](#)⁵⁶, C. Schiavi [id](#)^{57b,57a}, M. Schioppa [id](#)^{44b,44a}, B. Schlag [id](#)¹⁴⁸, S. Schlenker [id](#)³⁷,
 J. Schmeing [id](#)¹⁷⁶, E. Schmidt [id](#)¹¹¹, M.A. Schmidt [id](#)¹⁷⁶, K. Schmieden [id](#)²⁵, C. Schmitt [id](#)¹⁰¹,
 N. Schmitt [id](#)¹⁰¹, S. Schmitt [id](#)⁴⁸, N.A. Schneider [id](#)¹¹⁰, L. Schoeffel [id](#)¹³⁷, A. Schoening [id](#)^{63b},

P.G. Scholer ^{id}35, E. Schopf ^{id}146, M. Schott ^{id}25, S. Schramm ^{id}56, T. Schroer ^{id}56,
 H-C. Schultz-Coulon ^{id}63a, M. Schumacher ^{id}54, B.A. Schumm ^{id}138, Ph. Schune ^{id}137, H.R. Schwartz ^{id}7,
 A. Schwartzman ^{id}148, T.A. Schwarz ^{id}107, Ph. Schwemling ^{id}137, R. Schwienhorst ^{id}108,
 F.G. Sciacca ^{id}20, A. Sciandra ^{id}30, G. Sciolla ^{id}27, F. Scuri ^{id}74a, C.D. Sebastiani ^{id}37, K. Sedlaczek ^{id}117,
 S.C. Seidel ^{id}114, A. Seiden ^{id}138, B.D. Seidlitz ^{id}42, C. Seitz ^{id}48, J.M. Seixas ^{id}82b, G. Sekhniaidze ^{id}72a,
 L. Selem ^{id}60, N. Semprini-Cesari ^{id}24b,24a, A. Semushin ^{id}178, D. Sengupta ^{id}56, V. Senthilkumar ^{id}168,
 L. Serin ^{id}66, M. Sessa ^{id}72a,72b, H. Severini ^{id}122, F. Sforza ^{id}57b,57a, A. Sfyrta ^{id}56, Q. Sha ^{id}14,
 H. Shaddix ^{id}117, A.H. Shah ^{id}33, R. Shaheen ^{id}149, J.D. Shahinian ^{id}130, M. Shamim ^{id}37, L.Y. Shan ^{id}14,
 M. Shapiro ^{id}18a, A. Sharma ^{id}37, A.S. Sharma ^{id}169, P. Sharma ^{id}30, P.B. Shatalov ^{id}38, K. Shaw ^{id}151,
 S.M. Shaw ^{id}102, Q. Shen ^{id}14, D.J. Sheppard ^{id}147, P. Sherwood ^{id}97, L. Shi ^{id}97, X. Shi ^{id}14,
 S. Shimizu ^{id}83, I.P.J. Shipsey ^{id}128,* , S. Shirabe ^{id}89, M. Shiyakova ^{id}39,z, M.J. Shochet ^{id}40,
 D.R. Shope ^{id}127, B. Shrestha ^{id}122, S. Shrestha ^{id}121,an, I. Shreyber ^{id}39, M.J. Shroff ^{id}170, P. Sicho ^{id}133,
 A.M. Sickles ^{id}167, E. Sideras Haddad ^{id}34i,165, A.C. Sidley ^{id}116, A. Sidoti ^{id}24b, F. Siegert ^{id}50,
 Dj. Sijacki ^{id}16, F. Sili ^{id}62, J.M. Silva ^{id}52, I. Silva Ferreira ^{id}82b, M.V. Silva Oliveira ^{id}30,
 S.B. Silverstein ^{id}47a, S. Simion ^{id}66, R. Simoniello ^{id}37, E.L. Simpson ^{id}102, H. Simpson ^{id}151,
 L.R. Simpson ^{id}6, S. Simsek ^{id}81, S. Sindhu ^{id}55, P. Sinervo ^{id}160, S.N. Singh ^{id}27, S. Singh ^{id}30,
 S. Sinha ^{id}48, S. Sinha ^{id}102, M. Sioli ^{id}24b,24a, K. Sioulas ^{id}9, I. Siral ^{id}37, E. Sitnikova ^{id}48,
 J. Sjölin ^{id}47a,47b, A. Skaf ^{id}55, E. Skorda ^{id}21, P. Skubic ^{id}122, M. Slawinska ^{id}87, I. Slazyk ^{id}17,
 I. Sliusar ^{id}127, V. Smakhtin ^{id}174, B.H. Smart ^{id}136, S.Yu. Smirnov ^{id}139b, Y. Smirnov ^{id}81,
 L.N. Smirnova ^{id}38,a, O. Smirnova ^{id}99, A.C. Smith ^{id}42, D.R. Smith ^{id}164, J.L. Smith ^{id}102, M.B. Smith ^{id}35,
 R. Smith ^{id}148, H. Smitmanns ^{id}101, M. Smizanska ^{id}92, K. Smolek ^{id}134, P. Smolyanskiy ^{id}134,
 A.A. Snesarev ^{id}39, H.L. Snoek ^{id}116, R.M. Snyder ^{id}51, S. Snyder ^{id}30, R. Sobie ^{id}170,ab, A. Soffer ^{id}156,
 C.A. Solans Sanchez ^{id}37, E.Yu. Soldatov ^{id}39, U. Soldevila ^{id}168, A.A. Solodkov ^{id}34i, S. Solomon ^{id}27,
 A. Soloshenko ^{id}39, K. Solovieva ^{id}54, O.V. Solovyanov ^{id}41, P. Sommer ^{id}50, A. Sonay ^{id}13,
 A. Sopczak ^{id}134, A.L. Soppio ^{id}52, F. Sopkova ^{id}29b, J.D. Sorenson ^{id}114, I.R. Sotarriva Alvarez ^{id}140,
 V. Sothilingam ^{id}63a, O.J. Soto Sandoval ^{id}139c,139b, S. Sottocornola ^{id}68, R. Soualah ^{id}84a,
 Z. Soumami ^{id}36e, D. South ^{id}48, N. Soybelman ^{id}174, S. Spagnolo ^{id}70a,70b, D. Sperlich ^{id}54,
 B. Spisso ^{id}72a,72b, D.P. Spiteri ^{id}59, L. Splendori ^{id}103, M. Spousta ^{id}135, E.J. Staats ^{id}35, R. Stamen ^{id}63a,
 E. Stanecka ^{id}87, W. Stanek-Maslouska ^{id}48, M.V. Stange ^{id}50, B. Stanislaus ^{id}18a, M.M. Stanitzki ^{id}48,
 E.A. Starchenko ^{id}38, G.H. Stark ^{id}138, J. Stark ^{id}90, P. Staroba ^{id}133, P. Starovoitov ^{id}84b,
 R. Staszewski ^{id}87, C. Stauch ^{id}110, G. Stavropoulos ^{id}46, A. Stefl ^{id}37, A. Stein ^{id}101, P. Steinberg ^{id}30,
 B. Stelzer ^{id}147,161a, H.J. Stelzer ^{id}131, O. Stelzer ^{id}161a, H. Stenzel ^{id}58, T.J. Stevenson ^{id}151,
 G.A. Stewart ^{id}37, J.R. Stewart ^{id}123, G. Stoicea ^{id}28b, M. Stolarski ^{id}132a, S. Stonjek ^{id}111,
 A. Straessner ^{id}50, J. Strandberg ^{id}149, S. Strandberg ^{id}47a,47b, M. Stratmann ^{id}176, M. Strauss ^{id}122,
 T. Strebler ^{id}103, P. Striznec ^{id}29b, R. Ströhmer ^{id}171, D.M. Strom ^{id}125, R. Stroynowski ^{id}45,
 A. Strubig ^{id}47a,47b, S.A. Stucci ^{id}30, B. Stugu ^{id}17, J. Stupak ^{id}122, N.A. Styles ^{id}48, D. Su ^{id}148,
 S. Su ^{id}62, X. Su ^{id}62, D. Suchy ^{id}29a, A.D. Sudhakar Ponnu ^{id}55, K. Sugizaki ^{id}130, V.V. Sulin ^{id}38,
 D.M.S. Sultan ^{id}128, L. Sultanaliyeva ^{id}25, S. Sultansoy ^{id}3b, S. Sun ^{id}175, W. Sun ^{id}14, N. Sur ^{id}99,
 M.R. Sutton ^{id}151, M. Svatos ^{id}133, P.N. Swallow ^{id}33, M. Swiatlowski ^{id}161a, A. Swoboda ^{id}37,
 I. Sykora ^{id}29a, M. Sykora ^{id}135, T. Sykora ^{id}135, D. Ta ^{id}101, K. Tackmann ^{id}48,y, A. Taffard ^{id}164,
 R. Tafirout ^{id}161a, Y. Takubo ^{id}83, M. Talby ^{id}103, A.A. Talyshev ^{id}38, K.C. Tam ^{id}64b, N.M. Tamir ^{id}156,
 A. Tanaka ^{id}158, J. Tanaka ^{id}158, R. Tanaka ^{id}66, M. Tanasini ^{id}150, Z. Tao ^{id}169, S. Tapia Araya ^{id}139g,
 S. Tapprogge ^{id}101, A. Tarek Abouelfadl Mohamed ^{id}37, S. Tarem ^{id}155, K. Tariq ^{id}14, G. Tarna ^{id}37,
 G.F. Tartarelli ^{id}71a, M.J. Tartarin ^{id}90, P. Tas ^{id}135, M. Tasevsky ^{id}133, E. Tassi ^{id}44b,44a, A.C. Tate ^{id}167,
 Y. Tayalati ^{id}36e,aa, G.N. Taylor ^{id}106, W. Taylor ^{id}161b, R.J. Taylor Vara ^{id}168, A.S. Tegetmeier ^{id}90,
 P. Teixeira-Dias ^{id}96, J.J. Teoh ^{id}160, K. Terashi ^{id}158, J. Terron ^{id}100, S. Terzo ^{id}13, M. Testa ^{id}53,
 R.J. Teuscher ^{id}160,ab, A. Thaler ^{id}79, O. Theiner ^{id}56, T. Thevenaux-Pelzer ^{id}103, D.W. Thomas ^{id}96,

J.P. Thomas ^{id21}, E.A. Thompson ^{id18a}, P.D. Thompson ^{id21}, E. Thomson ^{id130}, R.E. Thornberry ^{id45}, C. Tian ^{id62}, Y. Tian ^{id56}, V. Tikhomirov ^{id81}, Yu.A. Tikhonov ^{id39}, S. Timoshenko ^{id38}, D. Timoshyn ^{id135}, E.X.L. Ting ^{id1}, P. Tipton ^{id177}, A. Tishelman-Charny ^{id30}, K. Todome ^{id140}, S. Todorova-Nova ^{id135}, L. Toffolin ^{id69a,69c}, M. Togawa ^{id83}, J. Tojo ^{id89}, S. Tokár ^{id29a}, O. Toldaiev ^{id68}, G. Tolkachev ^{id103}, M. Tomoto ^{id83}, L. Tompkins ^{id148,n}, E. Torrence ^{id125}, H. Torres ^{id90}, D.I. Torres Arza ^{id139g}, E. Torró Pastor ^{id168}, M. Toscani ^{id31}, C. Toscirci ^{id40}, M. Tost ^{id11}, D.R. Tovey ^{id144}, T. Trefzger ^{id171}, P.M. Tricarico ^{id13}, A. Tricoli ^{id30}, I.M. Trigger ^{id161a}, S. Trincaz-Duvoid ^{id129}, D.A. Trischuk ^{id170}, A. Tropina ^{id39}, D. Truncali ^{id76a,76b}, L. Truong ^{id34c}, M. Trzebinski ^{id87}, A. Trzupiek ^{id87}, F. Tsai ^{id150}, M. Tsai ^{id107}, A. Tsiamis ^{id157}, P.V. Tsiareshka ^{id39}, S. Tsigaridas ^{id161a}, A. Tsirigotis ^{id157,u}, V. Tsiskaridze ^{id154a}, E.G. Tskhadadze ^{id154a}, Y. Tsujikawa ^{id88}, I.I. Tsukerman ^{id38}, V. Tsulaia ^{id18a}, S. Tsuno ^{id83}, K. Tsuru ^{id120}, D. Tsybychev ^{id150}, Y. Tu ^{id64b}, A. Tudorache ^{id28b}, V. Tudorache ^{id28b}, S.B. Tuncay ^{id128}, S. Turchikhin ^{id57b,57a}, I. Turk Cakir ^{id3a}, R. Turra ^{id71a}, T. Turtuvshin ^{id39,ac}, P.M. Tuts ^{id42}, S. Tzamarias ^{id157,d}, Y. Uematsu ^{id83}, F. Ukegawa ^{id162}, P.A. Ulloa Poblete ^{id139c,139b}, E.N. Umaka ^{id30}, G. Unal ^{id37}, A. Undrus ^{id30}, G. Unel ^{id164}, J. Urban ^{id29b}, P. Urrejola ^{id139e}, G. Usai ^{id8}, R. Ushioda ^{id159}, M. Usman ^{id109}, F. Ustuner ^{id52}, Z. Uysal ^{id81}, V. Vacek ^{id134}, B. Vachon ^{id105}, T. Vafeiadis ^{id37}, A. Vaitkus ^{id97}, C. Valderanis ^{id110}, E. Valdes Santurio ^{id47a,47b}, M. Valente ^{id37}, S. Valentinetti ^{id24b,24a}, A. Valero ^{id168}, E. Valiente Moreno ^{id168}, A. Vallier ^{id90}, J.A. Valls Ferrer ^{id168}, D.R. Van Arneman ^{id116}, A. Van Der Graaf ^{id49}, H.Z. Van Der Schyf ^{id34i}, P. Van Gemmeren ^{id6}, M. Van Rijnbach ^{id37}, S. Van Stroud ^{id97}, I. Van Vulpen ^{id116}, P. Vana ^{id135}, M. Vanadia ^{id76a,76b}, U.M. Vande Voorde ^{id149}, W. Vandelli ^{id37}, E.R. Vandewall ^{id148}, D. Vannicola ^{id156}, L. Vannoli ^{id53}, R. Vari ^{id75a}, M. Varma ^{id177}, E.W. Varnes ^{id7}, C. Varni ^{id79}, D. Varouchas ^{id66}, L. Varriale ^{id168}, K.E. Varvell ^{id152}, M.E. Vasile ^{id28b}, L. Vaslin ^{id83}, M.D. Vassilev ^{id148}, A. Vasyukov ^{id39}, L.M. Vaughan ^{id123}, R. Vavricka ^{id135}, T. Vazquez Schroeder ^{id13}, J. Veatch ^{id32}, V. Vecchio ^{id102}, M.J. Veen ^{id104}, I. Veliscek ^{id30}, I. Velkovska ^{id94}, L.M. Veloce ^{id160}, F. Veloso ^{id132a,132c}, A.G. Veltman ^{id52}, S. Veneziano ^{id75a}, A. Ventura ^{id70a,70b}, A. Verbytskyi ^{id111}, M. Verducci ^{id74a,74b}, C. Vergis ^{id95}, M. Verissimo De Araujo ^{id82b}, W. Verkerke ^{id116}, J.C. Vermeulen ^{id116}, C. Vernieri ^{id148}, M. Vessella ^{id164}, M.C. Vetterli ^{id147,ai}, A. Vgenopoulos ^{id101}, N. Viaux Maira ^{id139g,af}, T. Vickey ^{id144}, O.E. Vickey Boeriu ^{id144}, G.H.A. Viehhauser ^{id128}, L. Vigani ^{id63b}, M. Vigi ^{id111}, M. Villa ^{id24b,24a}, M. Villaplana Perez ^{id168}, E.M. Villhauer ^{id40}, E. Vilucchi ^{id53}, M. Vincent ^{id168}, M.G. Vincter ^{id35}, A. Visibile ^{id116}, A. Visive ^{id116}, C. Vittori ^{id37}, I. Vivarelli ^{id24b,24a}, M.I. Vivas Albornoz ^{id48}, E. Voevodina ^{id111}, F. Vogel ^{id110}, J.C. Voigt ^{id50}, P. Vokac ^{id134}, Yu. Volkotrub ^{id86b}, L. Vomberg ^{id25}, E. Von Toerne ^{id25}, B. Vormwald ^{id37}, K. Vorobev ^{id51}, M. Vos ^{id168}, K. Voss ^{id146}, M. Vozak ^{id37}, L. Vozdecky ^{id122}, N. Vranjes ^{id16}, M. Vranjes Milosavljevic ^{id16}, M. Vreeswijk ^{id116}, N.K. Vu ^{id143b,143a}, R. Vuillermet ^{id37}, O. Vujanovic ^{id101}, I. Vukotic ^{id40}, I.K. Vyas ^{id35}, J.F. Wack ^{id33}, S. Wada ^{id162}, C. Wagner ^{id148}, J.M. Wagner ^{id18a}, W. Wagner ^{id176}, S. Wahdan ^{id176}, H. Wahlberg ^{id91}, C.H. Waits ^{id122}, J. Walder ^{id136}, R. Walker ^{id110}, K. Walkingshaw Pass ^{id59}, W. Walkowiak ^{id146}, A. Wall ^{id130}, E.J. Wallin ^{id99}, T. Wamorkar ^{id18a}, K. Wandall-Christensen ^{id168}, A. Wang ^{id62}, A.Z. Wang ^{id138}, C. Wang ^{id48}, C. Wang ^{id11}, H. Wang ^{id18a}, J. Wang ^{id64c}, P. Wang ^{id102}, P. Wang ^{id97}, R. Wang ^{id61}, R. Wang ^{id6}, S.M. Wang ^{id153}, S. Wang ^{id14}, T. Wang ^{id115}, T. Wang ^{id62}, W.T. Wang ^{id128}, W. Wang ^{id14}, X. Wang ^{id167}, X. Wang ^{id143a}, X. Wang ^{id48}, Y. Wang ^{id150}, Y. Wang ^{id62}, Z. Wang ^{id107}, Z. Wang ^{id143b}, Z. Wang ^{id107}, C. Wanotayaroj ^{id83}, A. Warburton ^{id105}, A.L. Warnerbring ^{id146}, S. Waterhouse ^{id96}, A.T. Watson ^{id21}, H. Watson ^{id52}, M.F. Watson ^{id21}, E. Watton ^{id37}, G. Watts ^{id141}, B.M. Waugh ^{id97}, J.M. Webb ^{id54}, C. Weber ^{id30}, M.S. Weber ^{id20}, S.M. Weber ^{id63a}, C. Wei ^{id62}, Y. Wei ^{id54}, A.R. Weidberg ^{id128}, E.J. Weik ^{id119}, J. Weingarten ^{id49}, C. Weiser ^{id54}, C.J. Wells ^{id48}, T. Wenaus ^{id30}, T. Wengler ^{id37}, N.S. Wenke ^{id111}, N. Wermes ^{id25}, M. Wessels ^{id63a}, A.M. Wharton ^{id92}, A.S. White ^{id61}, A. White ^{id8}, M.J. White ^{id1}, D. Whiteson ^{id164}, L. Wickremasinghe ^{id126}, W. Wiedenmann ^{id175}, M. Wielers ^{id136}, R. Wierda ^{id149}, C. Wiglesworth ^{id43}, H.G. Wilkens ^{id37}, J.J.H. Wilkinson ^{id33},

D.M. Williams , H.H. Williams ¹³⁰, S. Williams , S. Willocq , B.J. Wilson ,
D.J. Wilson , P.J. Windischhofer , F.I. Winkel , F. Winklmeier , B.T. Winter ,
M. Wittgen ¹⁴⁸, M. Wobisch , T. Wojtkowski ⁶⁰, Z. Wolffs , J. Wollrath ³⁷, M.W. Wolter ,
H. Wolters , M.C. Wong ¹³⁸, E.L. Woodward , S.D. Worm , B.K. Wosiek ,
K.W. Woźniak , S. Wozniowski , K. Wraight , C. Wu , C. Wu , J. Wu ,
M. Wu , M. Wu , S.L. Wu , S. Wu , X. Wu , Y.Q. Wu , Y. Wu ,
Z. Wu , Z. Wu , J. Wuerzinger , T.R. Wyatt , B.M. Wynne , S. Xella ,
L. Xia , M. Xie , A. Xiong , D. Xu , H. Xu , L. Xu , R. Xu , T. Xu ,
Y. Xu , Z. Xu , R. Xue , B. Yabsley , S. Yacoob , Y. Yamaguchi ,
E. Yamashita , H. Yamauchi , T. Yamazaki , Y. Yamazaki , S. Yan , Z. Yan ,
H.J. Yang , H.T. Yang , S. Yang , T. Yang , X. Yang , X. Yang ,
Y. Yang , Y. Yang , W.-M. Yao , C.L. Yardley , J. Ye , S. Ye , X. Ye , Y. Yeh ,
I. Yeletsikh , B. Yeo , M.R. Yexley , T.P. Yildirim , K. Yorita , C.J.S. Young ,
C. Young , N.D. Young ¹²⁵, Y. Yu , J. Yuan , M. Yuan , R. Yuan , L. Yue ,
M. Zaazoua , B. Zabinski , I. Zahir , A. Zaio ^{57b,57a}, Z.K. Zak , T. Zakareishvili ,
S. Zambito , J.A. Zamora Saa , J. Zang , R. Zanzottera , O. Zaplatilek ,
C. Zeitnitz , H. Zeng , D.T. Zenger Jr , O. Zenin , T. Ženiš , S. Zenz ,
D. Zerwas , D.F. Zhang , G. Zhang , J. Zhang , J. Zhang , L. Zhang ,
L. Zhang , P. Zhang , R. Zhang , S. Zhang , T. Zhang , Y. Zhang ,
Y. Zhang , Y. Zhang , Y. Zhang , Z. Zhang , Z. Zhang , Z. Zhang ,
H. Zhao , T. Zhao , Y. Zhao , Z. Zhao , Z. Zhao , A. Zhemchugov ,
J. Zheng , K. Zheng , X. Zheng , Z. Zheng , D. Zhong , B. Zhou , H. Zhou ,
N. Zhou , Y. Zhou , Y. Zhou , Y. Zhou ⁷, J. Zhu , X. Zhu ^{143b}, Y. Zhu , Y. Zhu ,
X. Zhuang , K. Zhukov , N.I. Zimine , J. Zinsser , M. Ziolkowski , L. Živković ,
A. Zoccoli , K. Zoch , A. Zografos , T.G. Zorbas , O. Zormpa , L. Zwalinski .

¹Department of Physics, University of Adelaide, Adelaide; Australia.

²Department of Physics, University of Alberta, Edmonton AB; Canada.

³(^a)Department of Physics, Ankara University, Ankara; (^b)Division of Physics, TOBB University of Economics and Technology, Ankara; Türkiye.

⁴LAPP, Université Savoie Mont Blanc, CNRS/IN2P3, Annecy; France.

⁵APC, Université Paris Cité, CNRS/IN2P3, Paris; France.

⁶High Energy Physics Division, Argonne National Laboratory, Argonne IL; United States of America.

⁷Department of Physics, University of Arizona, Tucson AZ; United States of America.

⁸Department of Physics, University of Texas at Arlington, Arlington TX; United States of America.

⁹Physics Department, National and Kapodistrian University of Athens, Athens; Greece.

¹⁰Physics Department, National Technical University of Athens, Zografou; Greece.

¹¹Department of Physics, University of Texas at Austin, Austin TX; United States of America.

¹²Institute of Physics, Azerbaijan Academy of Sciences, Baku; Azerbaijan.

¹³Institut de Física d'Altes Energies (IFAE), Barcelona Institute of Science and Technology, Barcelona; Spain.

¹⁴Institute of High Energy Physics, Chinese Academy of Sciences, Beijing; China.

¹⁵Physics Department, Tsinghua University, Beijing; China.

¹⁶Institute of Physics, University of Belgrade, Belgrade; Serbia.

¹⁷Department for Physics and Technology, University of Bergen, Bergen; Norway.

¹⁸(^a)Physics Division, Lawrence Berkeley National Laboratory, Berkeley CA; (^b)University of California, Berkeley CA; United States of America.

- ¹⁹Institut für Physik, Humboldt Universität zu Berlin, Berlin; Germany.
- ²⁰Albert Einstein Center for Fundamental Physics and Laboratory for High Energy Physics, University of Bern, Bern; Switzerland.
- ²¹School of Physics and Astronomy, University of Birmingham, Birmingham; United Kingdom.
- ²²(^a)Department of Physics, Bogazici University, Istanbul; (^b)Department of Physics Engineering, Gaziantep University, Gaziantep; (^c)Department of Physics, Istanbul University, Istanbul; Türkiye.
- ²³(^a)Facultad de Ciencias y Centro de Investigaciones, Universidad Antonio Nariño, Bogotá; (^b)Departamento de Física, Universidad Nacional de Colombia, Bogotá; Colombia.
- ²⁴(^a)Dipartimento di Fisica e Astronomia A. Righi, Università di Bologna, Bologna; (^b)INFN Sezione di Bologna; Italy.
- ²⁵Physikalisches Institut, Universität Bonn, Bonn; Germany.
- ²⁶Department of Physics, Boston University, Boston MA; United States of America.
- ²⁷Department of Physics, Brandeis University, Waltham MA; United States of America.
- ²⁸(^a)Transilvania University of Brasov, Brasov; (^b)Horia Hulubei National Institute of Physics and Nuclear Engineering, Bucharest; (^c)Department of Physics, Alexandru Ioan Cuza University of Iasi, Iasi; (^d)National Institute for Research and Development of Isotopic and Molecular Technologies, Physics Department, Cluj-Napoca; (^e)National University of Science and Technology Politehnica, Bucharest; (^f)West University in Timisoara, Timisoara; (^g)Faculty of Physics, University of Bucharest, Bucharest; Romania.
- ²⁹(^a)Faculty of Mathematics, Physics and Informatics, Comenius University, Bratislava; (^b)Department of Subnuclear Physics, Institute of Experimental Physics of the Slovak Academy of Sciences, Kosice; Slovak Republic.
- ³⁰Physics Department, Brookhaven National Laboratory, Upton NY; United States of America.
- ³¹Universidad de Buenos Aires, Facultad de Ciencias Exactas y Naturales, Departamento de Física, y CONICET, Instituto de Física de Buenos Aires (IFIBA), Buenos Aires; Argentina.
- ³²California State University, CA; United States of America.
- ³³Cavendish Laboratory, University of Cambridge, Cambridge; United Kingdom.
- ³⁴(^a)Department of Physics, University of Cape Town, Cape Town; (^b)iThemba Labs, Western Cape; (^c)Department of Mechanical Engineering Science, University of Johannesburg, Johannesburg; (^d)National Institute of Physics, University of the Philippines Diliman (Philippines); (^e)Department of Physics, Stellenbosch University, Matieland; (^f)University of South Africa, Department of Physics, Pretoria; (^g)University of Pretoria, Department of Mechanical and Aeronautical Engineering, Pretoria; (^h)University of Zululand, KwaDlangezwa; (ⁱ)School of Physics, University of the Witwatersrand, Johannesburg; South Africa.
- ³⁵Department of Physics, Carleton University, Ottawa ON; Canada.
- ³⁶(^a)Faculté des Sciences Ain Chock, Université Hassan II de Casablanca; (^b)Faculté des Sciences, Université Ibn-Tofail, Kénitra; (^c)Faculté des Sciences Semlalia, Université Cadi Ayyad, LPHEA-Marrakech; (^d)LPMR, Faculté des Sciences, Université Mohamed Premier, Oujda; (^e)Faculté des sciences, Université Mohammed V, Rabat; (^f)Institute of Applied Physics, Mohammed VI Polytechnic University, Ben Guerir; Morocco.
- ³⁷CERN, Geneva; Switzerland.
- ³⁸Affiliated with an institute formerly covered by a cooperation agreement with CERN.
- ³⁹Affiliated with an international laboratory covered by a cooperation agreement with CERN.
- ⁴⁰Enrico Fermi Institute, University of Chicago, Chicago IL; United States of America.
- ⁴¹LPC, Université Clermont Auvergne, CNRS/IN2P3, Clermont-Ferrand; France.
- ⁴²Nevis Laboratory, Columbia University, Irvington NY; United States of America.
- ⁴³Niels Bohr Institute, University of Copenhagen, Copenhagen; Denmark.
- ⁴⁴(^a)Dipartimento di Fisica, Università della Calabria, Rende; (^b)INFN Gruppo Collegato di Cosenza,

Laboratori Nazionali di Frascati; Italy.

⁴⁵Physics Department, Southern Methodist University, Dallas TX; United States of America.

⁴⁶National Centre for Scientific Research "Demokritos", Agia Paraskevi; Greece.

⁴⁷(^a) Department of Physics, Stockholm University; (^b) Oskar Klein Centre, Stockholm; Sweden.

⁴⁸Deutsches Elektronen-Synchrotron DESY, Hamburg and Zeuthen; Germany.

⁴⁹Fakultät Physik, Technische Universität Dortmund, Dortmund; Germany.

⁵⁰Institut für Kern- und Teilchenphysik, Technische Universität Dresden, Dresden; Germany.

⁵¹Department of Physics, Duke University, Durham NC; United States of America.

⁵²SUPA - School of Physics and Astronomy, University of Edinburgh, Edinburgh; United Kingdom.

⁵³INFN e Laboratori Nazionali di Frascati, Frascati; Italy.

⁵⁴Physikalisches Institut, Albert-Ludwigs-Universität Freiburg, Freiburg; Germany.

⁵⁵II. Physikalisches Institut, Georg-August-Universität Göttingen, Göttingen; Germany.

⁵⁶Département de Physique Nucléaire et Corpusculaire, Université de Genève, Genève; Switzerland.

⁵⁷(^a) Dipartimento di Fisica, Università di Genova, Genova; (^b) INFN Sezione di Genova; Italy.

⁵⁸II. Physikalisches Institut, Justus-Liebig-Universität Giessen, Giessen; Germany.

⁵⁹SUPA - School of Physics and Astronomy, University of Glasgow, Glasgow; United Kingdom.

⁶⁰LPSC, Université Grenoble Alpes, CNRS/IN2P3, Grenoble INP, Grenoble; France.

⁶¹Laboratory for Particle Physics and Cosmology, Harvard University, Cambridge MA; United States of America.

⁶²Department of Modern Physics and State Key Laboratory of Particle Detection and Electronics, University of Science and Technology of China, Hefei; China.

⁶³(^a) Kirchoff-Institut für Physik, Ruprecht-Karls-Universität Heidelberg, Heidelberg; (^b) Physikalisches Institut, Ruprecht-Karls-Universität Heidelberg, Heidelberg; Germany.

⁶⁴(^a) Department of Physics, Chinese University of Hong Kong, Shatin, N.T., Hong Kong; (^b) Department of Physics, University of Hong Kong, Hong Kong; (^c) Department of Physics and Institute for Advanced Study, Hong Kong University of Science and Technology, Clear Water Bay, Kowloon, Hong Kong; China.

⁶⁵Department of Physics, National Tsing Hua University, Hsinchu; Taiwan.

⁶⁶IJCLab, Université Paris-Saclay, CNRS/IN2P3, 91405, Orsay; France.

⁶⁷Centro Nacional de Microelectrónica (IMB-CNM-CSIC), Barcelona; Spain.

⁶⁸Department of Physics, Indiana University, Bloomington IN; United States of America.

⁶⁹(^a) INFN Gruppo Collegato di Udine, Sezione di Trieste, Udine; (^b) ICTP, Trieste; (^c) Dipartimento Politecnico di Ingegneria e Architettura, Università di Udine, Udine; Italy.

⁷⁰(^a) INFN Sezione di Lecce; (^b) Dipartimento di Matematica e Fisica, Università del Salento, Lecce; Italy.

⁷¹(^a) INFN Sezione di Milano; (^b) Dipartimento di Fisica, Università di Milano, Milano; Italy.

⁷²(^a) INFN Sezione di Napoli; (^b) Dipartimento di Fisica, Università di Napoli, Napoli; Italy.

⁷³(^a) INFN Sezione di Pavia; (^b) Dipartimento di Fisica, Università di Pavia, Pavia; Italy.

⁷⁴(^a) INFN Sezione di Pisa; (^b) Dipartimento di Fisica E. Fermi, Università di Pisa, Pisa; Italy.

⁷⁵(^a) INFN Sezione di Roma; (^b) Dipartimento di Fisica, Sapienza Università di Roma, Roma; Italy.

⁷⁶(^a) INFN Sezione di Roma Tor Vergata; (^b) Dipartimento di Fisica, Università di Roma Tor Vergata, Roma; Italy.

⁷⁷(^a) INFN Sezione di Roma Tre; (^b) Dipartimento di Matematica e Fisica, Università Roma Tre, Roma; Italy.

⁷⁸(^a) INFN-TIFPA; (^b) Università degli Studi di Trento, Trento; Italy.

⁷⁹Universität Innsbruck, Department of Astro and Particle Physics, Innsbruck; Austria.

⁸⁰Department of Physics and Astronomy, Iowa State University, Ames IA; United States of America.

⁸¹Istinye University, Sariyer, Istanbul; Türkiye.

⁸²(^a) Departamento de Engenharia Elétrica, Universidade Federal de Juiz de Fora (UFJF), Juiz de

Fora;^(b)Universidade Federal do Rio De Janeiro COPPE/EE/IF, Rio de Janeiro;^(c)Instituto de Física, Universidade de São Paulo, São Paulo;^(d)Rio de Janeiro State University, Rio de Janeiro;^(e)Federal University of Bahia, Bahia; Brazil.

⁸³KEK, High Energy Accelerator Research Organization, Tsukuba; Japan.

⁸⁴(^a)Khalifa University of Science and Technology, Abu Dhabi;^(b)University of Sharjah, Sharjah; United Arab Emirates.

⁸⁵Graduate School of Science, Kobe University, Kobe; Japan.

⁸⁶(^a)AGH University of Krakow, Faculty of Physics and Applied Computer Science, Krakow;^(b)Marian Smoluchowski Institute of Physics, Jagiellonian University, Krakow; Poland.

⁸⁷Institute of Nuclear Physics Polish Academy of Sciences, Krakow; Poland.

⁸⁸Faculty of Science, Kyoto University, Kyoto; Japan.

⁸⁹Research Center for Advanced Particle Physics and Department of Physics, Kyushu University, Fukuoka ; Japan.

⁹⁰L2IT, Université de Toulouse, CNRS/IN2P3, UPS, Toulouse; France.

⁹¹Instituto de Física La Plata, Universidad Nacional de La Plata and CONICET, La Plata; Argentina.

⁹²Physics Department, Lancaster University, Lancaster; United Kingdom.

⁹³Oliver Lodge Laboratory, University of Liverpool, Liverpool; United Kingdom.

⁹⁴Department of Experimental Particle Physics, Jožef Stefan Institute and Department of Physics, University of Ljubljana, Ljubljana; Slovenia.

⁹⁵Department of Physics and Astronomy, Queen Mary University of London, London; United Kingdom.

⁹⁶Department of Physics, Royal Holloway University of London, Egham; United Kingdom.

⁹⁷Department of Physics and Astronomy, University College London, London; United Kingdom.

⁹⁸Louisiana Tech University, Ruston LA; United States of America.

⁹⁹Fysiska institutionen, Lunds universitet, Lund; Sweden.

¹⁰⁰Departamento de Física Teórica C-15 and CIAFF, Universidad Autónoma de Madrid, Madrid; Spain.

¹⁰¹Institut für Physik, Universität Mainz, Mainz; Germany.

¹⁰²School of Physics and Astronomy, University of Manchester, Manchester; United Kingdom.

¹⁰³CPPM, Aix-Marseille Université, CNRS/IN2P3, Marseille; France.

¹⁰⁴Department of Physics, University of Massachusetts, Amherst MA; United States of America.

¹⁰⁵Department of Physics, McGill University, Montreal QC; Canada.

¹⁰⁶School of Physics, University of Melbourne, Victoria; Australia.

¹⁰⁷Department of Physics, University of Michigan, Ann Arbor MI; United States of America.

¹⁰⁸Department of Physics and Astronomy, Michigan State University, East Lansing MI; United States of America.

¹⁰⁹Group of Particle Physics, University of Montreal, Montreal QC; Canada.

¹¹⁰Fakultät für Physik, Ludwig-Maximilians-Universität München, München; Germany.

¹¹¹Max-Planck-Institut für Physik (Werner-Heisenberg-Institut), München; Germany.

¹¹²Graduate School of Science and Kobayashi-Maskawa Institute, Nagoya University, Nagoya; Japan.

¹¹³(^a)Department of Physics, Nanjing University, Nanjing;^(b)School of Science, Shenzhen Campus of Sun Yat-sen University;^(c)University of Chinese Academy of Science (UCAS), Beijing; China.

¹¹⁴Department of Physics and Astronomy, University of New Mexico, Albuquerque NM; United States of America.

¹¹⁵Institute for Mathematics, Astrophysics and Particle Physics, Radboud University/Nikhef, Nijmegen; Netherlands.

¹¹⁶Nikhef National Institute for Subatomic Physics and University of Amsterdam, Amsterdam; Netherlands.

¹¹⁷Department of Physics, Northern Illinois University, DeKalb IL; United States of America.

- ¹¹⁸(*a*) New York University Abu Dhabi, Abu Dhabi; (*b*) United Arab Emirates University, Al Ain; United Arab Emirates.
- ¹¹⁹Department of Physics, New York University, New York NY; United States of America.
- ¹²⁰Ochanomizu University, Otsuka, Bunkyo-ku, Tokyo; Japan.
- ¹²¹Ohio State University, Columbus OH; United States of America.
- ¹²²Homer L. Dodge Department of Physics and Astronomy, University of Oklahoma, Norman OK; United States of America.
- ¹²³Department of Physics, Oklahoma State University, Stillwater OK; United States of America.
- ¹²⁴Palacký University, Joint Laboratory of Optics, Olomouc; Czech Republic.
- ¹²⁵Institute for Fundamental Science, University of Oregon, Eugene, OR; United States of America.
- ¹²⁶Graduate School of Science, University of Osaka, Osaka; Japan.
- ¹²⁷Department of Physics, University of Oslo, Oslo; Norway.
- ¹²⁸Department of Physics, Oxford University, Oxford; United Kingdom.
- ¹²⁹LPNHE, Sorbonne Université, Université Paris Cité, CNRS/IN2P3, Paris; France.
- ¹³⁰Department of Physics, University of Pennsylvania, Philadelphia PA; United States of America.
- ¹³¹Department of Physics and Astronomy, University of Pittsburgh, Pittsburgh PA; United States of America.
- ¹³²(*a*) Laboratório de Instrumentação e Física Experimental de Partículas - LIP, Lisboa; (*b*) Departamento de Física, Faculdade de Ciências, Universidade de Lisboa, Lisboa; (*c*) Departamento de Física, Universidade de Coimbra, Coimbra; (*d*) Centro de Física Nuclear da Universidade de Lisboa, Lisboa; (*e*) Departamento de Física, Escola de Ciências, Universidade do Minho, Braga; (*f*) Departamento de Física Teórica y del Cosmos, Universidad de Granada, Granada (Spain); (*g*) Departamento de Física, Instituto Superior Técnico, Universidade de Lisboa, Lisboa; Portugal.
- ¹³³Institute of Physics of the Czech Academy of Sciences, Prague; Czech Republic.
- ¹³⁴Czech Technical University in Prague, Prague; Czech Republic.
- ¹³⁵Charles University, Faculty of Mathematics and Physics, Prague; Czech Republic.
- ¹³⁶Particle Physics Department, Rutherford Appleton Laboratory, Didcot; United Kingdom.
- ¹³⁷IRFU, CEA, Université Paris-Saclay, Gif-sur-Yvette; France.
- ¹³⁸Santa Cruz Institute for Particle Physics, University of California Santa Cruz, Santa Cruz CA; United States of America.
- ¹³⁹(*a*) Departamento de Física, Pontificia Universidad Católica de Chile, Santiago; (*b*) Millennium Institute for Subatomic physics at high energy frontier (SAPHIR), Santiago; (*c*) Instituto de Investigación Multidisciplinario en Ciencia y Tecnología, y Departamento de Física, Universidad de La Serena; (*d*) Universidad Andres Bello, Department of Physics, Santiago; (*e*) Universidad San Sebastian, Recoleta; (*f*) Instituto de Alta Investigación, Universidad de Tarapacá, Arica; (*g*) Departamento de Física, Universidad Técnica Federico Santa María, Valparaíso; Chile.
- ¹⁴⁰Department of Physics, Institute of Science, Tokyo; Japan.
- ¹⁴¹Department of Physics, University of Washington, Seattle WA; United States of America.
- ¹⁴²(*a*) Institute of Frontier and Interdisciplinary Science and Key Laboratory of Particle Physics and Particle Irradiation (MOE), Shandong University, Qingdao; (*b*) School of Physics, Zhengzhou University; China.
- ¹⁴³(*a*) State Key Laboratory of Dark Matter Physics, School of Physics and Astronomy, Shanghai Jiao Tong University, Key Laboratory for Particle Astrophysics and Cosmology (MOE), SKLPPC, Shanghai; (*b*) State Key Laboratory of Dark Matter Physics, Tsung-Dao Lee Institute, Shanghai Jiao Tong University, Shanghai; China.
- ¹⁴⁴Department of Physics and Astronomy, University of Sheffield, Sheffield; United Kingdom.
- ¹⁴⁵Department of Physics, Shinshu University, Nagano; Japan.
- ¹⁴⁶Department Physik, Universität Siegen, Siegen; Germany.

- ¹⁴⁷Department of Physics, Simon Fraser University, Burnaby BC; Canada.
- ¹⁴⁸SLAC National Accelerator Laboratory, Stanford CA; United States of America.
- ¹⁴⁹Department of Physics, Royal Institute of Technology, Stockholm; Sweden.
- ¹⁵⁰Departments of Physics and Astronomy, Stony Brook University, Stony Brook NY; United States of America.
- ¹⁵¹Department of Physics and Astronomy, University of Sussex, Brighton; United Kingdom.
- ¹⁵²School of Physics, University of Sydney, Sydney; Australia.
- ¹⁵³Institute of Physics, Academia Sinica, Taipei; Taiwan.
- ¹⁵⁴(^a)E. Andronikashvili Institute of Physics, Iv. Javakhishvili Tbilisi State University, Tbilisi; (^b)High Energy Physics Institute, Tbilisi State University, Tbilisi; (^c)University of Georgia, Tbilisi; Georgia.
- ¹⁵⁵Department of Physics, Technion, Israel Institute of Technology, Haifa; Israel.
- ¹⁵⁶Raymond and Beverly Sackler School of Physics and Astronomy, Tel Aviv University, Tel Aviv; Israel.
- ¹⁵⁷Department of Physics, Aristotle University of Thessaloniki, Thessaloniki; Greece.
- ¹⁵⁸International Center for Elementary Particle Physics and Department of Physics, University of Tokyo, Tokyo; Japan.
- ¹⁵⁹Graduate School of Science and Technology, Tokyo Metropolitan University, Tokyo; Japan.
- ¹⁶⁰Department of Physics, University of Toronto, Toronto ON; Canada.
- ¹⁶¹(^a)TRIUMF, Vancouver BC; (^b)Department of Physics and Astronomy, York University, Toronto ON; Canada.
- ¹⁶²Division of Physics and Tomonaga Center for the History of the Universe, Faculty of Pure and Applied Sciences, University of Tsukuba, Tsukuba; Japan.
- ¹⁶³Department of Physics and Astronomy, Tufts University, Medford MA; United States of America.
- ¹⁶⁴Department of Physics and Astronomy, University of California Irvine, Irvine CA; United States of America.
- ¹⁶⁵University of West Attica, Athens; Greece.
- ¹⁶⁶Department of Physics and Astronomy, University of Uppsala, Uppsala; Sweden.
- ¹⁶⁷Department of Physics, University of Illinois, Urbana IL; United States of America.
- ¹⁶⁸Instituto de Física Corpuscular (IFIC), Centro Mixto Universidad de Valencia - CSIC, Valencia; Spain.
- ¹⁶⁹Department of Physics, University of British Columbia, Vancouver BC; Canada.
- ¹⁷⁰Department of Physics and Astronomy, University of Victoria, Victoria BC; Canada.
- ¹⁷¹Fakultät für Physik und Astronomie, Julius-Maximilians-Universität Würzburg, Würzburg; Germany.
- ¹⁷²Department of Physics, University of Warwick, Coventry; United Kingdom.
- ¹⁷³Waseda University, Tokyo; Japan.
- ¹⁷⁴Department of Particle Physics and Astrophysics, Weizmann Institute of Science, Rehovot; Israel.
- ¹⁷⁵Department of Physics, University of Wisconsin, Madison WI; United States of America.
- ¹⁷⁶Fakultät für Mathematik und Naturwissenschaften, Fachgruppe Physik, Bergische Universität Wuppertal, Wuppertal; Germany.
- ¹⁷⁷Department of Physics, Yale University, New Haven CT; United States of America.
- ¹⁷⁸Yerevan Physics Institute, Yerevan; Armenia.
- ^a Also at Affiliated with an institute formerly covered by a cooperation agreement with CERN.
- ^b Also at An-Najah National University, Nablus; Palestine.
- ^c Also at Borough of Manhattan Community College, City University of New York, New York NY; United States of America.
- ^d Also at Center for Interdisciplinary Research and Innovation (CIRI-AUTH), Thessaloniki; Greece.
- ^e Also at Centre of Physics of the Universities of Minho and Porto (CF-UM-UP); Portugal.
- ^f Also at CERN, Geneva; Switzerland.
- ^g Also at Département de Physique Nucléaire et Corpusculaire, Université de Genève, Genève;

Switzerland.

^h Also at Departament de Física de la Universitat Autònoma de Barcelona, Barcelona; Spain.

ⁱ Also at Department of Financial and Management Engineering, University of the Aegean, Chios; Greece.

^j Also at Department of Mathematical Sciences, University of South Africa, Johannesburg; South Africa.

^k Also at Department of Modern Physics and State Key Laboratory of Particle Detection and Electronics, University of Science and Technology of China, Hefei; China.

^l Also at Department of Physics, Bolu Abant İzzet Baysal University, Bolu; Türkiye.

^m Also at Department of Physics, King's College London, London; United Kingdom.

ⁿ Also at Department of Physics, Stanford University, Stanford CA; United States of America.

^o Also at Department of Physics, Stellenbosch University; South Africa.

^p Also at Department of Physics, University of Fribourg, Fribourg; Switzerland.

^q Also at Department of Physics, University of Thessaly; Greece.

^r Also at Department of Physics, Westmont College, Santa Barbara; United States of America.

^s Also at Faculty of Physics, Sofia University, 'St. Kliment Ohridski', Sofia; Bulgaria.

^t Also at Faculty of Physics, University of Bucharest ; Romania.

^u Also at Hellenic Open University, Patras; Greece.

^v Also at Henan University; China.

^w Also at Imam Mohammad Ibn Saud Islamic University; Saudi Arabia.

^x Also at Institutio Catalana de Recerca i Estudis Avancats, ICREA, Barcelona; Spain.

^y Also at Institut für Experimentalphysik, Universität Hamburg, Hamburg; Germany.

^z Also at Institute for Nuclear Research and Nuclear Energy (INRNE) of the Bulgarian Academy of Sciences, Sofia; Bulgaria.

^{aa} Also at Institute of Applied Physics, Mohammed VI Polytechnic University, Ben Guerir; Morocco.

^{ab} Also at Institute of Particle Physics (IPP); Canada.

^{ac} Also at Institute of Physics and Technology, Mongolian Academy of Sciences, Ulaanbaatar; Mongolia.

^{ad} Also at Institute of Physics, Azerbaijan Academy of Sciences, Baku; Azerbaijan.

^{ae} Also at Institute of Theoretical Physics, Iliia State University, Tbilisi; Georgia.

^{af} Also at Millennium Institute for Subatomic physics at high energy frontier (SAPHIR), Santiago; Chile.

^{ag} Also at National Institute of Physics, University of the Philippines Diliman (Philippines); Philippines.

^{ah} Also at The Collaborative Innovation Center of Quantum Matter (CICQM), Beijing; China.

^{ai} Also at TRIUMF, Vancouver BC; Canada.

^{aj} Also at Università di Napoli Parthenope, Napoli; Italy.

^{ak} Also at University of Chinese Academy of Sciences (UCAS), Beijing; China.

^{al} Also at University of Colorado Boulder, Department of Physics, Colorado; United States of America.

^{am} Also at University of Sienna; Italy.

^{an} Also at Washington College, Chestertown, MD; United States of America.

^{ao} Also at Yeditepe University, Physics Department, Istanbul; Türkiye.

* Deceased